

Uplift, erosion and fault reactivation in southern West and South Greenland. Field report summer 2006

Peter Japsen, Johan M. Bonow, Jean-Pierre Peulvast & Robert W. Wilson



GEOLOGICAL SURVEY OF DENMARK AND GREENLAND
MINISTRY OF THE ENVIRONMENT



GEUS

Uplift, erosion and fault reactivation in southern West and South Greenland. Field report summer 2006

Peter Japsen, Johan M. Bonow, Jean-Pierre Peulvast & Robert W. Wilson

With contributions from James A. Chalmers & Adam A. Garde

1.	Summary	3
2.	Introduction	5
2.1	Aim of the project.....	6
2.2	Structural development of the Labrador Sea and Davis Strait.....	8
2.3	Cenozoic uplift history of central West Greenland	13
2.4	Existing AFTA data from South-west Greenland	14
2.5	Regional topography.....	16
3.	Akia (Nordlandet)	20
3.1	Geological setting	21
3.2	Geomorphological analysis.....	25
3.3	Structural analysis	29
3.4	Rock sampling	38
3.5	Discussion	38
4.	South Greenland	41
4.1	An overview of the crustal architecture of the Ketilidian orogen	42
4.2	Geomorphological analysis.....	46
4.3	Structural analysis	51
4.4	Rock sampling	60
4.5	Discussion	63
5.	Acknowledgements	66
6.	References	67
	Appendix. Location maps and list of rocks sampled	71

1. Summary

Fieldwork was carried out in two weeks of August 2006 along the north-western coast of Godthåbsfjord and in South Greenland focussed at Kobberminebugt. The work was part of the project 'Uplift, erosion and fault reactivation in Southwest Greenland' that is primarily funded by the Danish Natural Science Research Council (FNU) and involves studies of geomorphology, structural relations and apatite fission-track analysis of rock samples.

During the fieldwork in Godthåbsfjord the main question was whether the pronounced topographical contrast across the fjord can be explained by Cretaceous–Paleocene normal faulting. A characteristic of the lowlands of Akia (Nordlandet) is the pronounced width of the area compared to other strandflat-like features (coastal platforms) along the coast of West Greenland. Akia might thus represent the exhumed base of a graben structure and the high-lying terrain east of Godthåbsfjord the hanging wall of this rift system. Previous studies have identified a Precambrian fault along the fjord because it is characterized by a strong magnetic anomaly and because it marks the separation of different metamorphic grades. It was however, not possible to identify indications of normal fault movements in the study area along the north-western end of the fjord, and the saprolites found are probably young. Evidence of normal faulting is more likely to be present along the outer parts of the fjord, but planned work had to be given up due to weather conditions. Further studies, in particular analysis of rocks sampled during the fieldwork and mapping of large-scale landforms in the area between Sukkertoppen and Nuuk may lead to further clarification.

During the fieldwork in South Greenland the main objective was to analyse fault patterns and landforms in Kobberminebugt in order to investigate how the structures in this area relate to the Mesozoic rifting in the Labrador Sea. This region marks a distinct left-lateral step on the south-west margin of Greenland, and this step coincides with the transition from Archaean basement rocks to the north and rocks of the Ketilidian orogenic belt to the south. In the west there is a marked topographic change in the region of Kobberminebugt which is coincident with the Border zone of the Ketilidian Orogen. This topographic expression is not apparent on the east coast where the lithological contrast is the same, and this proves that the main control on the topography must be tectonic rather than related to the differential resistance of the rocks. Fault patterns and movements in Kobberminebugt all appear to be consistent with a regional NE–SW extension direction and the orientation of strike-slip faults appears to fit with an E–W-trending dextral wrench system. As the area studied lies in a left-lateral step on the rifted Labrador Sea margin, we suggest that this system may have developed as an oblique transfer zone during Cretaceous–Paleocene rifting. According to the model for mid-crustal partitioning of deformation within the Ketilidian Orogen (Garde et al. 2002) the upper crust underwent localised transpression along a number of discrete faults and shear zones, while the lower crust shows a more distributed zone of deformation. This upper block is more likely to be prone to reactivation during rifting than the lower block as it contains more discrete structures. Therefore the western margin shows a stepped/ transfer zone geometry and the development of an oblique margin segment, whereas the east does not.

The present-day elevations in south-western Greenland may be the result of the Cenozoic development: If the results from recent uplift studies in central West Greenland apply to southern Greenland, the relief is mainly due to late Neogene tectonic movements. Later, differential weathering controlled by lithological contrasts has overprinted the uplifted relief to different degrees. This opens the possibility that the transfer zone along Kobberrminebugt has been reactivated during the Neogene.

Our preliminary analysis of the large-scale topography indicates that the eastern and western coasts of Greenland have developed separately: the south-eastern coast is characterized by an elongate, anticlinal structure with elevations above 2 km almost to at 60°N near the southern tip of Greenland, whereas the south-western coast is dominated by near-horizontal surfaces reaching 1 km in elevation, and these can be traced only as far south as to the northern part of Kobberrminebugt at 61°N. How this configuration can be explained awaits the detailed follow-up on the fieldwork: Namely regional mapping of the landforms that may or may not verify a correlation with planation surfaces in central West Greenland and the analysis of the new apatite fission track data from the study area, in particular from an elevated transect sampled near Narsarsuaq to 1.8 km above sea level. The latter results may give insight into the magnitude and timing of cooling events that have affected the region and reveal to what extent such events correlate with those established north of Sukkertoppen Iskappe.

2. Introduction

The present report contains documentation of the Fieldwork carried out in 2006 as part of the project 'Uplift, erosion and fault reactivation in Southwest Greenland' that is primarily funded by the Danish Natural Science Research Council (FNU). The participants in the Fieldwork were geomorphologist Johan M. Bonow (GEUS), geophysicist Peter Japsen (GEUS), geomorphologist Jean-Pierre Peulvast (Université Paris-Sorbonne) and structural geologist Robert 'Woody' Wilson (University of Durham). This report also contains a compilation of various relevant information such as short descriptions of the regional geology, maps of magnetic anomalies, regional topography and existing data from apatite fission-track analysis (AFTA; cf. Green et al. 2002) of rock samples from the area.

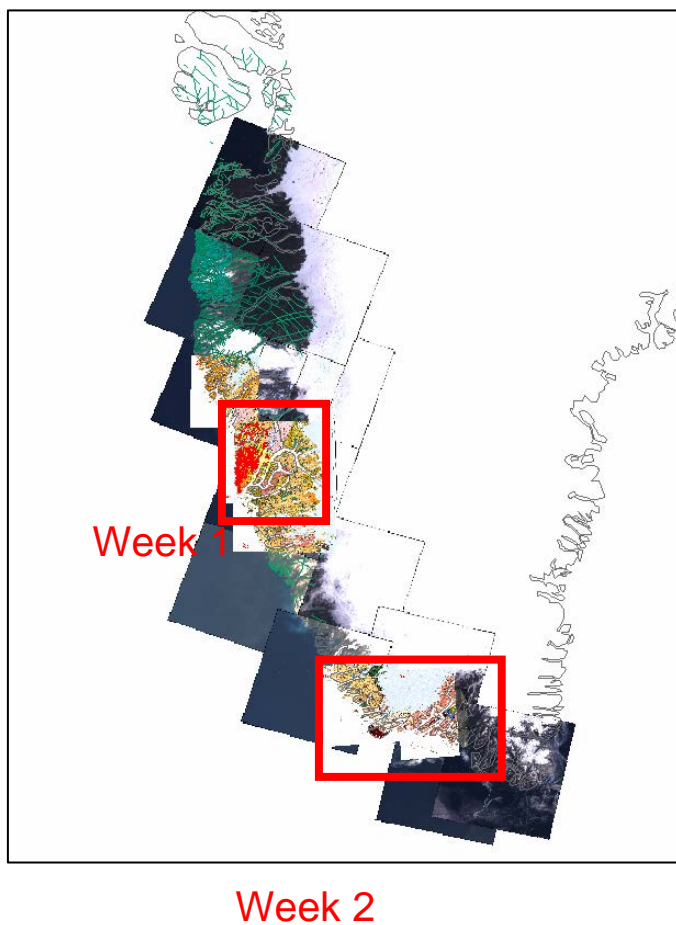


Figure 2.0-1. Location of the two study areas and of the ArcGIS datasets. Inserted geological maps are shown later in this report (cf. the geological map in Fig. 2.0-2).

The Fieldwork took place during two weeks from August 14 to 28 2006 (Fig. 2.0-1). The first week's work was along the north-western coast of Godthåbsfjord with a base camp in Kikiallit (August 14–20) and the second week's work was focussed in Kobberminebugt based on the M/S Gardar sailed by Carl-Aage Skovaa starting from Qaqartoq (August 21–27). The last week included three helicopter-borne surveys. Location maps for the study areas with indication of photos are shown in Appendix. Place names are according to modern Greenlandic spelling, which differs from the available geodetic maps in scale 1 : 250 000 ('Saga' maps; see reference list). Note that many geological units were named when the older spelling was prevailing, and these remain unchanged.

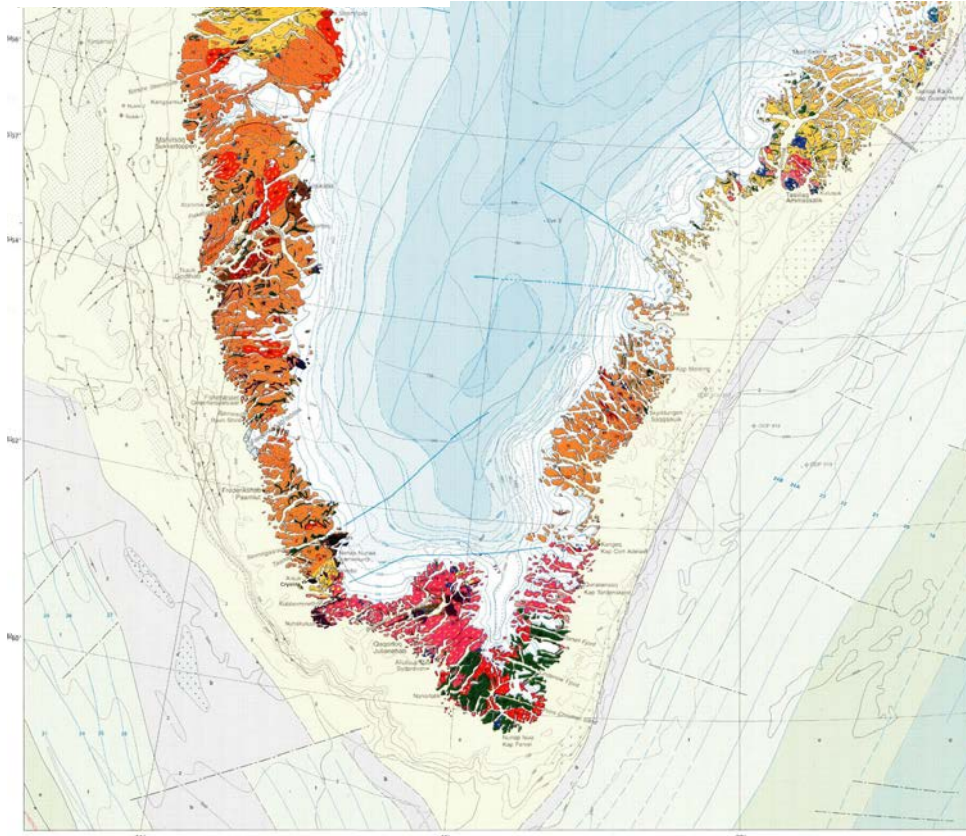


Figure 2.0-2. General geological map of the ice-free areas of Greenland (parts). Offshore geology of the shelf and sea floor shown based on geophysical interpretation and exploration wells. Note the narrow continental shelf offshore of SW Greenland. From Henriksen et al. 2000 (map legend on full map).

2.1 Aim of the project

The aim of the project was described in the application to the Danish Research Council in 2005 as “to carry out Fieldwork in Southwest Greenland to gather data that may further constrain our knowledge on which processes that have caused Neogene uplift around the North Atlantic. The investigations will seek to identify the extent, magnitude and timing of episodes of uplift, erosion and fault reactivation in SW Greenland. The work will be based

on methods that have proven to be effective in our previous studies in central West Greenland, 2002–2005. The model of the landscape evolution will be based on new apatite fission-track analysis of rock samples in combination with structural analysis of fault systems and geomorphological analysis of large landforms. The geomorphological analysis of landforms will provide a relative chronology for the development of the relief whereas timing of associated thermal events can be estimated from fission track analysis. The movement patterns and timing of the different fault systems will be assessed by various methods in order to investigate their control on the vertical movements of the crust; including fracture pattern analysis and $^{40}\text{Ar}/^{39}\text{Ar}$ geochronology for possible dating of fault movements. The history of Cenozoic vertical movements will be determined from stratigraphy based on offshore seismic data supplemented by interpretation of the onshore development. Based on these investigations we will establish a regional model for major events in the Phanerozoic burial and erosional history of onshore SW Greenland, in particular the Cenozoic components.

Differences between central W and SW Greenland will add important constraints to the evaluation of different hypotheses that have been suggested to explain Neogene uplift around the North Atlantic. This will be possible due to the differences between the sections of volcanic and non-volcanic margin along the coast, and because the areas off the coast of SW Greenland, in the Labrador Sea, were subject to substantial sea-floor spreading during the Palaeogene in contrast to the areas offshore central West Greenland.

The study area is from Nanortalik to Sukkertoppen Iskappe (60–66°N). Fieldwork will be carried out during the summer of 2006, but the initial phase of the study will be based on digital terrain models, aerial photos and on results from available studies. Furthermore, the results will be integrated with the outcome of the investigations carried out in our previous investigations in central West Greenland.

The Greenland society will benefit from a better understanding of the erosion level exposed in diamond-bearing kimberlites onshore and to burial of hydrocarbon generating strata offshore West Greenland.”

Specific targets and questions during the two weeks of Fieldwork in 2006 were:

Godthåbsfjord, week 1

- Observation of geomorphological and structural relations.
- Sampling of rocks for apatite fission track analysis across the fjord.
- Possible identification of any indications of Phanerozoic fault movements along the shear or thrust zone in Godthåbsfjord proven by aeromagnetic data. Can the present topographical contrast across the fjord be explained by Mesozoic normal faulting?

South Greenland, week 2

- Observation of geomorphological and structural relations.
- Sampling of rocks for apatite fission track analysis across the area.
- Sampling of rocks for apatite fission track analysis along a near-vertical profile to c. 2 km above sea level for possible identification of palaeo-geothermal gradients and estimation of magnitude and timing of exhumation.
- Analysis of the fault patterns and landforms in Kobberrminebugt to investigate how this area relates to the Mesozoic rifting in the Labrador Sea.

2.2 Structural development of the Labrador Sea and Davis Strait

By James A. Chalmers, GEUS

The present-day Labrador Sea/Davis Strait developed during two intra-cratonic rifting phases and a phase of sea-floor spreading (Fig. 2.2-1) (cf. Chalmers 1997; Chalmers & Laursen 1995; Chalmers & Pulvertaft 2001; Chalmers et al. 1993, 1999; Chian & Loudon 1994).

The first phase of rifting took place during the Early to mid-Cretaceous, with an initial sag that developed during the Berresian to Aptian followed by active rifting during the Aptian-Albian. Thermal subsidence continued during the later Cretaceous over the present-day Labrador, southern West Greenland and Nuussuaq Basins, but slow rifting appears to have continued to form the highly-extended “transition” zone, along the present-day margins of the oceanic crust.

New rifting took place during the Maastrichtian-Danian and was followed during the later Paleocene by major volcanism and the start of sea-floor spreading. The start of sea-floor spreading in the northern North Atlantic in the earliest Eocene caused a change in Euler Pole in the Labrador Sea and spreading rates declined steadily, finally ceasing during Chron 13 (Oligocene/Miocene), although true sea-floor spreading probably ceased earlier during Chron 20 (mid-Eocene).

Volcanism was high-temperature around the Davis Strait, shown by the eruption of picrites in the Nuussuaq Basin and the formation of Seaward-Dipping Reflectors (SDRs) in northern Labrador Sea and southern Baffin Bay, but the highly extended transition zone farther south stayed cool.

A major change in tectonic style occurred in the Oligocene when compression, volcanism and uplift caused erosion of the West Greenland shelf area as well as large areas in the Labrador Sea (Sørensen 2006). The period of uplift and erosion ended in mid-Miocene time, when renewed subsidence of the shelf began.

Uplift during the Neogene is recorded by tilting of the sediments that is substantially different in different places, but does not seem to have reactivated the faults to any significant extent. The section west of Disko and Nuussuaq has clearly been tilted up to the east relatively recently (cf. Fig. 2.3-1A and fig. 4 in Chalmers 2000) and the landward end eroded by an unconformity a short distance below the sea bed, or by the sea bed itself. A similar configuration is found in the Sisimiut Basin (Fig. 2.2-2).

What happened farther south is not so clear on the offshore data. On the landward ends of both Figs 2.2-3 and 2.2-4, Plio–Pleistocene sediments rest directly on Mesozoic sediments and there are hints of tilting of the Palaeogene and Mesozoic section farther seawards. Both observations indicate that uplift and erosion took place before deposition of the Plio–Pleistocene prograding wedges. However, the situation is not so clear cut as farther north

and needs more extensive seismic stratigraphic analysis of the Neogene section than has yet been done.

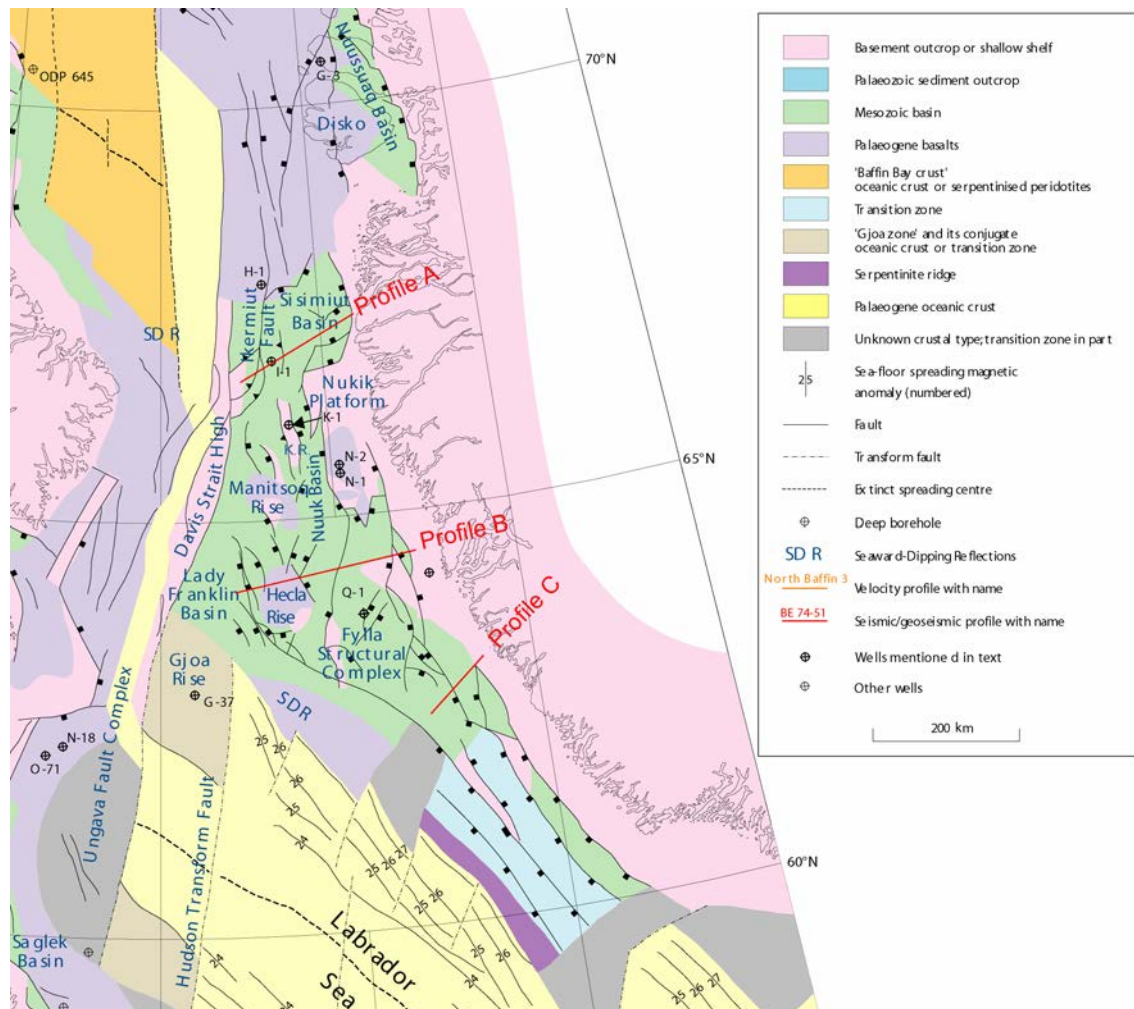
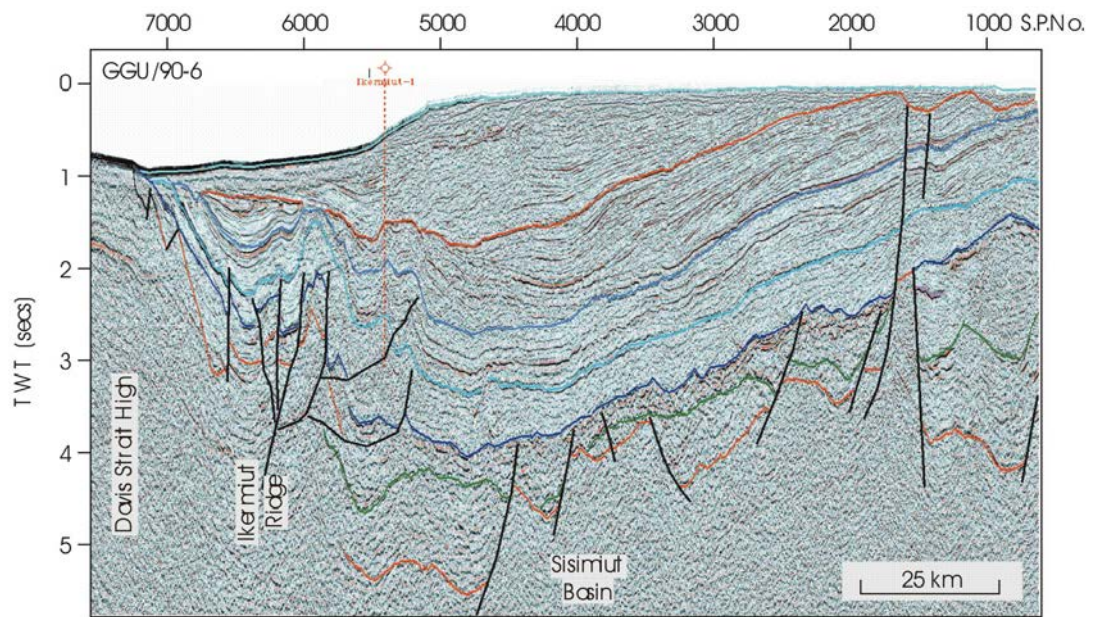


Fig. 2.2-1. Geology of the area between Greenland and Canada with indications of the profiles A, B and C shown in Figs 2.2-2 to -4. Modified after Chalmers in press.



SW

NE

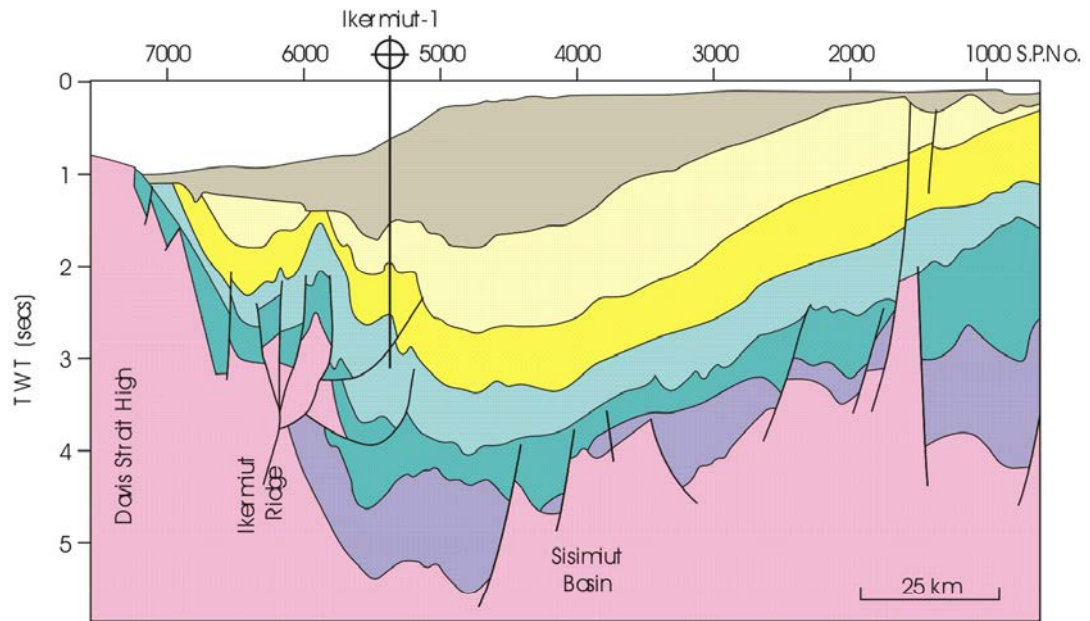


Figure 2.2-2. Profile across the Sisimiut Basin indicating late truncation of the thick Palaeogene section. Profile A on Fig. 2.2-1. From Chalmers in press.

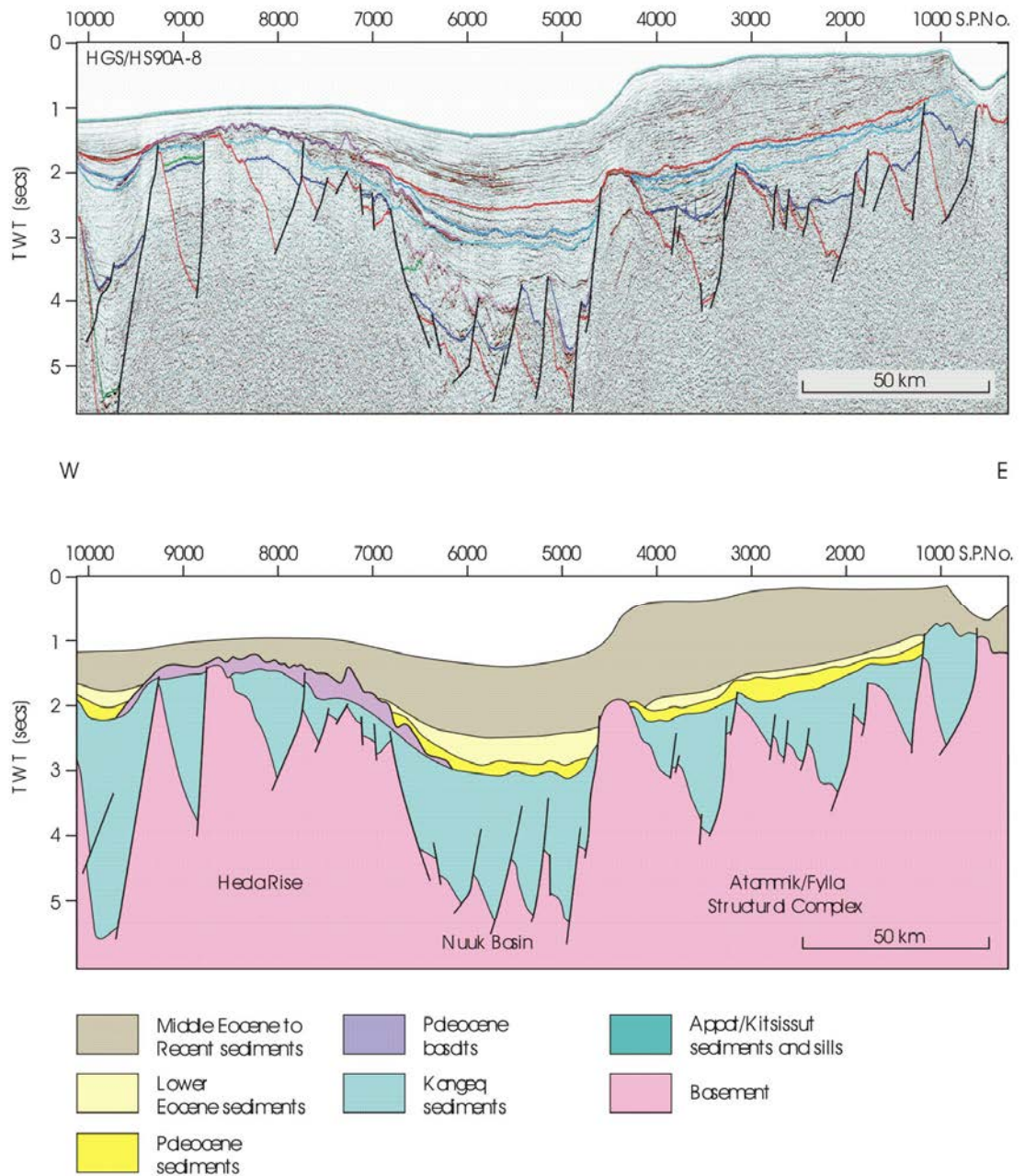


Figure 2.2-3. Profile across the Nuuk Basin and the Fylla structural complex, west of Akia (Nordlandet). Note the thin Palaeogene section and the presence of Mesozoic rift basins just west of Akia. Profile B on Fig. 2.2-1. From Chalmers in press.

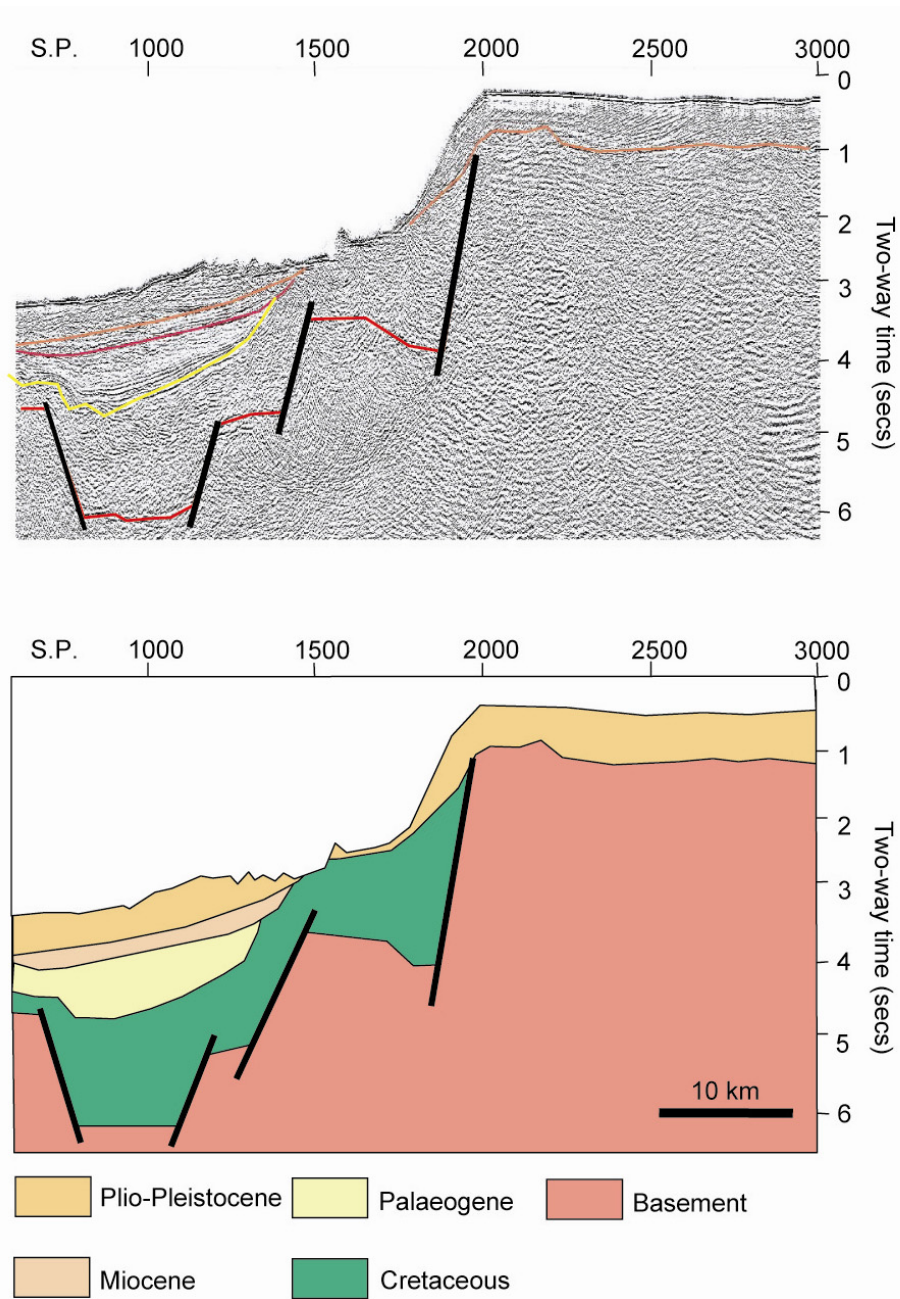


Figure 2.2-4. Profile across the area just south of the Fylla structural complex. Note that Plio–Pleistocene sediments rest directly on the Mesozoic graben fill. Profile C on Fig. 2.2-1 (Interpretation of GGU line 90-21).

2.3 Cenozoic uplift history of central West Greenland

The preserved Mesozoic–Cenozoic sedimentary and volcanic record of central West Greenland (65–71°N) has made it possible to decipher the Cenozoic uplift history of this passive continental margin. The development of West Greenland landscapes across areas with substantially different geology was investigated by combining apatite fission-track analysis data with landform analysis (Fig. 2.3-1) (Bonow 2005; Bonow et al. 2006a, b; Japsen et al. 2005, 2006).

The present-day mountains of central West Greenland have thus been found to be the end result of three Cenozoic phases of uplift and erosion. The first phase that began between 36 and 30 Ma led to the formation of a planation surface during the Oligocene–Miocene. This surface was offset by reactivated faults, resulting in megablocks that were tilted and uplifted to present-day altitudes of up to 2 km in two phases that began between 11 and 10 and between 7 and 2 Ma. These late Neogene uplift phases postdate rifting by c. 50 million years and sea-floor spreading west of Greenland by c. 30 million years, while the first of these phases predates onset of glaciation in Greenland by c. 3 million years. The regional nature of these uplift movements and their considerable distance from active plate boundaries suggest that the causal mechanisms must be located in the deep crust or the upper mantle where the thickness of the crust and lithosphere changes substantially over a short distance.

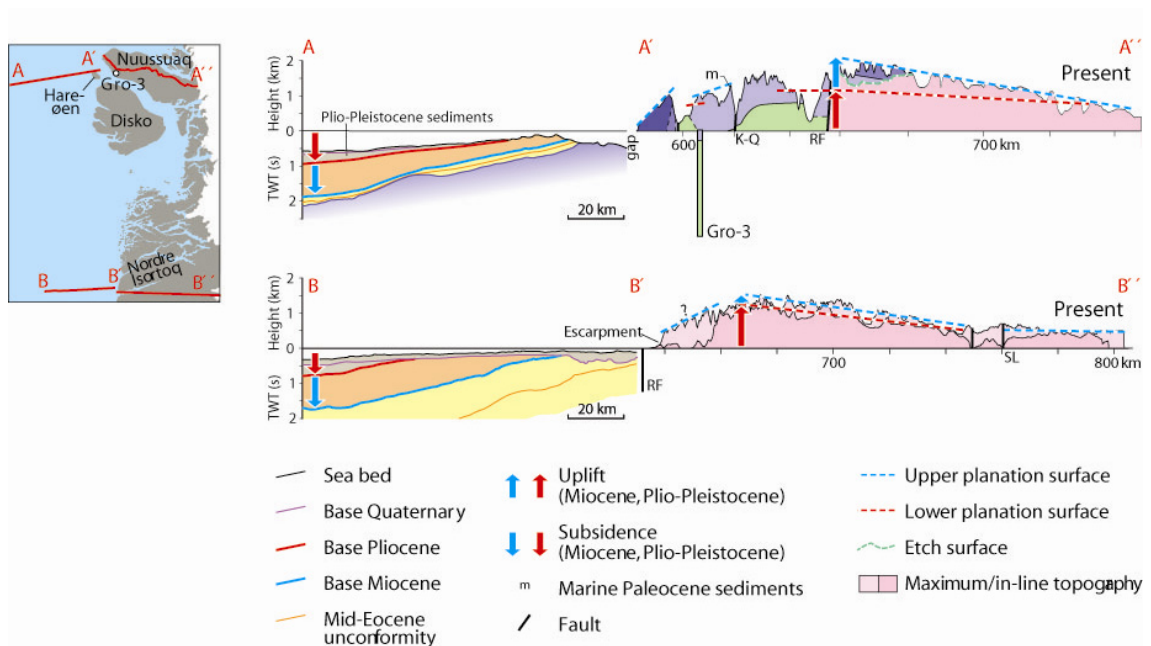


Figure 2.3-1. Onshore-offshore correlation. Present-day profiles across Nuussuaq (AA'A'') and Nordre Isortoq (BB'B'') reveal uplift of the upper planation surface onshore and subsidence offshore during the Neogene. Note that late Cenozoic erosion along the coast near Nordre Isortoq has resulted in a c. 500 m high escarpment. Pink: Precambrian basement. Green: Cretaceous sediments. Violet: Palaeogene basalt formations. K-Q: Kuugannguaq–Qunnilik fault. RF: Rift fault (c. 65 Ma). SL: Sisimiut Line. TWT: Two-way traveltime. Modified from Japsen et al. (2006).

2.4 Existing AFTA data from South-west Greenland

AFTA data exist for 4 samples in SW Greenland (south of 65°N, Manitsoq; Table 2.4-1; Fig. 2.4-1) (Green 2004). The palaeotemperature analysis of the three southernmost samples shows a cooling episode that began at 70-60 Ma, contrasting with all samples from north of 65°N where a cooling episode beginning 36-30 Ma has been identified (Japsen et al. 2006). The mid-Cenozoic cooling episode was interpreted by Japsen et al. (2006) as indicating continued burial until uplift and exhumation was initiated at the Eocene–Oligocene transition in agreement with the presence of Paleocene–Eocene sediments offshore central West Greenland (Figs 2.3-1, -2) (e.g. Chalmers 2000). The cooling starting at 70-60 Ma in south Greenland probably reflects events related to rifting or break-up. The fact that a mid-Cenozoic event (if present) cannot be resolved in these samples may indicate that Palaeogene burial was less pronounced in South-west than in central West Greenland or alternatively higher Paleocene heat flow towards the south than around e.g. Sukkertoppen Iskappe. Note that maximum palaeotemperatures occurred around 60 Ma in the central parts of the British Isles (cf. Green et al. 2002). At this time South Greenland was situated west of the Rockall Plateau (Fig. 2.4-2).

All four samples cooled to temperatures within the partial annealing zone (<105-125°C) during the Late Jurassic event (beginning 160-150 Ma) as recorded by almost all basement samples along the coast further north. This timing coincides with the Jurassic magmatism in south-western Greenland south of 66°N reported by Larsen (2006), in particular with the approximate ages of two carbonatite intrusions (158-166 Ma). According to Larsen the triggering of the melting could be incipient Lithospheric stretching leading to localised asthenospheric upwelling or due to passive uplift alone. Increased extension occurred around 150 Ma as indicated by magmatic rocks produced by larger degrees of melting than during the preceding episodes; e.g. the dyke swarm around Frederikshåb Isblink (c. 62°30'N). During the early Cretaceous (140-133 Ma) the SW Greenland coast-parallel dyke swarm was emplaced indicating a significant regional stretching and rifting event (Larsen 2006).

There is no significant difference between the palaeothermal history derived from AFTA of the two samples on either side of Godthåbsfjord (GC891-29, -30)



Figure 2.4-1. Timing constraints derived from AFTA in individual samples from SW Greenland (part of figure in Green 2004; see Table 2.4-1). Constraints on certain cooling episodes in samples labelled “*” are not consistent with those in other samples (GC891-33). Note the cooling episode beginning 70–60 Ma as identified in the three southernmost samples in contrast to all samples north of 65°N.

Table 2.4-1: Paleotemperature analysis summary: AFTA data in four outcrop samples, SW Greenland (Geotrack Report #891, Green 2004)

Sample No.	Elevation (m)	Stratigraphic age (Ma)	Present temperature ⁺¹ (°C)	FT age (Ma)	Mesozoic		Cenozoic	
					Maximum paleotemperature ⁻² (°C)	Onset of cooling ⁻² (Ma)	Maximum paleotemperature ⁻² (°C)	Onset of cooling ⁻² (Ma)
27 Manitsoq South	0	>570	0	113±9	>105	160-115	60-85	40-0
29 Nordlandet, Nipisat	0	>570	0	116±8	>125	260-110	80-110 30-70	82-28 45-0
30 Nuuk, Sømands-hjemmet	0	>570	0	116±8	>105	175-115	75-90	70-10
33 Nanortalik	0	>570	0	72±3	>110	150-80	100-110 50-85	85-60 18-0

Synthesis of all data (not shown) suggests four discrete episodes of cooling (vertical bands in Fig.2.4-1). See also Japsen et al. 2006:

160-150 Ma Late Jurassic

70-60 Ma Late Cretaceous-Palaeogene (orange in Fig. 2.4-1)

36-30 Ma Late Eocene–Early Oligocene

18-0 Ma Neogene

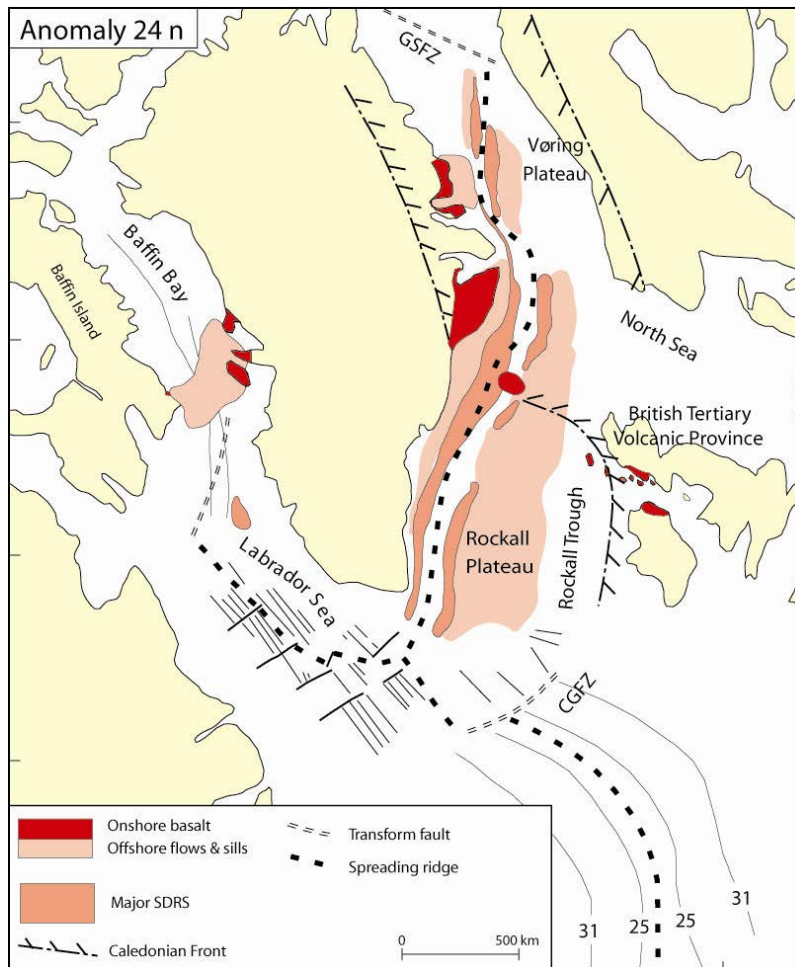


Figure 2.4-2. Reconstruction of the geography in the North Atlantic region at the time of break-up (c. 54 Ma, anomaly 24 N). Note the location of Southern Greenland west of the Rockall Plateau. Courtesy of Trine Dahl-Jensen.

2.5 Regional topography

A regional map of the elevation above sea level of the bedrock in southern Greenland (south of 65°N) has been produced by interpolation of a 5 km grid based on airborne ice-penetrating radar measurements over the Inland Ice (Fig. 2.5-1) (Layberry & Bamber 2001). Note that the density of the flight routes is sparse in many areas and that the southernmost east-west line is along 61°45'N and that no north-south line covers the southwestern tongue of the Inland Ice (NE of Kobberrminebugt) (cf. Fig. 2.5-2).

The regional map reveals a symmetrical pattern of elevated margins along both the western and the eastern coast of Greenland. This pattern is confirmed by topographic maps at the scale 1: 250 000 (see list of maps at the end of the reference list).

- Along the west coast, the detailed maps show that the elevation of the ice-free bedrock reach c. 1 km from south of Nuuk to just north of Kobberrminebugt. Elevations up to 1.5 km are reached along a major anticline parallel to the coast below the margin of the Inland Ice as seen from the regional map.

- Along the east coast elevations reach 2 km along much of the coast and in particular on the southern tip of Greenland as is confirmed by the more detailed maps. The southern tip (south of Narsarsuaq, c. 61°15'N) is thus a well-defined anticline where bedrock elevations above 2 km are reached on either side of the ice cover.

Each side of southern Greenland is thus characterized by bedrock anticlines that parallel the coasts. The thickness of the Inland Ice is limited in southern Greenland (Layberry & Bamber 2001) and the depression of the bedrock due to the load of the ice thus plays a minor role. The anticlinal pattern along the coasts of South Greenland most likely reflect the Neogene uplift of the margins of the Greenland craton such as it has been documented in central West Greenland (Bonow et al. 2006a, b; Japsen et al. 2006) and also in parts of East Greenland (e.g. Thomson et al. 1999). From this distinction it follows that the vertical section of samples from Illerfissalik (up to 1750 m, SE of Narsarsuaq) is located on the anticline along eastern Greenland.

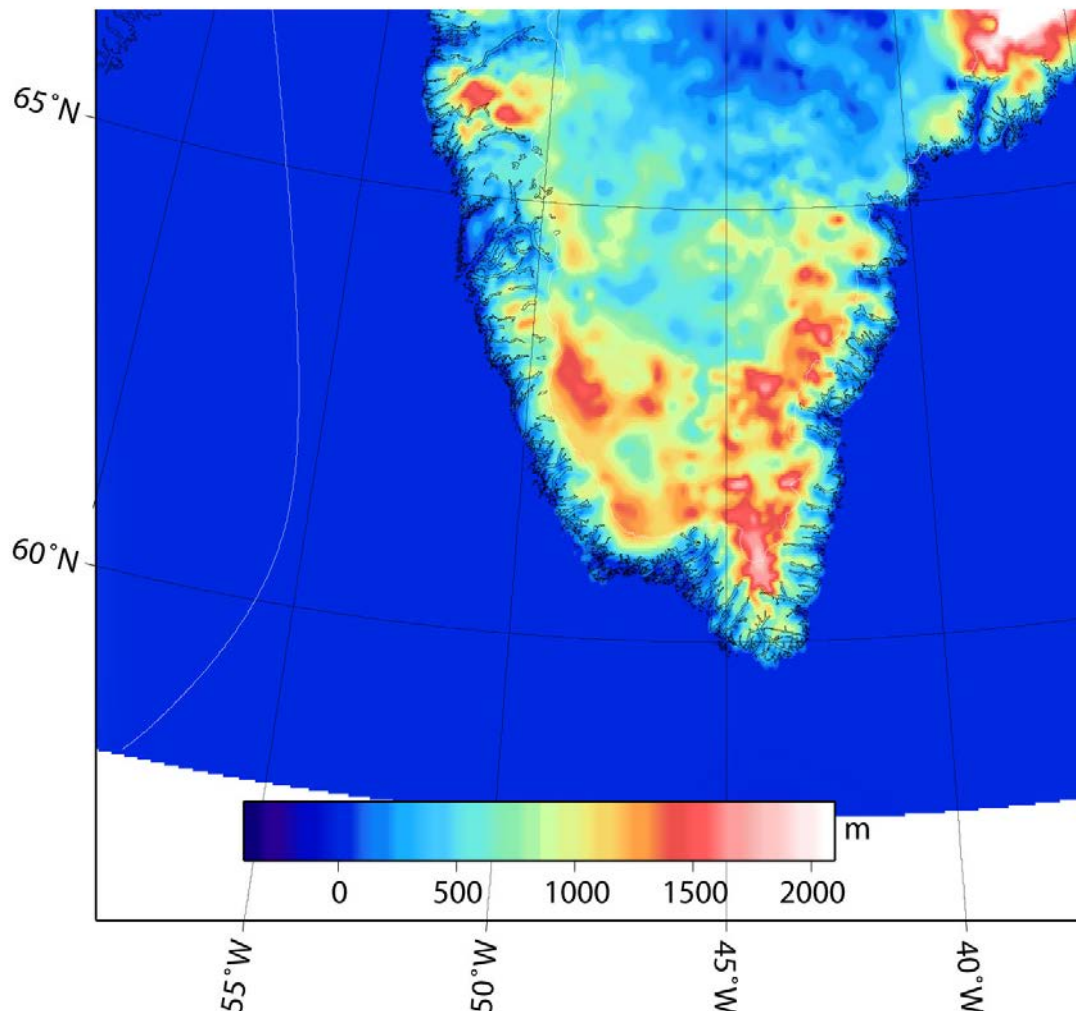


Figure 2.5-1. Elevation of the bedrock in southern Greenland above sea level. Interpolation of a 5 km grid based on airborne ice-penetrating radar measurements over the Inland Ice (Layberry & Bamber 2001).

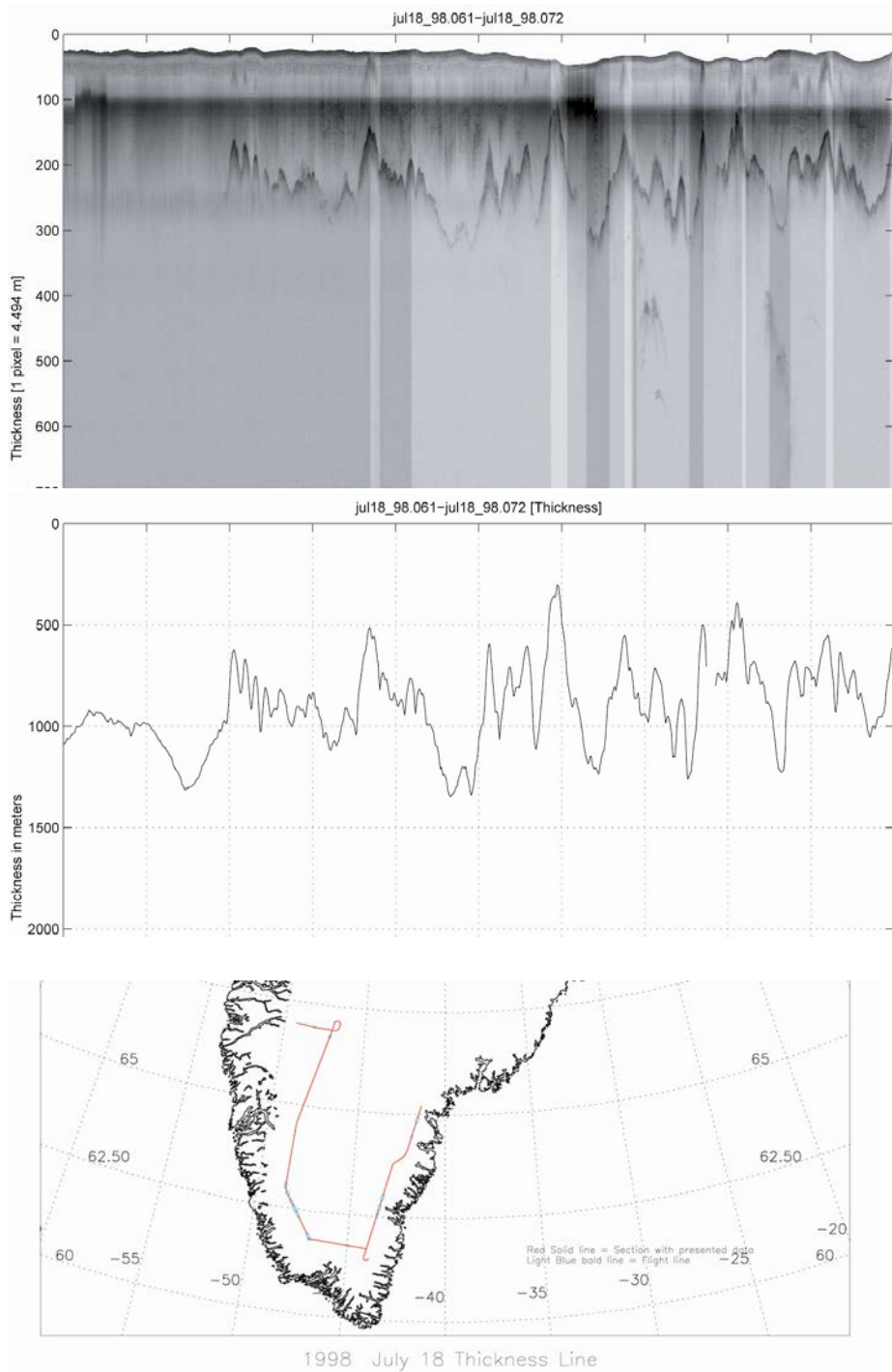


Figure 2.5-2. Airborne radar echo sounder measurement (upper panel) across South Greenland along c. 61.8°N, interpretation of the ice thickness along the line (mid panel) and map with the flight route, east-west line in red (lower panel). This line is the southernmost data used for the bedrock topography map of Layberry & Bamber (2001) (Fig. 2.5-1). The bedrock topography is remarkably rugged compared to that further north shown in Fig. 2.5-3. The ice thickness varies typically between 500 and 1000 m. Western corner: 47.05°W, 61.84°N; eastern corner: 44.38°W, 61.73°N. Data from CReSIS (Center for Remote Sensing of Ice Sheets; www.cresis.ku.edu/research/data/greenland_data.html).

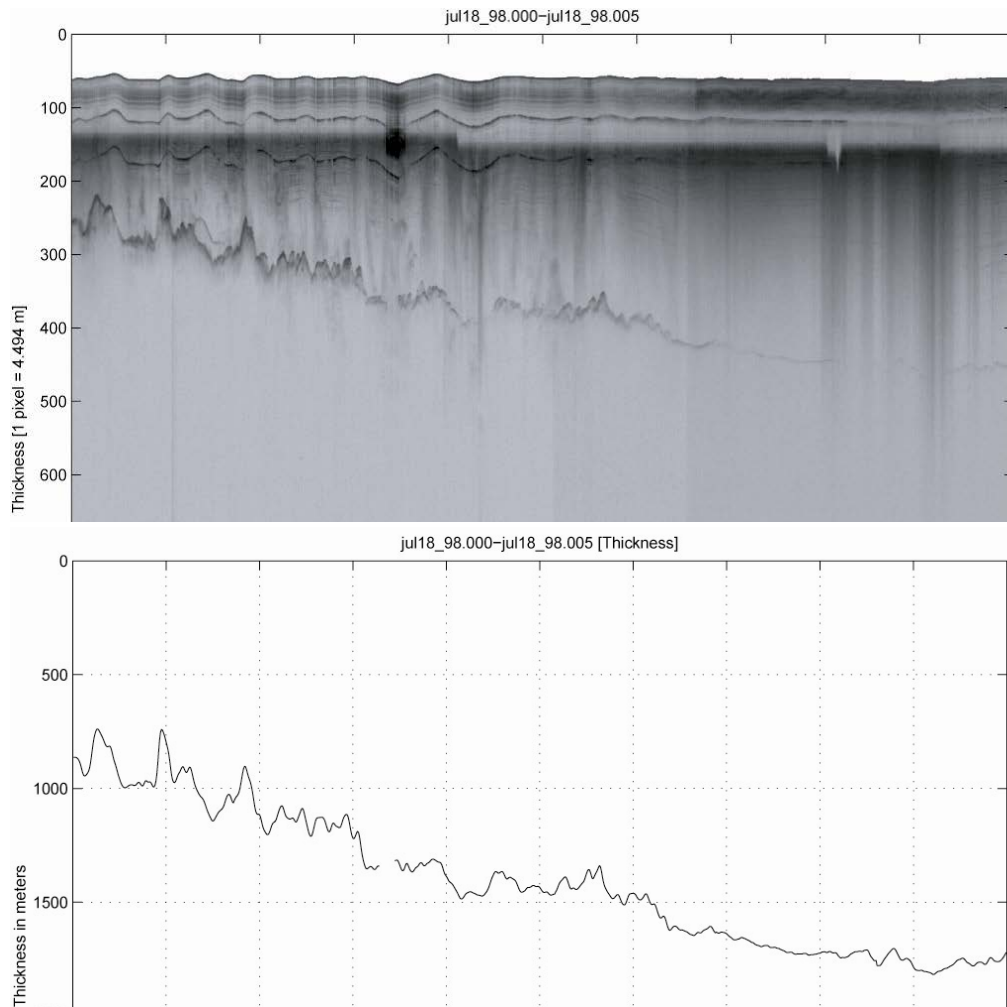


Figure 2.5-3. Airborne radar echo sounder measurement (upper panel) across western Greenland along c. 67°N, interpretation of the ice thickness along the line (lower panel). Map with the flight route, east-west line in red is shown in Fig 2.5-2. The bedrock topography is remarkably smooth compared to that shown in Fig. 2.5-2. Western corner: 49.30°W, 66.98°N; eastern corner: 46.58°W, 67.06°N. Data from CReSIS (Center for Remote Sensing of Ice Sheets).

3. Akia (Nordlandet)

Two relief types occur in the northern study area on either side of Godthåbsfjord, viz: in the west, a low relief surface at low elevation in Akia (Nordlandet), characterized by a rolling plain bearing vigorous rounded rocky hills up to 400-600 m, which is clearly different from the 100 km wide strip of dissected highlands (above 1000 m a.s.l.) in the east, between Akia and the ice sheet (Fig. 3.0-1). Several causes, separate or in combination, may be responsible for formation of this difference. Possible causes for such contrasting topography and landscape characteristics may either be that these elements have a tectonic origin (a fault or flexure scarp separating the highlands from the lowlands) or that they represent stepped planation landforms of different ages, incised into the uplifted continental margin and separated by erosional scarps.

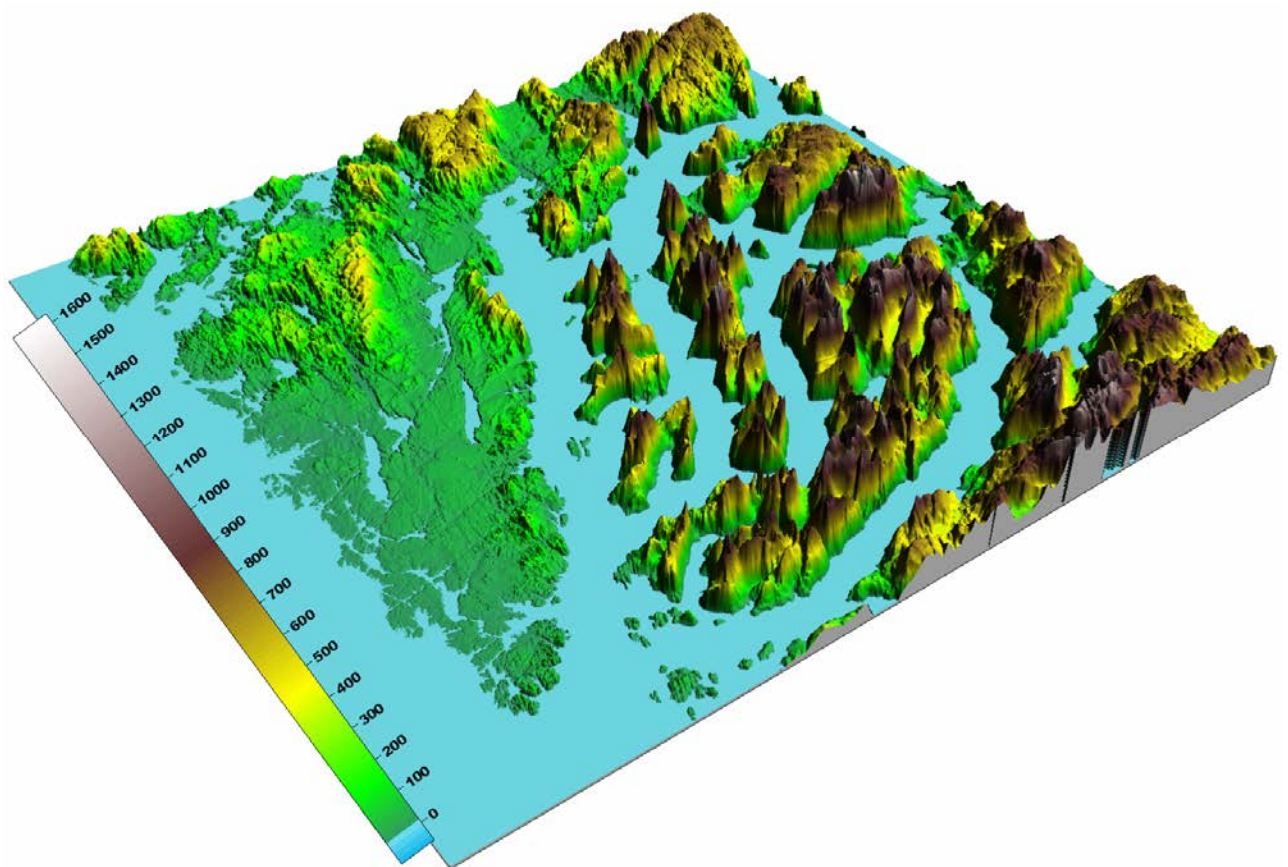


Figure 3.0-1. 3-D map based on a digital terrain model of Nuuk area. The high areas in the east are the remnants of a highly dissected plateau and this area is in the east bounded by an escarpment, in general parallel to Godthåbsfjord. The dissected plateau is distinct from the low-relief area in Akia.

3.1 Geological setting

An overview of the Archaean evolution of the Nuuk region in southern West Greenland is given by Adam A. Garde in GEUS report 2003/94 (Appel et al. 2003). According to this summary the Nuuk region is part of the Archaean North Atlantic craton in southern Greenland and eastern Labrador. The region consists of three different tectono-stratigraphic terranes. From south-east to north-west these are the Tasiusarsuaq, Akulleq and Akia terrane (Fig. 3.1-1). Together the three terranes comprise (1) the c. 3.8 Ga Isua greenstone belt which is the largest coherent segment of early Archaean supracrustal rocks known on Earth, (2) a group of c. 3.8-3.6 Ga orthogneisses, (3) middle to late Archaean supracrustal rocks holding the Ivisârtoq greenstone belt and the greenstones on Storø, (4) fragments of layered anorthosite-gabbro complexes, (5) voluminous 3.2-2.8 Ga orthogneisses, and (6) the 2.5 Ga Qôrqt granite complex.

In all three terranes, greenstone belts and smaller enclaves of supracrustal rocks in upper amphibolite and locally granulite facies are magmatically and tectonically intercalated with orthogneisses. The greenstone belts are dominated by metamorphosed tholeiitic pillow lavas and sills and lesser mica-garnet schists and may have been formed in oceanic or island arc environments. Magnesium-rich siliceous units are also locally important and have been interpreted as weathered or hydrothermally altered and then metamorphosed acid volcanic rocks. Quartzitic metasediments are rare but have been found e.g. south of Nuuk.

There are also several large fragments of metamorphosed anorthosite-gabbro complexes, which may represent the deeper plutonic counterparts of the metamorphosed pillow lavas and sills in an original layered oceanic crust that is now totally disrupted by magmatic and tectonic intercalation with grey gneisses and granitic rocks. Two large, late-kinematic, dome-shaped, tonalitic-granodioritic plutons, the Finnefeld gneiss and Taseressuaq tonalite complex, occur in the north-western part of the region, and late Archaean (c. 2.97-2.75 Ga) granodioritic and granitic intrusions are common in the central and eastern parts of the region and are thought to have formed by partial melting of the orthogneisses. The c. 2.5 Ga Qôrqt granite complex was emplaced after the terrane assembly, apparently contemporaneously with the development of local steep shear zones. It forms a dense swarm of inclined and undeformed granite sheets and related pegmatites that occupy an area of c. 20 by 50 km along the eastern part of Godthåbsfjord. Swarms of N-S, E-W and NE-SW trending basic dykes of Palaeoproterozoic age are related to the early rifting stages of two contemporaneous orogenies to the north and south of the Archaean craton. A system of conjugate, WNW- and ENE-trending faults are presumed to reflect the brittle response of the craton to the subsequent contractional phases of these events.

The Akulleq terrane in the central part of the Nuuk region preserves a higher crustal level than the two adjacent terranes. This can be seen both from the inverse distributions of granitic rocks and granulite facies areas in the three terranes. The higher crustal exposure within the Akulleq terrane - or a geographical area that largely overlaps with it - shows that it has experienced a major downthrow relative to the neighbouring areas. The downthrow may have occurred during the late Archaean terrane assembly, or in the Palaeoproterozoic. The major aeromagnetic boundary visible on Fig. 3.1-2 along the northwestern margin of

Godthåbsfjord may represent a major NW-dipping thrust fault that could account for part of the downthrow.

3.1.1 Magnetic data

A presentation and interpretation of the aeromagnetic data available in the Nuuk region is given by Thorkild M. Rasmussen and Adam A. Garde in Appel et al. (2003). Here it is shown that the data provide information on large-scale crustal segments and that the data are useful in the structural interpretation of the geology. In particular a boundary between the Akia terrane and the Akulleq terrane can be mapped from the aeromagnetic data and is found to dip towards northwest. The north-western boundary of the Akulleq terrane between 64°N and 64°30'N from the Nuuk area through Sermitsiaq, Bjørnøen and western Storø is juxtaposed against the Akia terrane along the Ivinnguit fault (Fig. 3.1-1). This terrane boundary has not been detected on the aeromagnetic maps. However, a major magnetic boundary follows north-western Godthåbsfjord inside the Akia terrane between 5 and 15 km to the north-west of the terrane boundary (Fig. 3.1-2). This magnetic boundary separates the c. 3.2 Ga granulite facies dioritic orthogneiss on Akia (Garde et al. 2000), which displays a magnetic high, from a large area of c. 3.0 Ga amphibolite facies orthogneiss and supracrustal rocks with a magnetic low in the south-eastern Akia terrane and south-western Akulleq terrane. Rasmussen and Garde interpret the aeromagnetic boundary as a major shear zone or thrust fault. In outer Godthåbsfjord it has a large vertical offset, juxtaposing amphibolite and granulite facies rocks from significantly different crustal levels. It dies out towards the head of Fiskefjord in the north-north-east, where the amphibolite and granulite facies domains are now separated by a wide, diffuse zone of partially retrograde rocks. Modelling of the aeromagnetic data carried out by Rasmussen and Garde, has identified the surface location of the boundaries between the main crustal segments and the results suggests that the boundary between the Akia and Akulleq terranes along Godthåbsfjord dips c. 45° towards NW (Fig. 3.1-3).

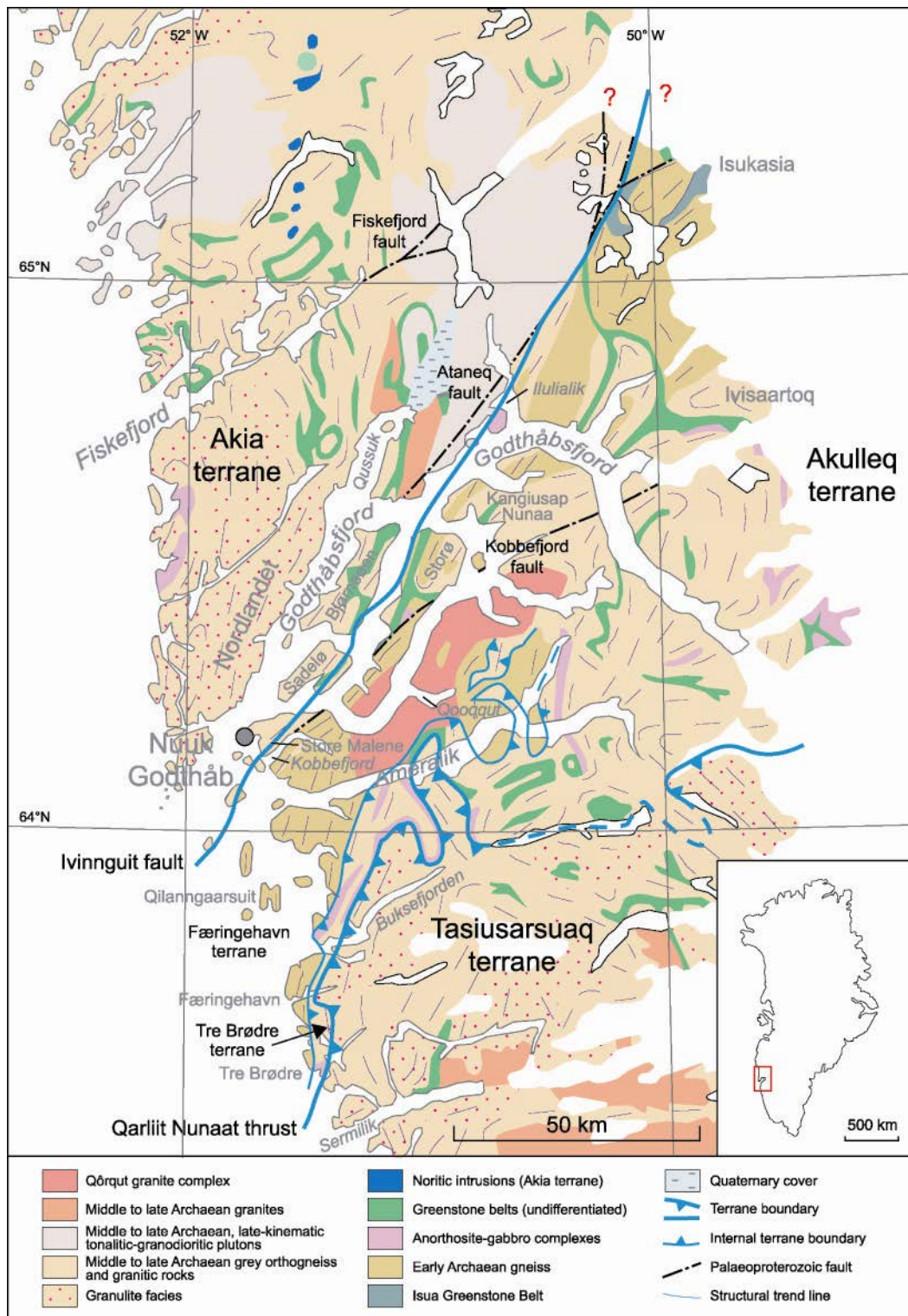


Figure 3.1-1. Simplified geological map of the Nuuk region with terrane boundaries and Palaeoproterozoic brittle faults. The extent of early Archaean orthogneiss is uncertain in some areas, especially in the eastern part of the Akulleq terrane. Map from Appel et al (2003) as modified from Escher & Pulvertaft (1995).

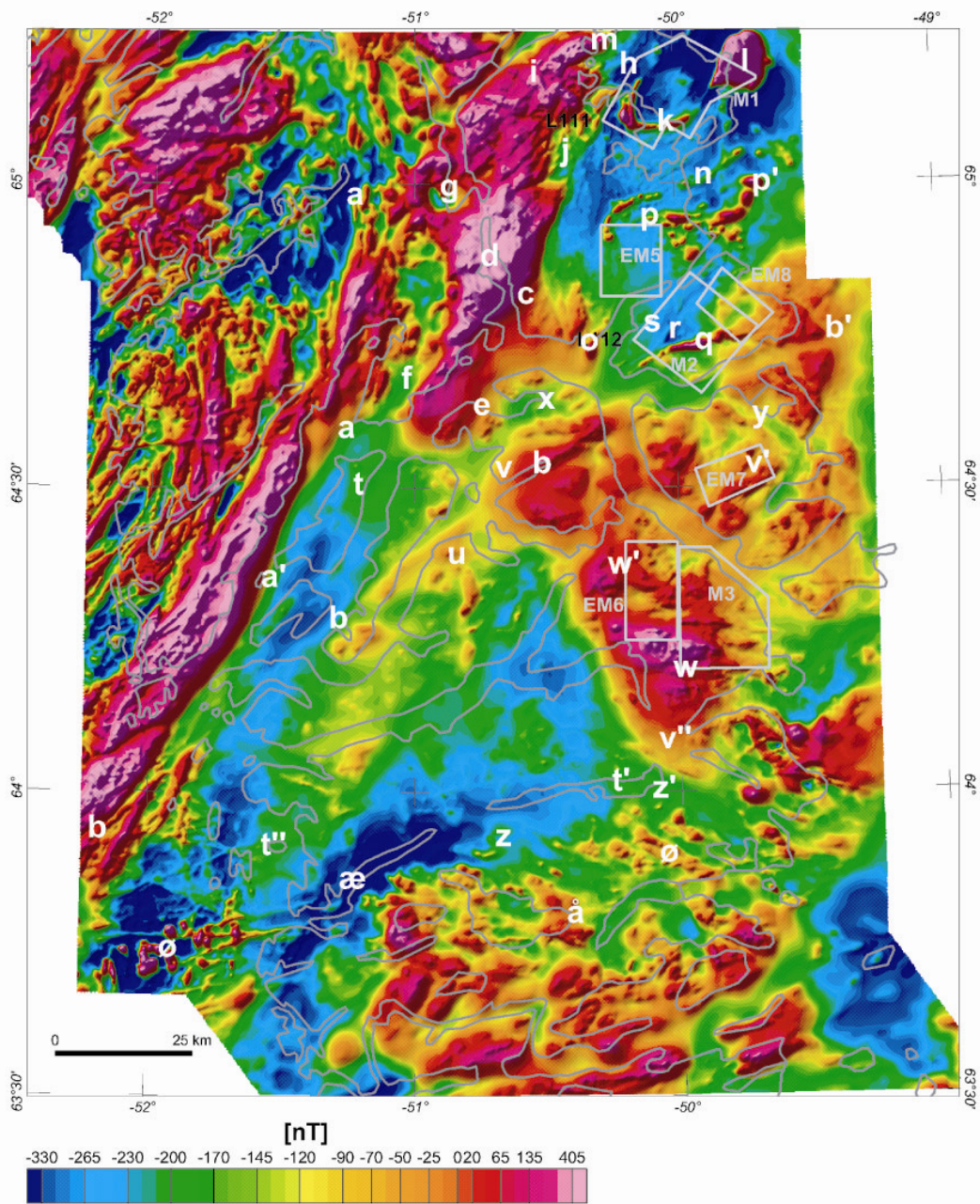


Figure 3.1-2. Magnetic total field anomalies from the regional aeromagnetic surveys. The labels in white are all referenced in Appel et al. (2003). Five areas covered by detailed surveys are indicated with grey lines. The area studied during the Fieldwork is the area west of letter 'a'. Map by Rasmussen and Garde from Appel et al. (2003).

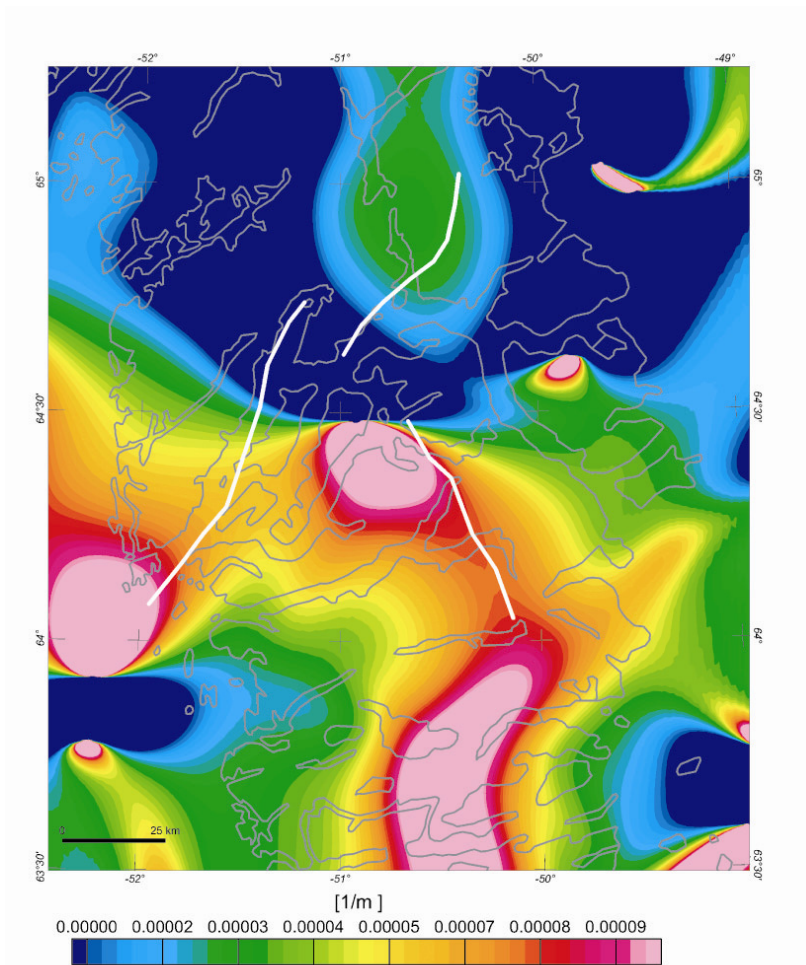


Figure 3.1-3. Interpretation of the aeromagnetic data with white lines showing the major boundaries separating crustal segments with distinct differences in magnetic properties. The colour overlay shows a calculated source parameter function. Map by Rasmussen and Garde from Appel et al. (2003).

3.2 Geomorphological analysis

The objective of the geomorphological analysis was to investigate the cause for the pronounced topography difference between Akia and the area east of Godthåbsfjord. In the study area (Fig. A-1; see Appendix) the low relief area is situated mainly below 200 m a.s.l. It is separated from the eastern highlands by a 1000 m high escarpment along which is excavated the western arm of Godthåbsfjord. It is not clear whether the surface above the escarpment is planated, but a very irregular and deeply dissected plateau can be identified above 800 m a.s.l. Possible explanations for this topography could be:

1: The Akia area is a southern equivalent of a presently exhumed sub-Cretaceous etch surface that has been identified close to the sea level on Disko, submerged in the Disko Bugt, and in the area immediately south of Disko Bugt (Bonow 2005, Bonow et al. 2006a). The preservation of such an etch surface of former regional extent on Akia should require a down-faulting of the Akia area along the escarpment, thus formed by reactivation of a fault in Godthåbsfjord prior to the formation of the presently higher planated relief. Late regional

uplift (maybe Neogene, see Bonow et al. 2006a) could have caused stripping of cover-rocks re-exposing an old relief. Thus this would imply that the landscape development in the study area is similar to the development in the Disko Bugt area, and that a reactivated fault zone of NS direction is identified along the western arm of Godthåbsfjord.

2: In another version of the hypothesis of exhumation of a Cretaceous palaeosurface, the Akia lowland represents an old piedmont surface of erosive origin, incised into an uplifted landmass and then buried (post-rift subsidence?) before being more recently re-exposed. In this case, the escarpment, at least the part identified west of Godthåbsfjord, would be a buried and then exhumed paleo-escarpment, possibly derived by retreat from local or more remote faults scarps, during or after the Cretaceous rifting. This hypothesis might be suggested by the geometry of the scarp-surface system and by the known development and preservation of similar surfaces in Cretaceous intracontinental rift zones of other regions of the world (e.g. northeast Brazil: Peulvast & Claudino Sales 2004; 2005). It is compatible with a scenario including later formation of the higher planated relief consecutive to a first phase of moderate margin uplift, still without exhumation of the buried palaeosurface (mid-Cenozoic? Japsen et al. 2006). Such development does not require a post-Cretaceous reactivation of the west Godthåbsfjord fault system.

3: The low surface represents a so called "strandflat", *i.e.* a much more recent base-level plain shaped by erosion into the uplifted landmass. The term "strandflat" was introduced by Reusch (1894) refereeing to the coastal platform in Norway characterised by low relief, uneven topography, partly submerged and with unknown or complex origin. If true the "Akia strandflat" could have developed during or after (Neogene) uplift, until the Plio–Pleistocene. In that case the "Akia strandflat" is significantly younger than the highland surfaces. Its wide development here might be linked with a particular sensitivity of the bedrock to weathering and erosion.

4. The Akia area is a composite surface, containing inherited sub-Cretaceous or younger landforms, more or less reshaped by "strandflat processes" in connexion with the evolution of the base level. This development has been suggested for parts of the strandflat in Norway (Peulvast 1988; Guilcher et al. 1994; Holtedahl 1998).

3.2.1 Methods

The study area was analysed in a digital terrain model with 50 m grid spacing, in order to depict the large-scale landforms. Analysis of the regional topographical overview map covering Godthåbsfjord area (Fig. 3.0-1) combined with analysis of the geology (lithology and structures) (Fig. 3.1-1) was decisional for selecting the field-work location and key sites for investigations. Complementary analysis was made in B/W aerial photographs at the scale 1:40.000 and 1: 150.000, interpreted in a stereoscope. On location the relationships between large-scale landforms and bedrock was observed. Photographs and sketches were used to document landform characteristics. Saprolites (weathered rocks) were collected from fracture zones for clay mineral analysis that are yet to be made.

3.2.2 Results

3.2.2.1 Large-scale landscape characteristics

The study area (Fig. 3.0-1, 3.2-1, A-1) is dominated by an elevated plateau east of Godthåbsfjord, highly dissected by deeply incised valleys local glaciers (Fig. 3.2-2). The area between the Ameralik (south) and northern Godthåbsfjord seems to be arranged in two main topographic levels: narrow and often sharp ridges or peaks between 1200 and 1600 m a.s.l., and more regular plateaus or benches between 700 and 1000 m to the north and the east of Godthåbsfjord system and also southeast of Nuuk. Well developed to the south of the inner Godthåbsfjord, the highest level forms a 50-60 km wide NS mountain region separating Akia and the coast line from the more regular plateau that bears the ice sheet to the east (Fig. 3.2-2). This upland plateau resembles much of the landscape north of Sukkertoppen Ice Cap (Bonow et al. 2006a), and a similar landform development in the study area is possible. However, no detailed survey has yet been undertaken and this issue will not specifically be treated in this report.

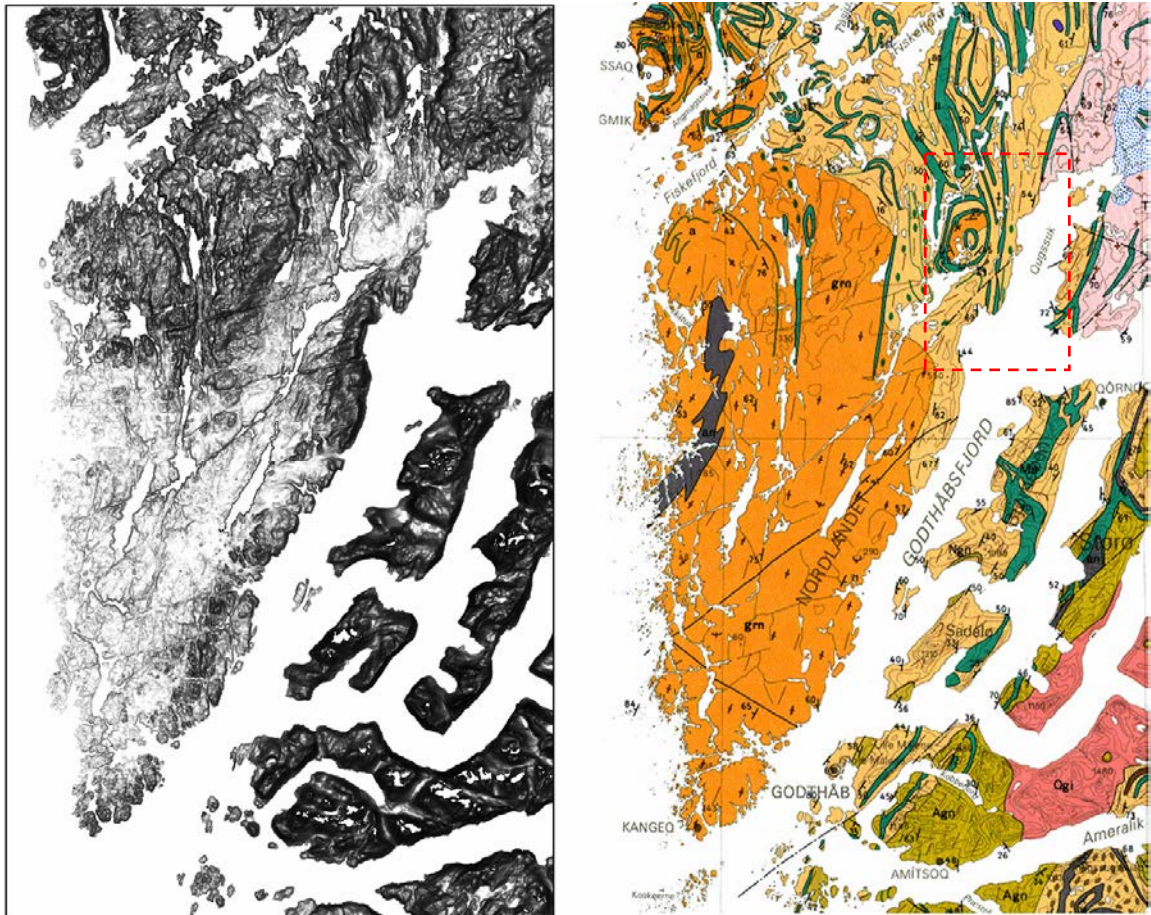


Figure 3.2-1. a) Map with vertical shading, based on a digital terrain model, of the topography in the Akia area. The vertical shading enhances the slopes (black=steep, white=flat). Hills and fracture systems are distinct. Akia with its characteristic individual hills and the strong structural control is significantly different from the areas east of Godthåbsfjord. b) General geology in the study area. Red rectangle marks the field-work area in Fig A-1.



Figure 3.2-2. A highly dissected surface is present in the Nuuk region. It is mainly visible close to the ice sheet as a horizontal line. In the foreground small remnants forming flat summits can be seen. Photo from Kingittoq towards the east (Fig. A-1).

To the west the plateau is bordered by a complex escarpment, more or less parallel to the outer, NNE–SSW running part of Godthåbsfjord (Fig 3.2-1). The eastern wall of the fjord (Qugssuk-western Godthåbsfjord) is the steepest and most visible part of this escarpment, but it should be underlined that a narrow and discontinuous ridge of rocky hills, up to 550 m a.s.l., is also present on the western flank of the fjord, forming a secondary and discontinuous escarpment parallel to the main one, separating the fjord from the lowlands of Akia. A narrow, discontinuous and irregular ice-scoured bench can be locally identified in the main escarpment, between 600 and 700 m a.s.l., from Ivnarssuaq, east of the Qugssuk, to the southwest tip of Bjørneøen (Fig 3.2-3, 3.2-1 for location).



Figure 3.2-3. An ice-scoured valley bench appears on both sides of Godthåbsfjord, best developed on the western side. Photo towards the south along Godthåbsfjord (Fig. A-1).

Roughly inclined westward, this bench does not show any clear connection with the other flat levels of the area, and the asymmetry of the fjord walls does not allow us to interpret them as remnants of possible former valley floors of pre-glacial origin, such as proposed along several Norwegian fjords (Peulvast 1985).

The landscape west of the fjord, Akia, is dominated by a low relief plain with individual hills and narrow over-deepened corridors often occupied by lakes. Its southern part has a relative relief of maximum c. 200 m, with wide plains below 60 m in altitude, while in the northern parts hill complexes with rounded summits up to 600 m high also occurs, between wide flat-floored valleys of NNE–SSW direction merging into the plain (Fig. 3.2-1). The extensive low-relief surface has mainly been developed within metamorphic rocks of granulite facies and the hill-complexes in the northern part, on the contrary, are mainly within areas where the bedrock is in amphibolite facies (Fig. 3.1-1). To the north of the Quassuup lake (Fig. 3.2-1, for location see A-1), these hills, low ridges and corridors underline the straight or curved patterns of the gneisses and supracrustal rocks. The area was interpreted as parts of a wide and shallow pre-glacial valley, with a floor characterised by complex patterns of differential weathering and erosion. The geometric patterns of valleys and lakes show strong structural control by fault or fracture zones, and in the southern parts the intersections of valleys are often perpendicular. The widest valleys run parallel to Godthåbsfjord. The western parts are dominated by thousands of small islands and skerries, forming a coastal archipelago over a 5 to 10 km wide fringe (Fig. 3.2-1).

3.3 Structural analysis

3.3.1 Regional studies

Landsat TM, aerial photographs, topographic maps and pre-existing geology maps have all been used to construct structural lineament maps at a regional scale. Lineaments were picked from Landsat images at both 1:500,000 and 1:100,000 scales in ArcGIS (Fig. 3.3-1). Attribute data (i.e. trend; length; offset; comments) were also recorded and stored in the GIS database. After interpretation, lineaments were then compared to a DTM (Digital Terrain Model) and refined using GIS analysis. Particular care was taken to distinguish between basement fabrics and other structural lineaments (e.g. faults, dykes, etc) in the lineament database. This was done mainly by studying pre-existing geological maps during lineament analysis, and where possible additionally checked during fieldwork. The main lineament trends identified at 1:500,000 scale are:

- N–S
- NE–SW
- ENE–WSW
- ESE–WNW

The most pronounced trend is NE–SW which is parallel to Godthåbsfjord. These trends are similar to those identified by Japsen et al. (2002) in the Nordre Strømfjord region.

A similar set of lineaments can also be identified at 1:100,000 scale, though here the dominant trend now appears to be ENE–WSW (Fig. 3.3-1b). However, the rose diagrams shown in Figure 3.1 are simply based on frequency, and when plotted against lineament length we see that NE–SW lineaments are again the dominant set (i.e. NE–SW lineaments are fewer in number but much longer than ENE–WSW lineaments).

A distinct change in lineament pattern and density can be seen either side of Godthåbsfjord (Fig. 3.3-1). To the east of Godthåbsfjord, in amphibolite facies rocks, the main lineament trends are NE–SW and WNW–ESE, while to the west, in the granulite facies rocks of Akia, lineament densities are far higher, with dominant trends being N–S, NE–SW, and ENE–WSW. This is consistent with the marked topographic and geomorphologic changes described in previous sections.

Aerial photographs have also been used to map out structures at 1:40,000 scale in order to link regional and outcrop scale studies. A detailed study of cross-cutting relationships and offsets is currently being carried out through aerial photograph analysis in GIS. Initial results suggest that NE–SW and ENE–WSW trending lineaments are the youngest sets as they appear to truncate all other systems. Both NE–SW and ENE–WSW structures appear to consistently offset basement fabrics and other lineament sets in a dextral sense of slip. The age relationship between these two sets however, is a little less clear. In some cases NE–SW lineaments appear to curve round to become ENE–WSW trending, however, in other cases these NE–SW lineaments cross-cut ENE–WSW structures.

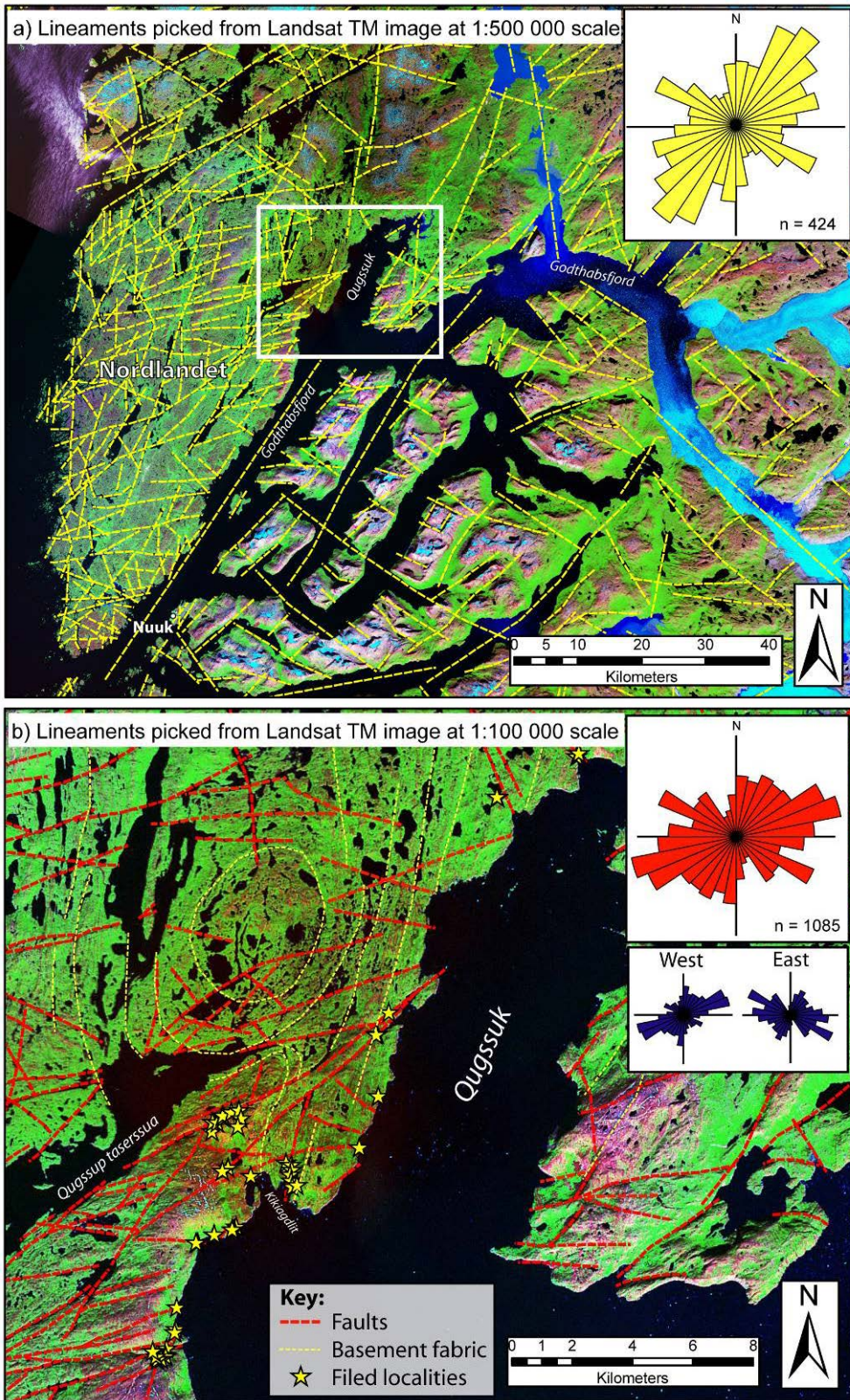


Figure 3.3-1. (a) Landsat TM with structural lineaments picked at 1:500,000 scale. Inset: rose diagram showing main lineament trends. (b) Zoom in of main field mapping area showing location of main field localities. Also shown are structural lineaments picked at 1:100,000 scale. Inset: rose diagrams showing main lineament trends at 1:100,000, bulk data (red) and east and west of Godthåbsfjord (blue).

3.3.2 Outcrop studies

Field investigations were carried out in the granulite facies basement rocks of NE Akia (Figs. 3.3-1, A-1) in key areas of interest identified during aerial photograph analysis prior to departure. Aerial photographs were also used during field data acquisition, allowing ground-truthing and modifications of regional structures identified in pre-fieldwork analysis. During Fieldwork, fault and fracture systems were mapped and the following structural data were collected for statistical/structural analysis:

- Fault attributes including: orientation; kinematics; fault surface characteristics; mineralization;
- Relative ages relationships;
- Fault rock samples (see **section 3.4.3**)

All field data were geospatially located (to 5m resolution) using GPS (Geographical Positioning Systems) waypoint collection, and were subsequently stored in a computer database with links to GIS (Geographic Information System) based maps.

Fresh fault exposures were relatively hard to find in the area as most coastal gullies were filled with deep raised beach deposits, while inland fault gullies have weathered out to form vegetated and boggy areas. This makes remote sensing of fault patterns relatively easy, but is not conducive to detailed kinematic studies.

The main fault trends recorded at outcrop were N–S, NE–SW, ENE–WSW and SE–NW (Fig. 3.3-2). The following paragraphs describe some of the field observations of fault characteristics for each of these fault sets (see also Table 3.3-1 and Figs. 3.2-2 – 3.2-5).

N–S:

A prominent N–S trending lineament may be easily distinguished from aerial photographs of the area (Fig. 3.3-3). This structure trends parallel to basement fabrics depicted by pre-existing geological maps. A number of very good coastal outcrop exposures were found for this lineament. Following the V-ing into valleys rule, it is clear that this lineament dips moderately (~60°) to the east, which is confirmed by outcrop studies. Kinematic indicators (i.e. slickenlines) suggest a dextral-I oblique movement sense (i.e. east side down to the SE). This fault comprises a number of different fault rocks. A 5-10 m wide mylonitic (ductile) deformation/ shear zone comprising mylonite and phyllonite fault rocks. While localised within the centre of this zone are a few discreet fine cataclasite deformation bands (e.g. Locality RW-1.06; Fig. 3.3-3). The cataclasite has a distinct green colour which may be due to the presence of the mineral epidote, and in places the cataclasite also has a weak fabric/ foliation (sample 468806, Locality RW-1.17; Fig. 3.3-3). This overprinting of brittle (cataclasite) on ductile (mylonite) suggests a re-working of a shear zone at a shallower depth (e.g. Holdsworth et al. 1997).

NE–SW:

The most continuous lineaments in the area trend NE–SW, and are characterised by wide deep gullies (e.g. Locality RW-1.11; Fig. 3.3-4). Although these structures are very easily distinguished from both aerial photographs and on the ground, coastal exposures of these structures yielded very little information as the fault zones deeply eroded and covered by

thick Quaternary marine sediments. Therefore detailed analysis was limited to a few small exposures inland (mainly in streams and craggy outcrops at the edge of gullies; Fig. 3.3-4). Most NE–SW faults recorded dip to the SE, and where observed all shear sense indicators show dextral strike-slip movements (Fig. 3.3-4). Furthermore, the fault exposed at Locality RW-1.11 appears to dextrally offset an N–S trending gully by >200m. Fault rocks observed suggest both semi-brittle (phyllonite) and brittle (cataclasite) deformation, and again epidote appears to be a common mineral deposit.

ENE–WSW

A large number of the faults encountered in the field trend ENE–WSW. These dip both NW and SE, and again shear sense indicators (slickenlines and Reidel shears) all suggest dextral strike-slip movement (Fig. 3.3-5). An epidote-rich cataclasite fault rock was observed at one locality (sample 468812, Locality RW-1.17).

SE–NW:

A system of SE–NW trending, NE–dipping joints and pegmatite filled fractures were also encountered at a number of localities. No shear sense indicators were recorded on these structures, though may represent opening mode-I fractures (Hancock 1985).

3.3.3 Summary of structural observations

Heavily weathered fault cores and poor coastal exposures all suggest that current exposures have been at the surface for relatively long periods of time. The age of the faults observed is difficult to determine from the current data available (geomorphologic studies, dating of fault rocks and offshore studies may be able to better constrain this), however some relative ages have been identified. Cross-cutting relationships from aerial photo analysis suggest that the oldest structure is the N–S trending faults, though as these reactivate Precambrian basement fabrics, this observation is to be expected. However, the age of brittle (cataclastic) re-working is unclear. The similar sense of movement (dextral) on NE–SW and ENE–WSW faults, along with their mutual dominance in cross-cutting relationships suggests that these faults are the most recent structures, and develop contemporaneously. The relative age of the NW-SE trending joints have not as yet been constrained, though assuming an opening mode-I origin, this would suggest a NE–SW extension direction which may be consistent with dextral movements on NE–SW and ENE–WSW faults.

Although fault patterns identified from remote sensing appear consistent with those identified further north in the Nordre Strømfjord region (Japsen et al. 2002; Wilson et al. in press) Fault kinematics observed in this study are NOT consistent with the sinistral wrench movements as observed further north, which may be linked to Eocene movements on the Ungava Fault Zone offshore (Wilson et al. in press). Sørensen (2006) describe a phase of Late Cretaceous strike-slip faulting (driven by compression) and the development of NE–SW trending faults on the Fylla Platform (Fig. 3.5-1 - Sørensen 2006). It is possible that the dextral strike-slip faults observed during this study developed at a similar time, however, further investigation is required to verify this.

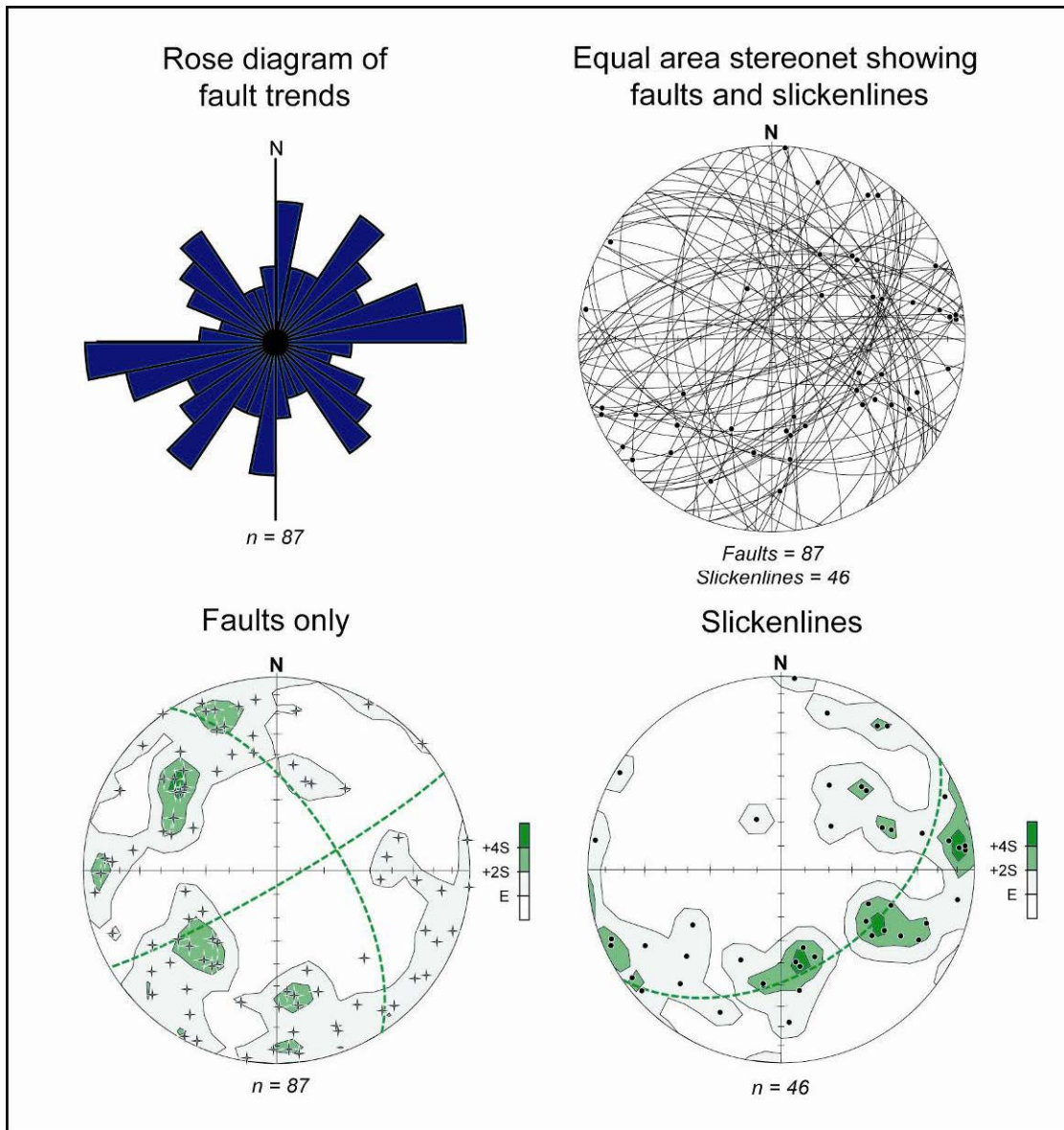


Figure 3.3-2. Fault and slickenlines data recorded during field mapping in Akia.

Table 3.3-1. Summary of main fault trends and their attributes.

Trend	Dip direction	Kinematics	Fault rocks	Comments
N-S	E	Dextral- oblique	Mylonite, ultracataclasite	Re-worked basement shear zone
NE-SW	SE	Dextral strike-slip	Cataclasite	
ENE-WSW	NNW and SSE	Dextral strike-slip	Cataclasite	
SE-NW	NE	?	Pegmatite veining	

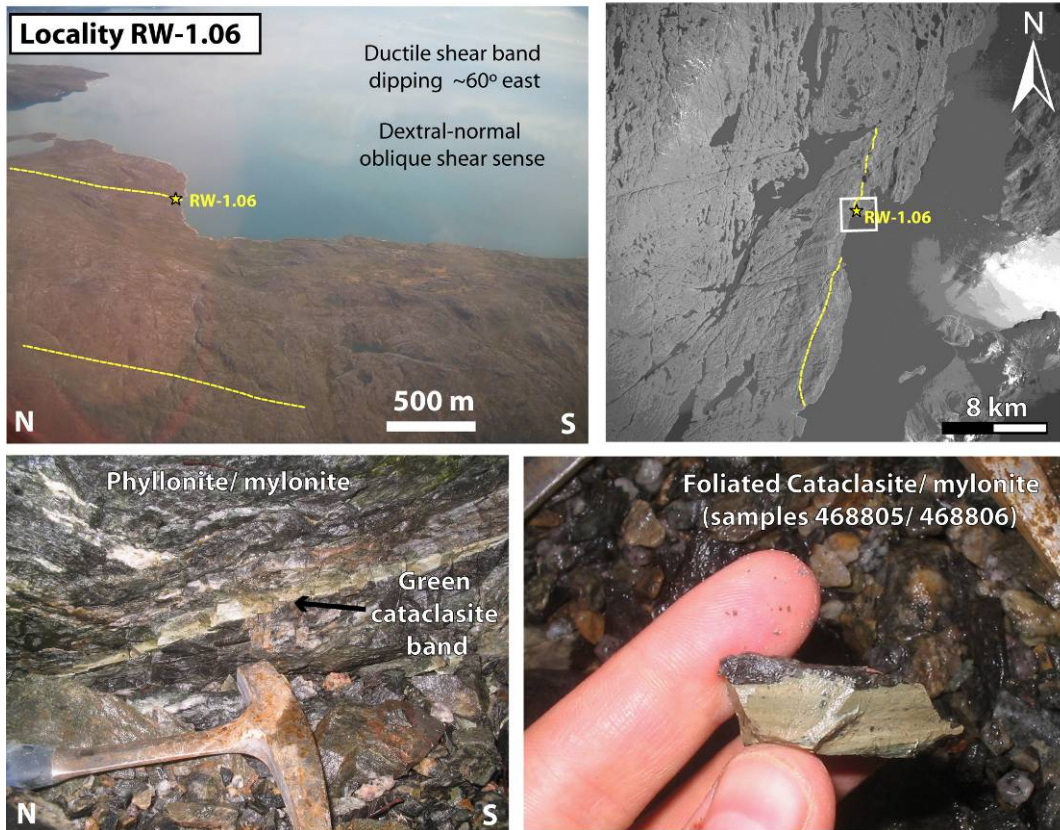


Figure 3.3-3. N-S trending (basement parallel) lineaments (Locality RW_1.06).

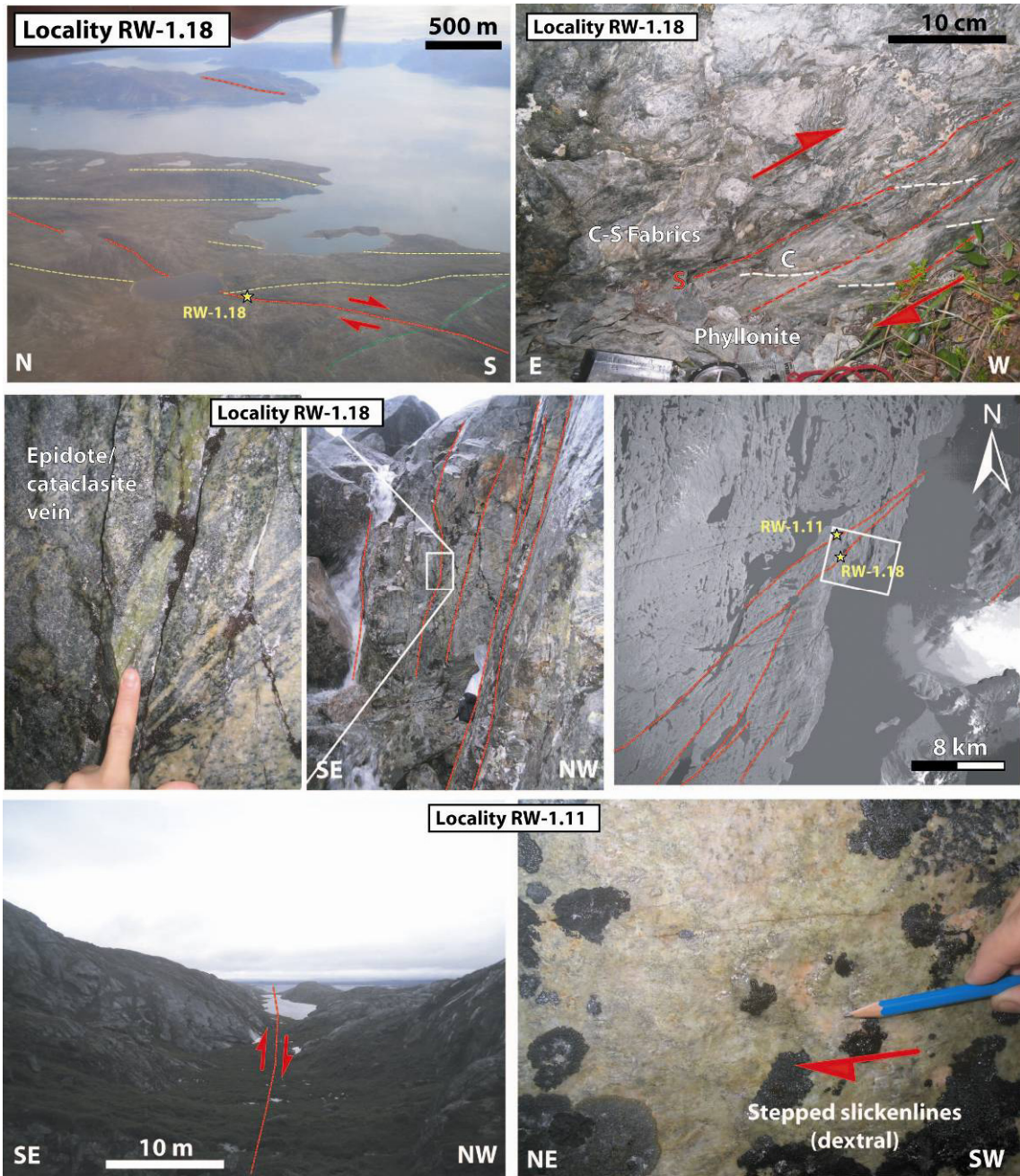


Figure 3.3-4. NE-SW lineaments at localities RW_1.11 and RW_1.18.

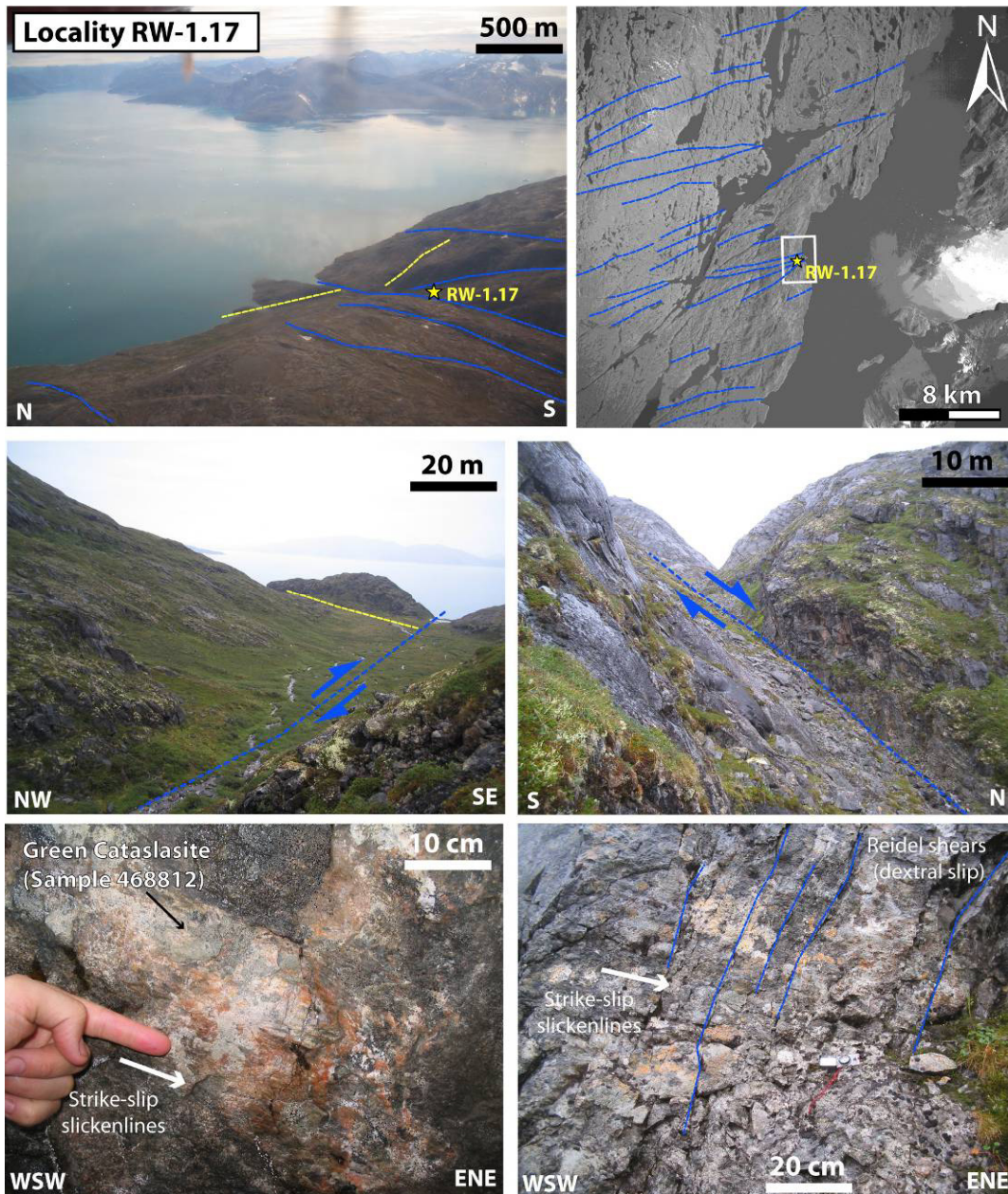


Figure 3.3-5. ENE–WSW lineaments. (Locality RW_1.17)

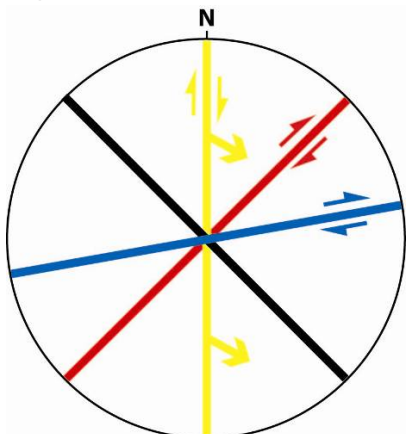


Figure 3.3-6. Summary of main fault trends and apparent movements.

3.4 Rock sampling

3.4.1 Sampling of rocks for apatite fission-track analysis

Sampling of rocks for fission-track analysis was not a primary target during the Fieldwork in Godthåbsfjord mainly due to the logistic conditions that prevented sampling across a major region and in particular along vertical transect of any considerable height. A few samples were gathered along Godthåbsfjord within the limited area of investigation and may eventually be supplemented with rocks that already exist at GEUS (see Appendix).

3.4.2 Sampling of rocks from faults

A number of oriented fault rock samples were also collected from various localities or thin section analysis. These include:

- Mylonite and cataclasite samples from N–S fault (sample 468806, Locality RW-1.17; Fig. 3.3-3).
- Epidote-rich cataclasite sample from ENE–WSW fault (sample 468812, Locality RW-1.17 Fig. 3.3-5).
- Epidote-cataclasite vein and a phyllonite rock sample from a NE–SW fault (sample 468813, Locality RW-1.18; Fig. 3.3-4).

3.5 Discussion

A number of past studies have suggested the presence of a large fault or shear zone in Godthåbsfjord as it marks a aeromagnetic boundary and juxtaposes basement rocks from markedly different depths (i.e. granulite and amphibolite facies) (e.g. Rasmussen and Garde in Appel et al. 2003; Fig. 3.1-3). A key question of this study was could the present topography across Godthåbsfjord be explained by a Mesozoic normal fault related to rifting and exhumation of this structure from below Mesozoic-Cenozoic cover rocks.

The Cretaceous–Paleocene rift system, shown in Fig 2.2-3, has its easternmost graben only 50 km west of Akia. Thus, Akia might represent the exhumed base of an additional graben and the high-lying terrain east of Godthåbsfjord the hanging wall of this rift system (cf. model 1 outlined in section 3.2).

The only brittle faulting observed onshore in this study show strike-slip movements and therefore do not support the hypothesis that the present day topography reflects a faulted half graben in Godthåbsfjord. The only structures that may suggest any such fault within the fjord are the N–S trending ductile shear zones (Fig. 3.3-5), which do indicate an ESE–movement direction (dextral oblique), and would be consistent with the predicted fault movements of a major fault/shear zone in the fjord. These faults likely reflect the older basement deformation events (Appel et al. 2003) rather than recent (i.e. Mesozoic) movements. However, it should be noted that as the main mapping area covered by this study is in the northernmost part of the fjord, this is likely to be in the vicinity of the fault tip, and thus

little onshore expression would be expected. Further studies to the south (along SE Akia), where the throw on any fault in the fjord would be at its greatest, were planned, however these had to be called off due to bad weather conditions. It is also noteworthy that the relative relief of southern Akia is less than in the investigated area and also more structurally controlled. Southern Akia is thus more likely to represent an old, re-exhumed surface.

An alternate explanation for this major contrast in topography across Godthåbsfjord could simply be that the fjord marks a major lithological boundary between basement terranes of differing rock strength and chemical stability and thus that terrain difference is due to the development of an escarpment without fault activity. This explanation corresponds to models 2 and 3 outlined in section 3.2 where the difference between these models is when the escarpment developed; in model 2 the main development was during the Mesozoic followed burial and subsequent (recent) exhumation from below the sedimentary cover. Model 3 predicts that the removal of basement rocks occurred during the Plio–Pleistocene whereas model 4 represents a combination of model Mesozoic and Neogene processes. The results from the Fieldwork have not made it possible to verify any of these models.

Granulites are metamorphic rocks that have experienced high temperatures of metamorphism (Fig. 3.5-2). As granulites form at high metamorphic grades (cf. Yardley 1996) the mineral phases that develop are likely to be more compositionally unstable at surface temperatures and pressures than a lower grade rock such as amphibolite, and are therefore more likely to breakdown due to weathering and alteration. This may account for some topographic difference across the fjord, but it is unlikely that this could account for the full ~800 m contrast. This suggestion however, is in contrast to observations from the exposed basement north of Sukkertoppen, where Bonow et al. (2006a) found that erosion is less in areas of gneiss in granulite facies, than in areas of gneiss in amphibolite facies.

In summary it was not possible during the fieldwork to establish conclusive evidence to explain not only the topographic contrast across Godthåbsfjord but also the pronounced width of the lowlands of Akia compared to other strandflat-like features along the coast of West Greenland (e.g. at Nordre Isortoq). The faults studied in the north-western end of Godthåbsfjord did not appear to be related to Mesozoic normal faulting and remnants of saprolites of possible Mesozoic age were not found (but laboratory studies have not yet been carried out). However, in the outer parts of the fjord, where evidence of normal faulting is more likely to be present, planned work had to be given up due to weather conditions. Further studies, in particular analysis of rocks sampled during the fieldwork and mapping of large-scale landforms in the area between Sukkertoppen and Nuuk may lead to further clarification.

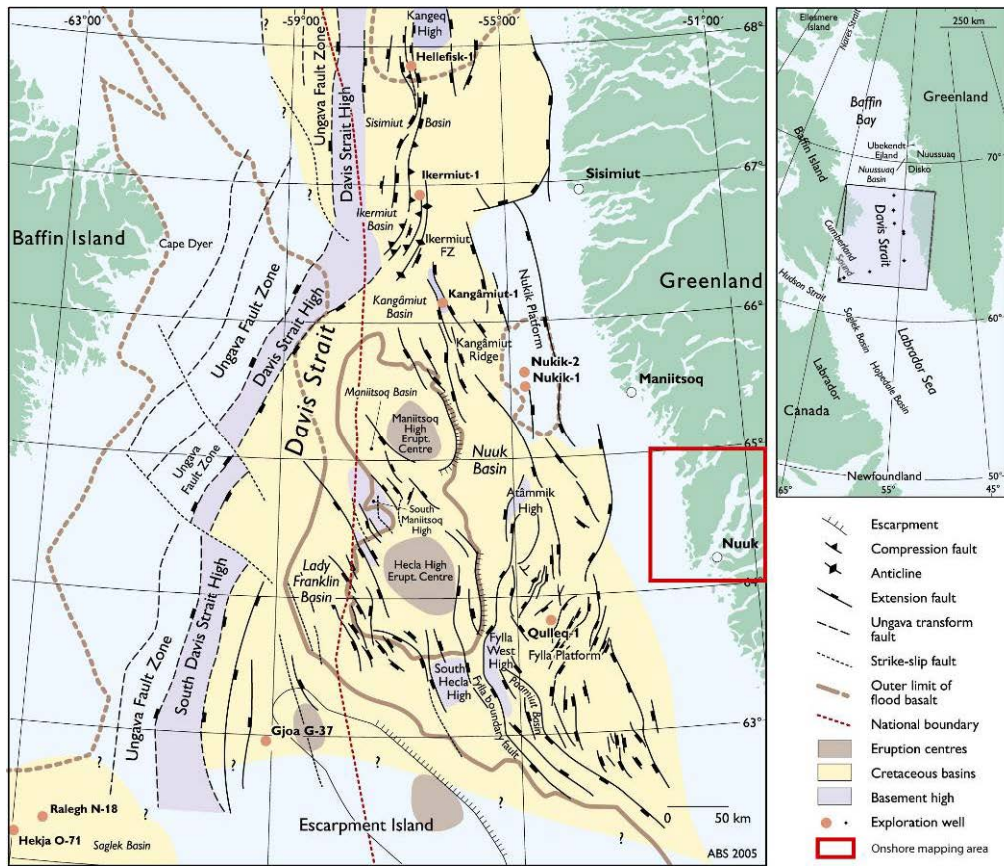


Figure 3.5-1. Cretaceous basins, regional structural elements and extent of flood basalts offshore southern West Greenland with indication of the onshore mapping area. Modified from Sørensen (2006).

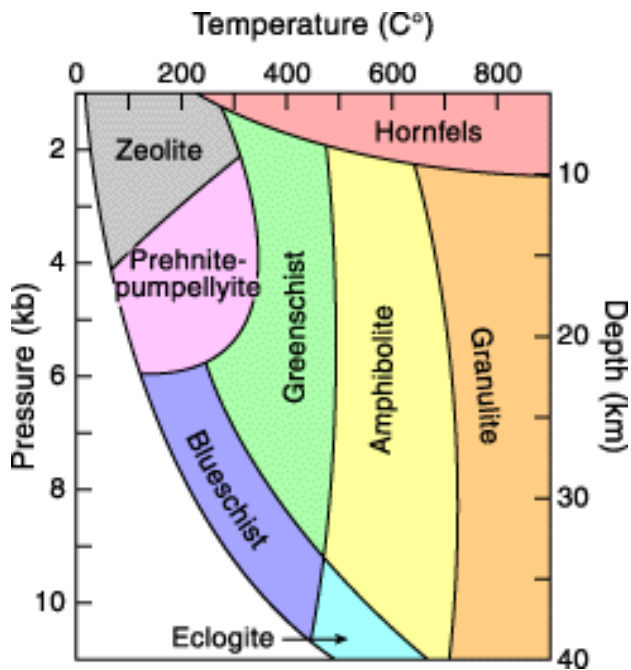


Figure 3.5-2. A temperature vs. pressure/ depth graph showing metamorphic facies derived from mafic rocks (after Yardley 1996).

4. South Greenland

This region marks a distinct left-lateral step on the margin of SW Greenland (e.g. Fig. 2.0-2). This step is coincident with the transition from Archaean basement rocks to the north and rocks of the Ketilidian orogenic belt to the south (Fig. 2.0-2). In the west there is a marked topographic change in the region of Kobberrminebugt (Fig. 4.0-1) This is coincident with the Border zone of the Ketilidian Orogen, which may lead some to suggest that the topographic change may be the result of differential erosion between the granites of the Ketilidian (Julianehåb batholith) and the stronger Archaean basement to the north (Fig. 4.1-1). However this topographic expression is not apparent on the east coast where the lithological contrast is the same. Therefore an alternate explanation is required.

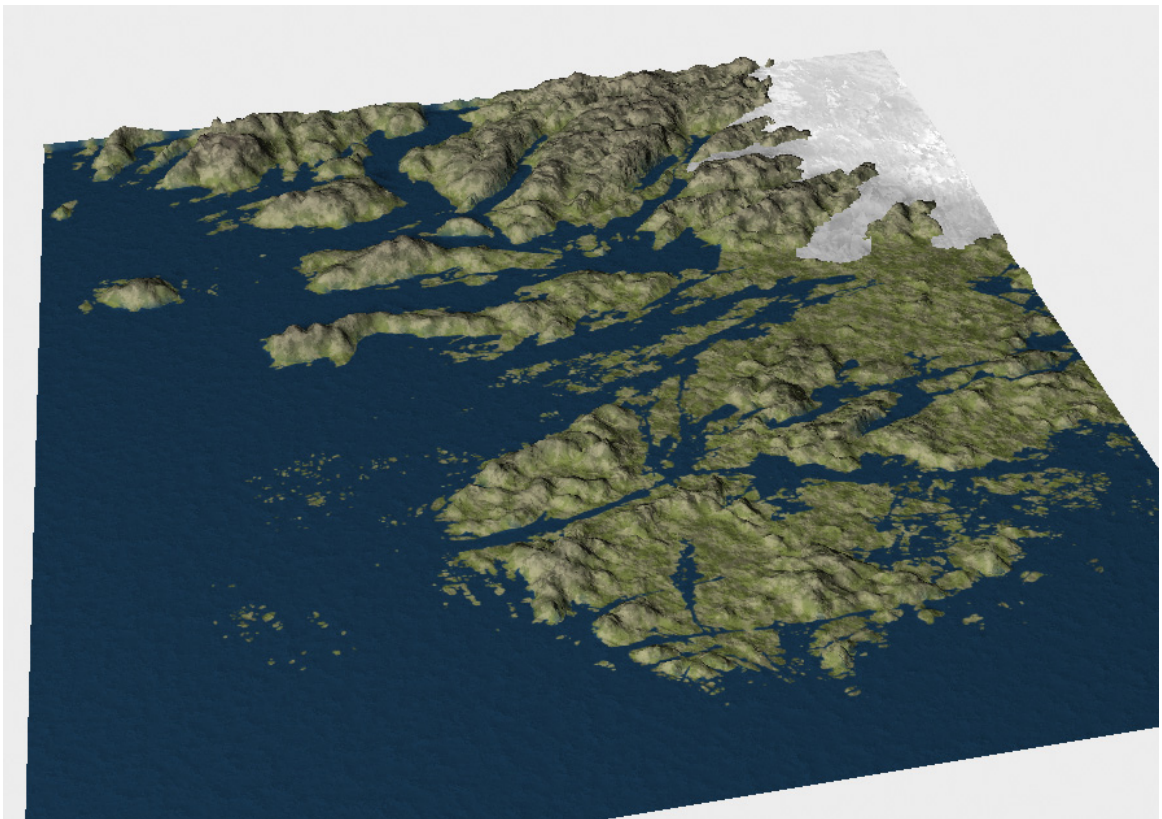


Figure 4.0-1. 3D model of the Kobberrminebugt area. Left margin indicates the north direction. Location in fig A-2.

The Ketilidian orogen is viewed as the result of oblique convergence between the Archaean craton of southern Greenland and a supposed oceanic plate located south of the present orogen, which was subducted towards the north (Garde et al. 2002b – see next section). Chadwick & Garde (1996) suggested the Ketilidian orogen be divided into four distinct zones (Fig. 4.1-1): a ‘Border Zone’ adjacent to the Archaean craton, the ‘Julianehåb batholith’ (formerly the Julianehåb granite) in the central part of the orogen, and the ‘Psammite Zone’ and ‘Pelite Zone’ to the south-east, which largely consist of deformed and metamorphosed erosion products derived from the evolving batholith.

The northern boundary between the Archaean and Ketilidian basement terranes is marked by a complex 'Border Zone' and it is this zone in Kobberminebugt area (and its transition to the Julianehåb batholith to the south) that the main mapping in this study was concentrated.

4.1 An overview of the crustal architecture of the Ketilidian orogen

By Adam A. Garde, GEUS

The Ketilidian orogen straddles the southern tip of Greenland (Fig. 1; Allaart 1972; Garde et al. 2002a). It is the southernmost of three E–W-trending Palaeoproterozoic orogens in western Greenland that formed at 2.1–1.7 Ga ago in response to long-lived, N–S-orientated plate-tectonic convergence that is also recorded in eastern Canada. In contrast to the collisional Nagssugtoqidian orogen in central West Greenland, the Ketilidian orogen in the south mainly consists of juvenile igneous rocks. These were emplaced at the southern margin of the North Atlantic craton, presumably during oblique subduction of an oceanic plate from the south (which is nowhere exposed).

The overall crustal architecture of the Ketilidian orogen is relatively simple, with four main components (Chadwick & Garde 1996):

(a) The Border Zone at the southern margin of the North Atlantic craton is the oldest part of the orogen (pre- c. 1850 Ma) and comprises greenschist to low amphibolite facies epiclastic metasedimentary rocks which were deposited unconformably on the Archaean basement, tectonically overlain by primitive metabasaltic pillow lavas, which most likely represent obducted oceanic crust. The Border Zone is about 50 km wide in the western part of the orogen. The structure is flat-lying to moderately south-dipping, reflecting the original bedding accentuated by early craton-directed thrusting. Subsequent upright, up to crustal-scale folds are related to sinistral transpression during the subsequent convergent stage of the orogeny. The folding becomes more intense and of shorter wavelength towards south-east and thus reflects progressive reworking and softening of the Archaean basement towards the south and south-east.

(b) The Julianehåb batholith is an 1850–1795 Ma juvenile continental arc, not unlike the Andean batholith. Covering some 30 000 km² it forms the bulk of the orogen; a large part is covered by the Inland Ice. The batholith consists of numerous individual, elongate plutons with steep fabrics, which were emplaced during long-lived sinistral transpression, and the batholith contains several large subvertical, syn-magmatic shear zones. The most prominent one is the 1815 Ma Sârdloq shear zone in the south/central part of the orogen (Fig. 1). Other important shear zones of similar or slightly younger age are located along the margins of the batholith, namely at Kobberminebugt on its north-western, continental side (McCaffrey et al. 1998; 2004), and e.g. at the head of Danell Fjord on its south-eastern, oceanic side.

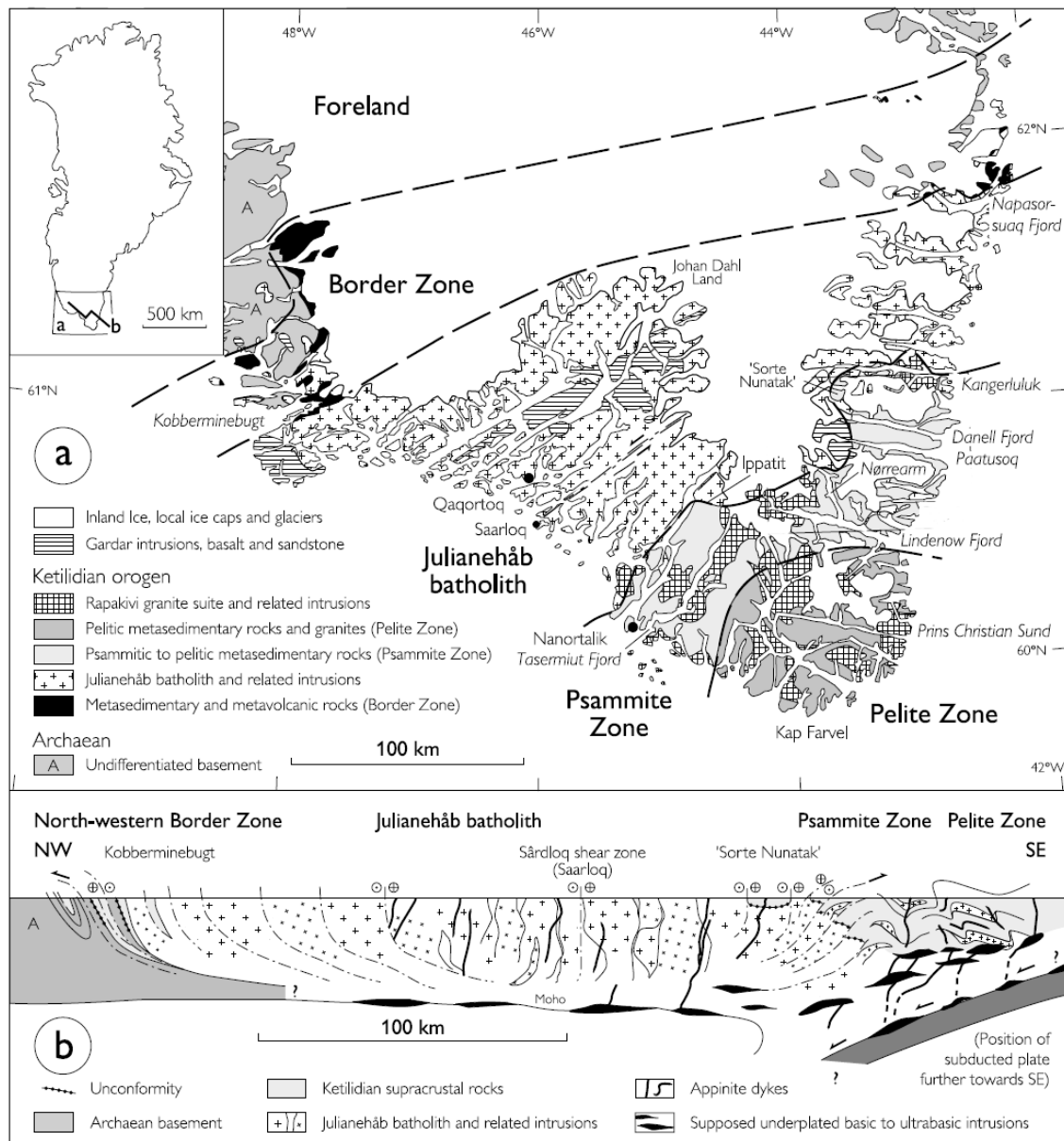


Figure 4.1-1. Overview geological map of Ketilidian Orogen showing four main subdivisions. a) Main map, b) cross-section. From Garde et al. (2002a)

(c) The Ketilidian forearc south-east of the batholith (also known as the Psammite and Pelite Zones, Fig. 1) comprises proximal arkoses and conglomerates and more distal turbiditic greywackes, which were intensely deformed and metamorphosed during the later parts of the Ketilidian orogeny. The detritus was mainly derived directly from the Julianehåb batholith itself and was deposited on its south-eastern, outboard margin. Sedimentation began already at c. 1795 Ma, while the magmatic activity of the batholith was still active. Whereas the boundary structure against the batholith is steep along most of its length, much of the forearc itself, as well as certain parts of the adjacent batholith, have a prominent flat-lying structure. Both the steep and flat-lying structures can be ascribed to the Ketilidian transpression (Garde et al. 2002b; McCaffrey et al. 2004).

Shortly after its deposition the forearc was intensely heated, and substantial partial melting took place in its outer parts. A traverse along the presently exposed land surface from the batholith margin towards the south-south-east exposes an oblique crustal section, from low-pressure amphibolite facies at the batholith-forearc contact e.g. at the head of Danell Fjord (c. 3 kbar, 580°C) to upper granulite facies well into the forearc (e.g. at Prins Christian Sund, c. 5 kbar, >800°C). The P–T gradient reflects crustal tilting in this part of the orogen, but the timing of the tilting event is not known with certainty; it could predate the emplacement of the rapakivi granites (see below).

(d) The rapakivi suite. Very voluminous, tabular bodies of rapakivi-type granite and related noritic intrusions were emplaced into the upper crust in the period 1755–1725 Ma, both at the batholith-forearc contact and within the forearc itself (Grocott et al. 1999; Garde et al. 2002a). The rapakivi plutons represent substantial transfer of magma from the lower/middle to the uppermost crust through narrow dykes. The magmatic activity may be regarded as a delayed consequence of the intense heating of the lower and middle crust after c. 1795 Ma, probably due to basic/ultrabasic magmatic underplating. The rapakivi sheets, which may originally have been more than 2.5 km thick, were folded into large, broad anticlines and narrow synclinal cusps during the waning stages of the Ketilidian transpression. The upper parts of the rapakivi intrusions have generally been removed by erosion, so that only their bases and lower parts are preserved, commonly at high topographic elevations.

The present-day physiography of South Greenland is influenced by the generally steep, NE–SW-trending (and in some areas flat-lying) Ketilidian structures, also by the massive, homogeneous nature of the rapakivi plutons, and not least by structures related to the c. 1340–1140 Ma Gardar rifting and magmatism. A number of ENE–WSW- to E–W-trending faults were developed during the rifting. Many of the Gardar dykes follow these trends, which have also governed the orientations of many of the fjords in South Greenland.

4.1.1 Regional magnetic data

Aeromagnetic data across South Greenland clearly reveal the crustal architecture. The outline of the Julianehåb Batholith is indicated by high magnetic intensity (red) and the Borderzone as low intensity (blue) (Fig. 4-2).

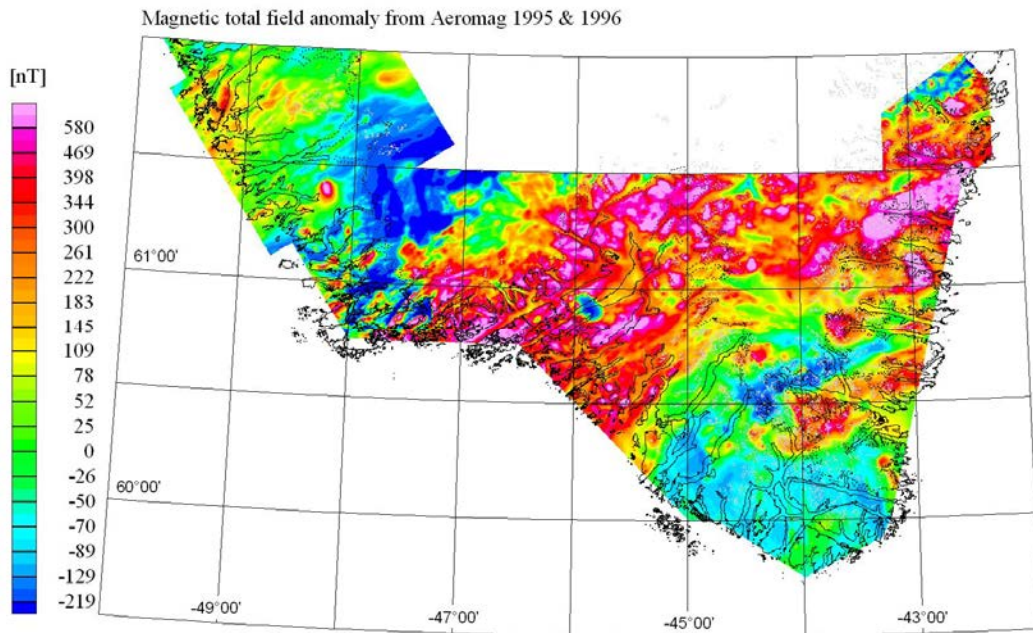


Figure 4.1-2. Magnetic total field anomaly from Aeromag 1995 and 1996. The outline of the Julianehåb Batholith is clearly indicated as high magnetic intensity (red) and the Border-zone as low intensity (blue). From Schjøth et al. 2000.

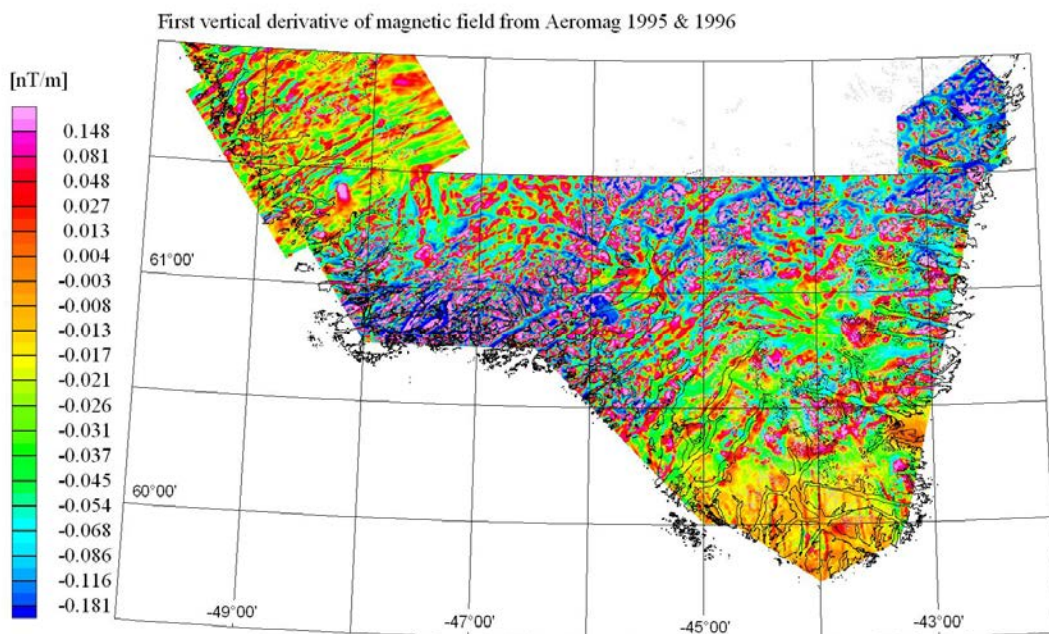


Figure 4.1-3. First vertical derivative of magnetic field from Aeromag 1995 and 1996. From Schjøth et al. 2000.

4.2 Geomorphological analysis

The study area in the south is more dissected than in Godthåbsfjord area, split into hundreds of promontories, islands, islets and skerries by a tight grid of ENE–WSW and NW-SE fjords and straits in which some outlets of the ice sheet bring icebergs. The interpretation of landforms is therefore more difficult and thus less confident. Two distinct landform types can be distinguished: namely inland tracts of highlands and a low relief surface in the costal areas.

The preliminary analysis of landforms suggested that the relief difference in a general prospective were connected to the geological border-zone between the Ketilidian mobile belt and the Archaean craton. Similar questions about the landscape development as in the Godthåbsfjord area were thus addressed. Can the present landscape be explained by either 1) fault reactivation and differential uplift or by 2) differential weathering and erosion within an uplifted landmass?

4.2.1 Methods

The large-scale landforms in the study area were analysed from overview topographical and geological maps. Complementary analysis was made in B/W aerial photographs at the scale 1:40.000 and 1: 150.000, interpreted in a stereoscope. In the field the large-scale landforms were described according to their characteristics, and also documented by ground-, helicopter- and aerial photographs and sketches. Systematic mapping of the large-scale landforms across the area from topographical maps and profiles is planned subsequent to the Fieldwork.

4.2.2 Results

4.2.2.1 Large-scale landscape characteristics

The elevated areas are mainly covered by the inland ice (see Fig. 2.5-1), but remnants of a summit plateau can be identified along the ice margin and east of the Narssaq-Qaqortoq region (Fig. 4.2-1). In the east, the Narsarsuaq-Søndre Sermilik area, the summits are about 1500-1700 m a.s.l., but field observations indicate that there might also be a lower level at c. 1200 m a.s.l.. These surface(s) have however not yet been mapped. In the west, north of the Kobberminebugt area, only one high level was identified at about 850 to 1000 m a.s.l.. It is difficult to correlate the summit surface from the Kobberminebugt area to the Narsarsuaq area because of the Inland Ice. However, the regional plateau system can be described either as one tilted block which is highest in the east, or as the juxtaposition of a high dissected plateau belonging to the eastern mountains of South Greenland, and a lower plateau developed to the west along the south-western margin of the Inland Ice (cf. section 2.5).



Fig 4.2-1 View from the top of Illerfissalik towards the north with the summit surface at c 1700 m a.s.l. in the eastern parts of the study area. To the left is the Qooroq fjord. Location in Fig. A-4.

In the east, a roughly north-south escarpment separates an upper and an intermediate surface based on observations in the Narsarsuaq-Igaliko-Uunartoq region (Fig. 4.2-2). The intermediate plateau seems to represent a surface level of rather regular altitude, between 400 and 600 m a.s.l. (slightly higher to the west – Qoroqssuaq – and the east – around the Nordre Sermilk), over a low and very rugged platform dissected between the fjords by multitudes of intersecting fracture zones and basins. The contact between the different surface levels is often confused by deep dissection and glacial scouring of the landscape, but locally, escarpments are better defined, for example with the NS scarp visible south of Igaliko (Fig. 4.2-2), between the high and intermediate levels, and in the Qaarsuarsuk-Tuttutooq area, between the intermediate and low levels (Fig. 4.2-3, 4.2-4). Higher mountains rise over these surfaces, related to the Gardar sediments and volcanics of the Eriks Fjord Formation, SW of Narsarsuaq (Redekammen, 1210 m; Ilimmaasaq, 1440 m), and to metamorphic rocks of the border zone of the Ketilidian orogen, in the west (Sanerut, Tallorutit, 943 m).

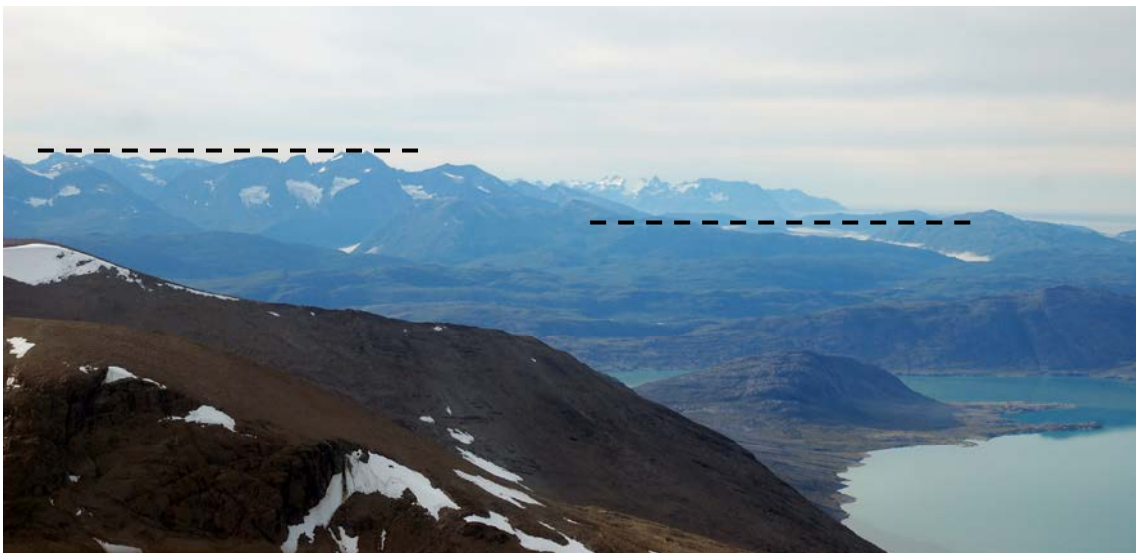


Fig 4.2-2. Three surfaces on one photo, and the NS escarpment between the higher and intermediate surfaces. The lowest surface is near sea level. Photo from Igaliko towards SSE. Location in Fig A-4.



Fig. 4.2-3. Helicopter photo of an intermediate surface (foreground) and a low surface (background) at Sermilik, from SW of Qalerallit Sermia towards SW. Photo taken further along the valley seen in Fig. 4.2-4. Location in Fig. A-3.



Fig. 4.2-4. Glacial erosion has contributed to destruction of the intermediate surface, here seen as a valley, connecting to the low surface, making the distinction between them somewhat difficult. Photo from Sermilik, SW of Qalerallit Sermia towards SW. Location in Fig. A-3.

The lowest relief is primary developed in the southern and western parts of the study area, south-west of Inland Ice. It consists of an undulating or rugged topography of knobs, basins, fracture corridors and hundreds of lakes, with a relative relief reaching about 200 m (Fig. 4.2-5).



Fig. 4.2-5. View from Qarmat Qaqa towards the west across the Kobberminebugt. The summit surface is at c 900 m a.s.l. and the low relief surface – here a true strandflat - has a maximum relief of 50 m. Location in Fig. A-2.

Higher hill complexes stand on this surface as steep residual hills or mountains up to 600 m high, with the highest mountains in Alanngorsuaq and the western and southern parts of Nunarssuit (new maps: Nunakuluut). Their altitude is close to that of the 20 to 50 km wide zone of rugged “intermediate” plateaus that separate the ice margin and the eastern mountains from narrow tracts of strandflat-like platforms represented in the Kobberminebugt and at the mouth of the fjords between Nunarssuit and Qaqortoq (Fig. 4.2-3).

In the Kobberminebugt area, a distinction can be made between wide and shallow basins in inner locations, with extremely rugged floors, mainly shaped into the Julianehåb granites (northern Ilorleq) or in pyroxene syenites of the Gardar intrusions (central Nunarssuit), very flat and low-lying strandflats of composite (glacial and possibly pre-glacial) origin, shaped into metasediments of the border zone (Ikerassaaqqap Nunaa), and typical and narrow wave-cut benches, intact (post-glacial) or more or less re-shaped by ice scouring (northern shore of Alanngorsuaq) (Fig. 4.2-4).

4.2.2.2 Weathering

Across considerable areas on Nunarssuit, the bedrock has been heavily weathered, disintegrated to a sandy, gravelly saprolite, many metres thick, covering the steep mountain slopes and the hollows of the low rugged platform (Figs. 4.2-6, 4.2-7). This type of weathering seems to be closely connected to granites of the Gardar intrusive complex, although these rocks, as well as peripheral parts of the adjacent syenite intrusion form prominent residual reliefs on the lowest surface (Fig. 4.2-8). The apparent contrast between this high sensitivity to weathering and the salient position in the landscape will require a detailed study of the history of differential erosion, since a first observation of the structural controls of the outlines of these landforms suggest lithological rather than tectonic influences (contrast with low-lying surfaces developed into the Julianehåb granites).



Fig. 4.2-6. A sandy to gravelly saprolite cover the mountainsides of Nunarssuit. Photo along the Torsukattak fjord. Location in Fig. A-2.



Fig. 4.2-7. The thick saprolite is in contact with fresh rock. Note the hammer for scale. (Sample site 48; A-2).



Fig. 4.2-8. A flat surface at intermediate level (c. 200 m a.s.l.), western Nunarsuit (Nunakuluut) with Kap Desolation rising to 600 m in the background. Helicopter photo towards SSE from the mouth of the Torsukattak fjord. Location in Fig. A-2.

4.3 Structural analysis

4.3.1 Regional studies

A similar mapping procedure to that outlined for Akia was also carried out for this region. Structural lineaments were picked from Landsat images at both 1:500,000 and 1:100,000 scales in ArcGIS (Fig. 4.3-1) and supplemented by observations made from DTM and pre-existing geological map data.

The main lineament trends identified at 1:500,000 scale for the region are:

- NE–SW
- ENE–WSW
- ESE –WNW
- SE–NW

With the most dominant system being SE–NW.

A similar set of lineaments can also be identified at 1:100,000 scale, though here there is no one dominant, just a range from NE–SW through to SE–NW (Fig. 4.3-1b). In the central part of the Julianehåb batholith the dominant trends are NE–SW/ ENE–WSW, as depicted by major fjords such as Bredefjord and Sermilik, and a roughly orthogonal set of SE–NW trends (Fig. 4.3-1). As you move west across the Julianehåb batholith a set of ESE–WNW lineaments becomes more pronounced, some of which may be traced eastwards offshore and parallel to the present day coastline (Fig. 4.3-1).

When comparing the lineament trends of the Archaean Craton/ Border Zone with those of the Julianehåb batholith, some distinct differences can be seen. The contact between the border zone and the batholith is marked by a distinct zone of contact parallel ENE–WSW trending lineaments and fjords, where as north of this there are few ENE–WSW trending structures (Fig. 4.3-1). On the other hand E-W and ESE–WNW trending structures are far more pronounced. A few lineaments appear to be traceable across the Border Zone, though their trends appear to change along strike, from SE–NW in the Julianehåb batholith and curving round into an ESE–WNW/ E-W trend in the Border Zone.

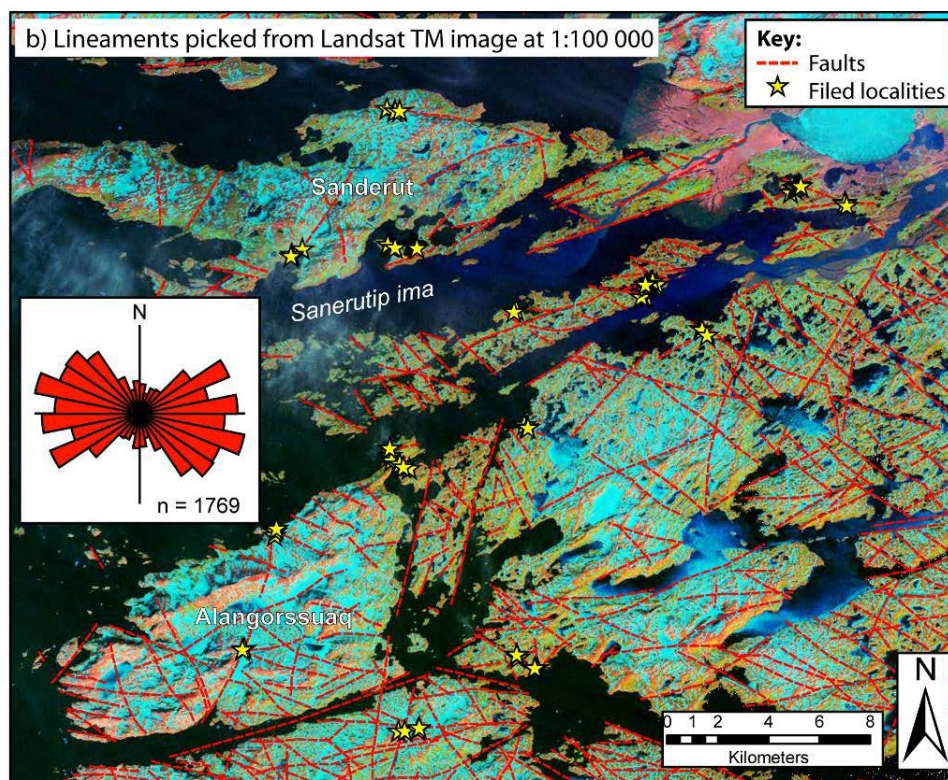
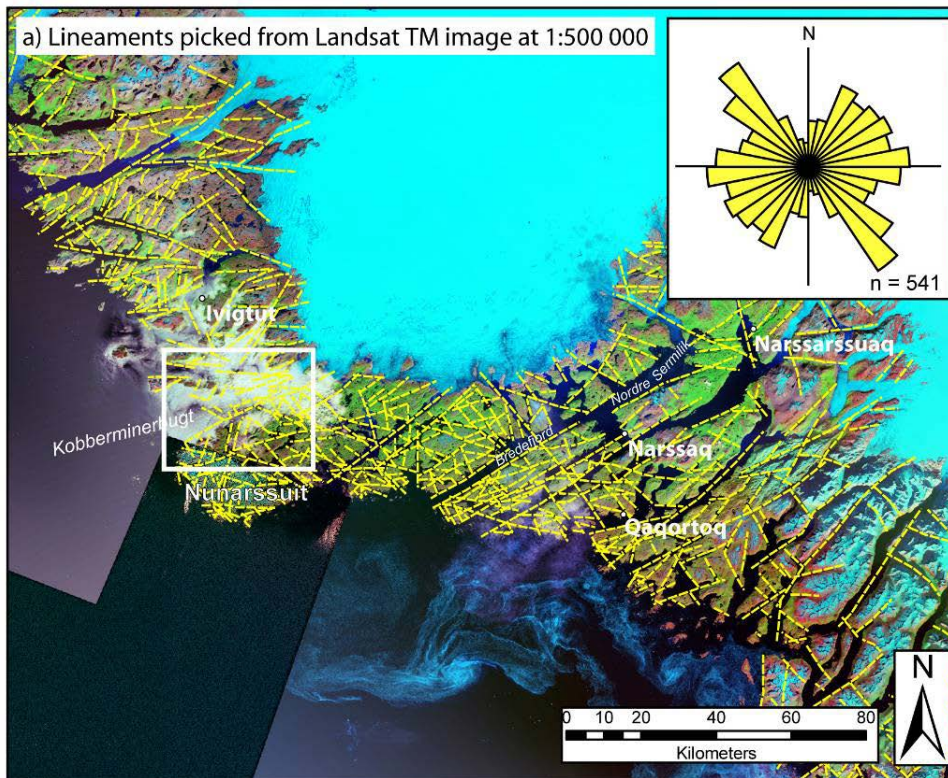


Figure 4.3-1. (a) Landsat TM with structural lineaments picked at 1:500,000 scale. Inset: rose diagram showing main lineament trends. (b) Zoom in of main field mapping area (outlined in a) showing location of main field localities. Also shown are structural lineaments picked at 1:100,000 scale. Inset: rose diagrams showing main lineament trends at 1:100,000.

4.3.2 Outcrop studies

Field investigations were mainly carried out in the Kobberminebugt region looking at the faults and structures in contact between the Border Zone and the Julianehåb batholith (Figs. 4.1-1 and 4.3-1b). Aerial photographs were used during field data acquisition to identify key areas of interest, and also allow ground-truthing of lineaments. In total 18 localities were visited and 171 fault measurements recorded. A similar set of attributes were recorded to those outlined in **section 3.3.2**. All field data were geospatially located using GPS waypoint collection, and stored in a computer database with links to GIS. Outcrop exposures in the region were excellent, with fresh exposures in both coastal and inland areas. The main fault trends recorded at outcrop were NE–SW to ENE–WSW, E–W, ESE–WNW, and to a lesser extent, N–S (Fig. 4.3-2). The following paragraphs describe some of the filed observations of fault characteristics for each of these fault sets (see also Table 4.3-1 and Figs. 4.3-2 – 4.3-6).

N–S:

A prominent set of N–S to NNE–SSW lineaments can be found in the western part of the mapping area (e.g. fjords bounding the east margin of Alanngorsuaq, Fig. 4.3-1). These correspond to steeply-dipping (to both E and W) major sinistral strike-slip faults. Two key localities were studied RW-2.16 and RW-2.17, both of which exhibit a wide (~5m) fault breccia damage zone (Figs. 4.3-3 and 4.3-4). The fault zone at locality RW-2.16 has a distinct green colouration which is likely to be due to the presence of epidote (Fig. 4.3-3). At locality RW-2.17, adjacent to Josvamine (an old copper mine), the breccia has a strong haematite red colouration indication iron oxide (Fig. 4.3-4).

NE–SW / ENE–WSW

The most pronounced system of faults seen at outcrop has to be the NE–SW to ENE–WSW (basement parallel) faults. Most faults of this orientation dip to the SE and exhibit dextral strike-slip movements, though a few dextral-normal oblique faults were also observed (Fig. 4.3-5c). Cataclastite fault rock was found in some ENE–WSW trending fault zones, though many of these faults are characterised by smooth epidote slickenlines (Fig. 4.3-5c).

E–W:

In many cases E–W trending faults may simply be a continuation of ENE–WSW faults described above; however, in some localities distinct set of E–W faults with distinctly different fault characteristics can be found (e.g. Locality RW-2.4, Fig. 4.3-6). These faults generally dip to the south, and show normal dip-slip and dextral-normal oblique-slip movements. At Locality RW-2.4 fault breccia/ cataclasite crush zones and pseudotachylite bands can be found within the fault zone (Fig. 4.3-6).

ESE–WNW / SE–NW:

Cutting much of the areas is also a set of ESE–WNW to SE–NW trending faults (Fig. 4.3-1). These dip both NE–and SW and show both dextral strike-slip and normal dip-slip movements. Many of these faults have cataclastic fault rocks exposed. Locally some of these faults appear to reactivate NW–SE trending dolerite dykes (Gardar dykes?; Fig. 4.3-5e).

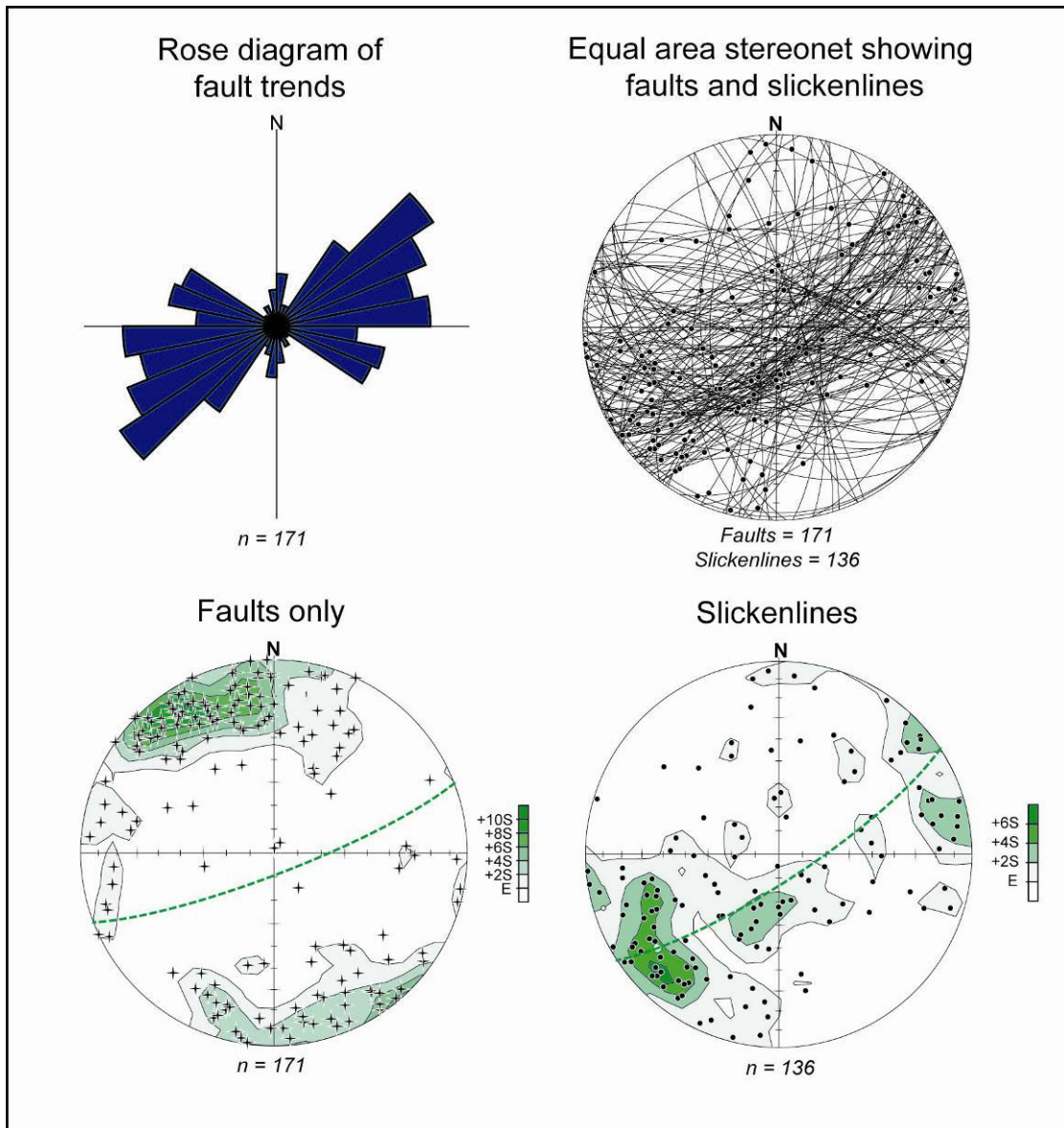


Figure 4.3-2. Fault and slickenline data recorded during field mapping in Kobberminebugt.

Table 4.3-1. Summary of main fault trends and their attributes.

Trend	Dip direction	Kinematics	Fault rocks	Comments
N-S to NNE-SSW	E and W	Sinistral strike-slip	Fault breccia	
NE-SW to ENE-WSW	SE	Dextral strike-slip and dextral normal oblique -slip	Cataclasite, smooth epidote slicks	Basement parallel
E-W	S	Normal dip-slip and dextral normal oblique-slip	Fault breccia/ cataclasite and Pseudotachylite	
ESE-WNW	NE and SW	Dextral and normal oblique-slip	Cataclasite	Some reactivate Gardar Dykes

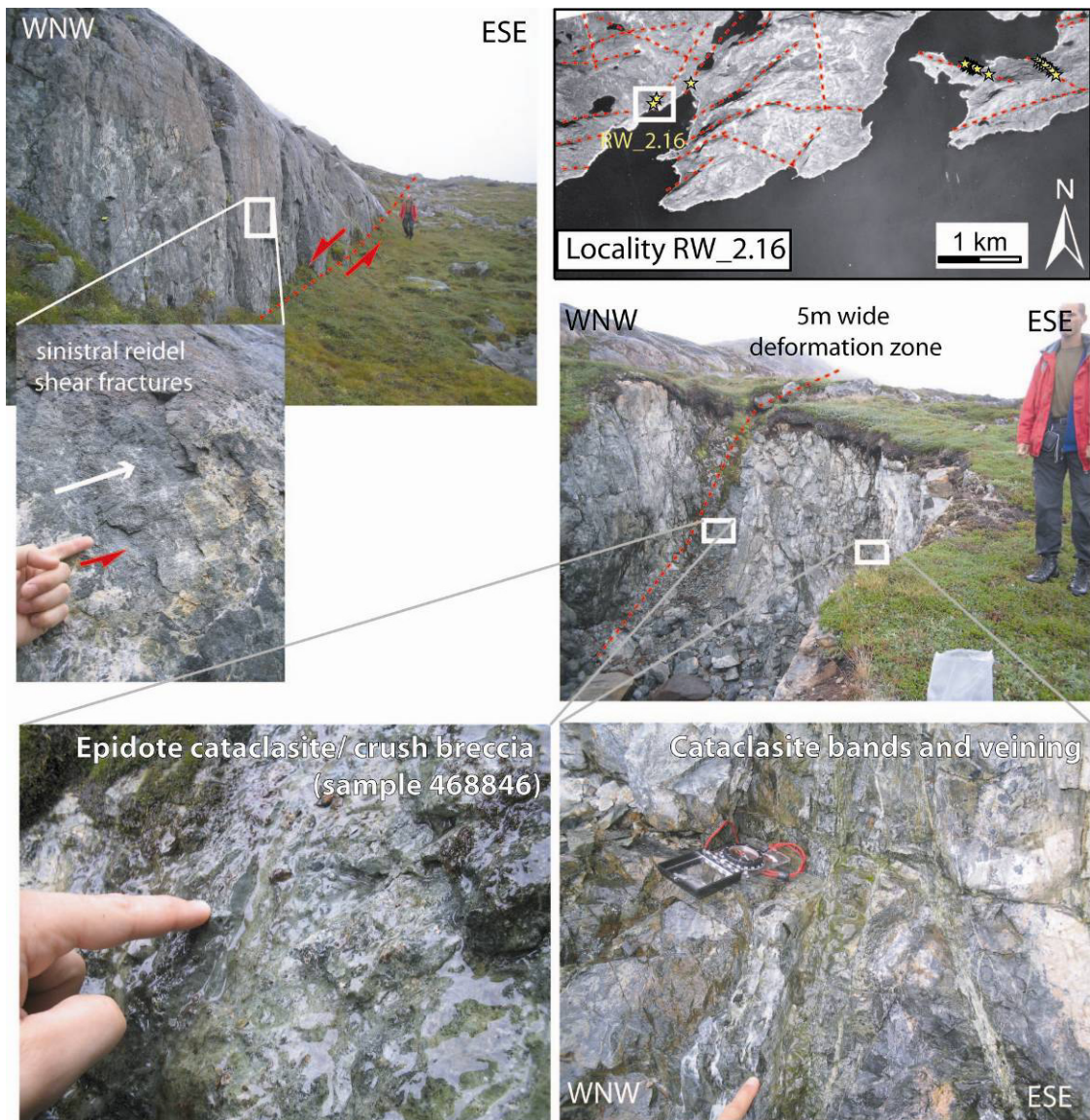


Figure 4.3-3. NNE–SSW lineament. Sinistral strike-slip fault with 5 m wide cataclasite/ fault breccia crush zone (Locality RW_2.16)

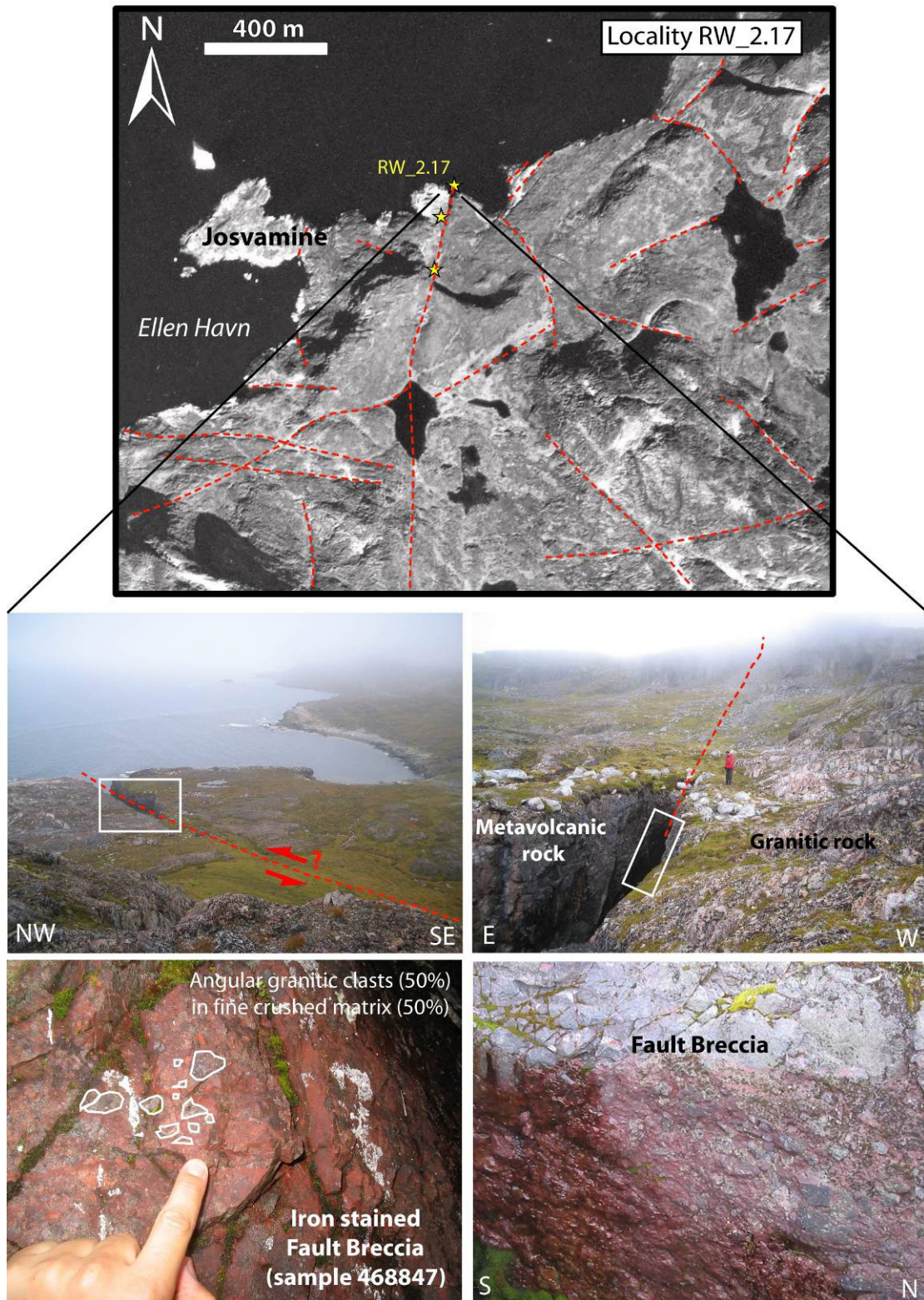


Figure 4.3-4. NNE–SSW trending lineament near Josvamine. Possible sinistral strike-slip fault with 1-2m wide fault breccia zone (Locality RW_2.17).

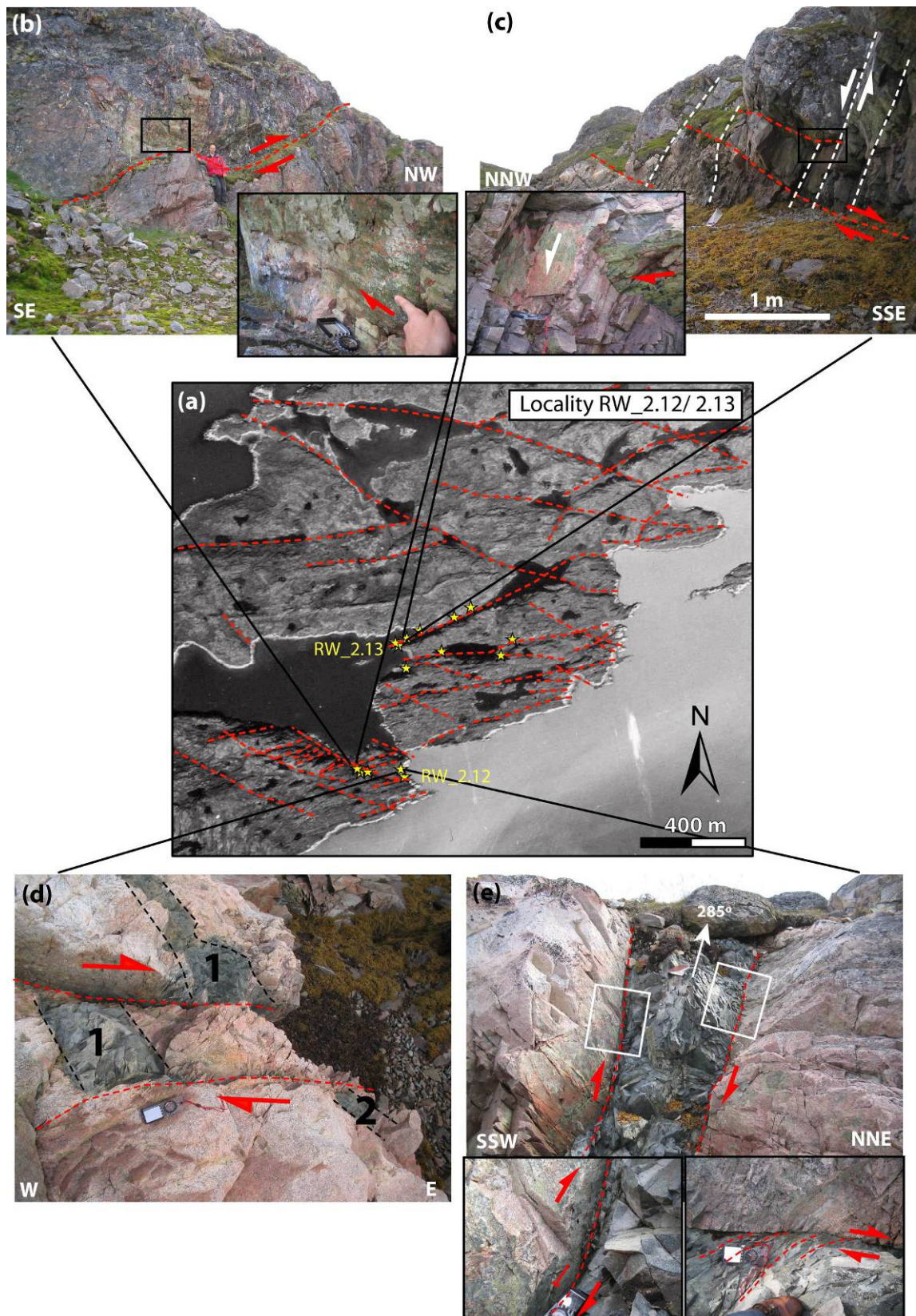


Figure 4.3-5. a) ENE–WSW and SE–NW trending lineaments (Locality RW_2.12 and 2.13). b) & c) ENE–WSW trending dextral strike-slip and normal-slip faults with clear epidote slickenlines. d) ENE–WSW trending dextral strike-slip faults cross-cutting dolerite dykes. e) Dextral reactivation of SE–NW trending (Gardar?) dykes.

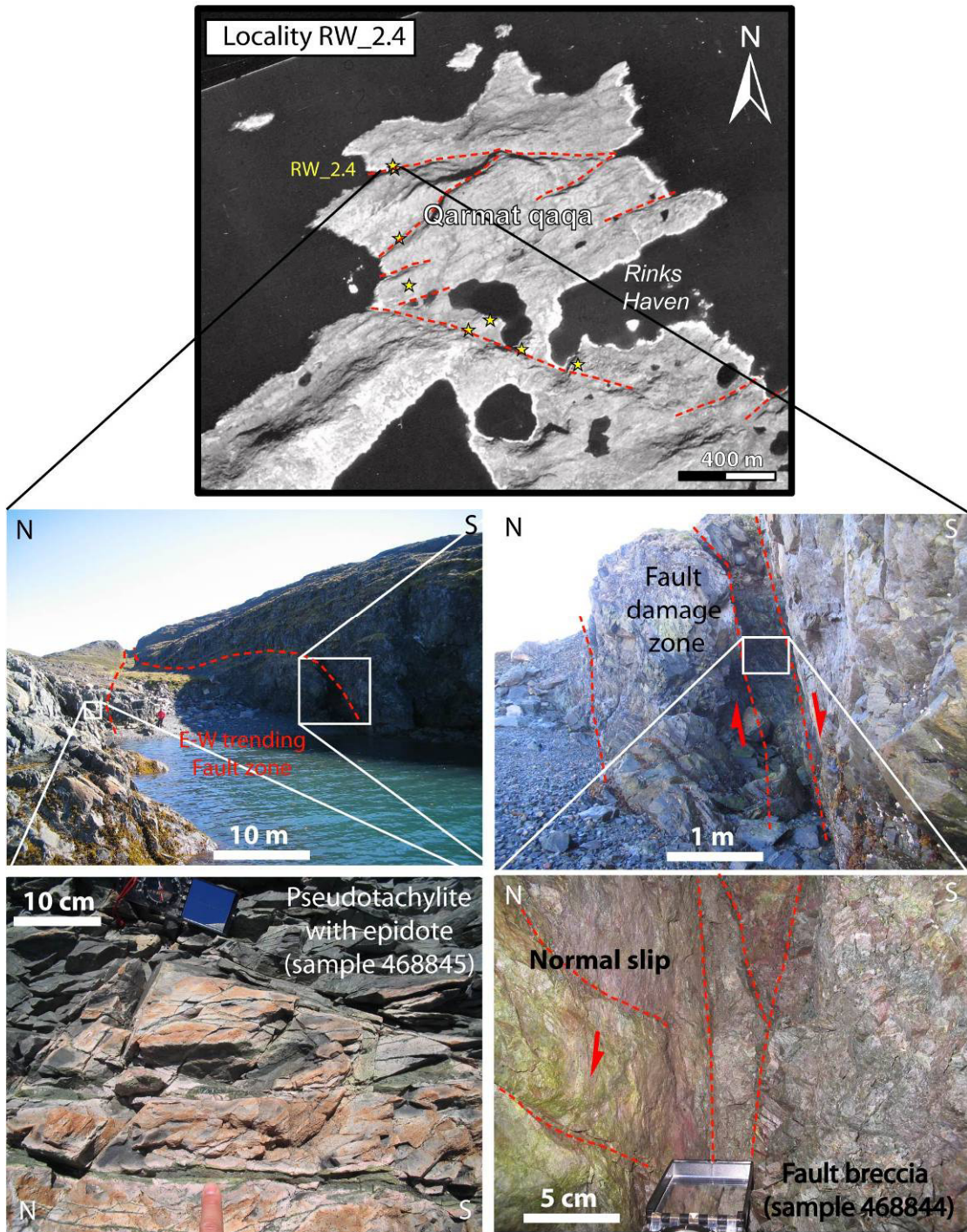


Figure 4.3-6. E-W trending lineament. Dextral/ normal-oblique slip fault with both fault breccia and pseudotachylite fault rocks (Locality RW_2.4).

4.4 Rock sampling

4.4.1 Sampling of rocks for apatite fission-track analysis

The main objective for rock sampling in South Greenland was sampling along a near-vertical transect to get AFTA data to establish palaeogeothermal gradients during episodes of palaeothermal maxima and thus to establish the amount of section removed since these episodes (Fig. 4.4-1). The original plan for sampling in the deep fjord of Søndre Sermilik, SE of Narsarsuaq airport had to be given up due to weather conditions. The alternative solution became the 1752 m high mountain Illerfissalik (or Burfjeld) just 10 km SE of Narsarsuaq (see Appendix). The location close to the airport was very convenient because sampling above 100 m had to be given up on the first day (August 21) due to low clouds, but was successfully resumed in bright weather and a total of 9 rocks were sampled (August 23). The seven samples above 100 m were gathered during a helicopter flight with only 75 minutes between take-off and landing in Narsarsuaq (Fig. 4.4-2).

A second vertical section was sampled north of Kobberminebugt on the island of Tallorutit with 4 samples up to 814 m. Additional samples were taken across the area to get a regional coverage. The sampling thus included a transect from Illerfissalik in the eastern interior of the region to islands south of Qaqortoq and a transect along Kobberminebugt with samples on either side of the bay.

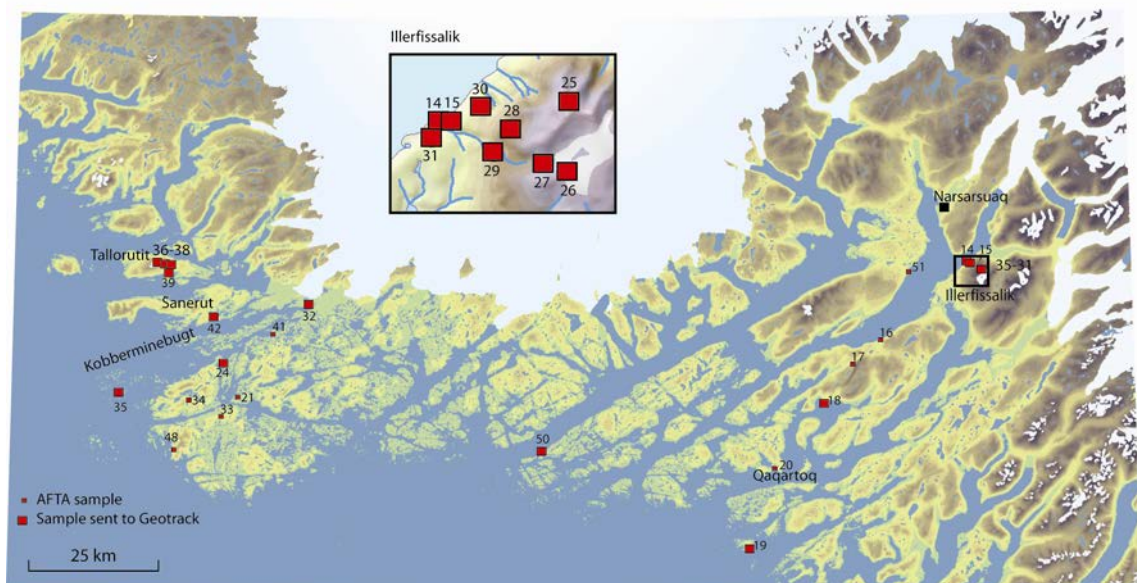


Figure 4.4-1. Location of AFTA samples in SW Greenland with indication of the first samples sent to Geotrack for analysis.

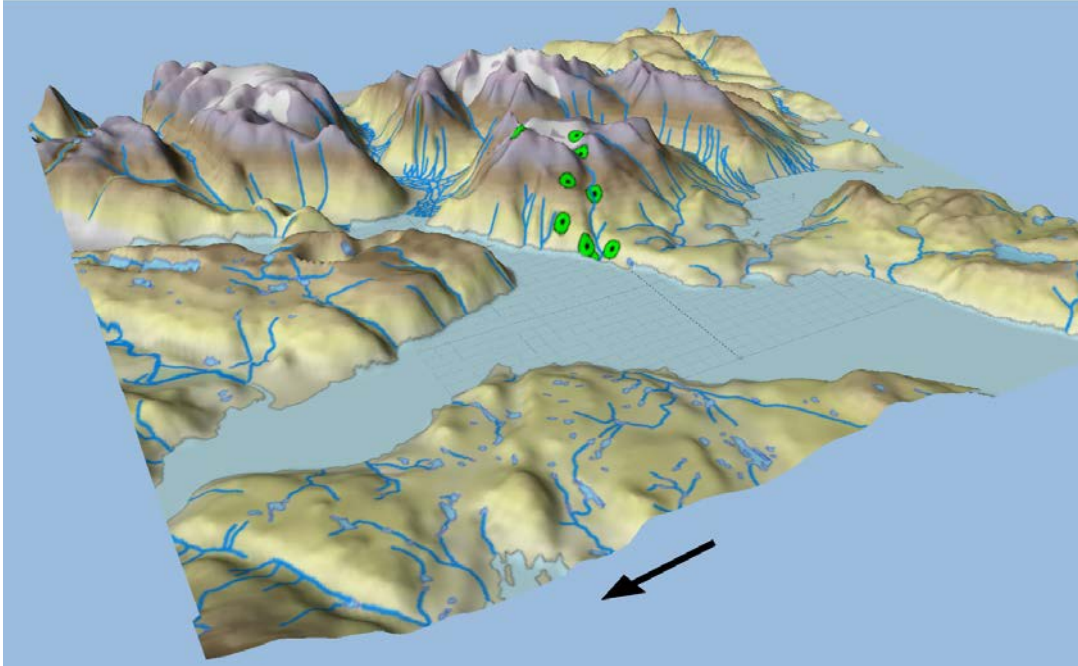


Figure 4.4-2. 3D model of the Illerfissalik mountain with location of the rocks sampled up to 1757 m a.s.l. for fission-track analysis. Viewpoint from north-west.

4.4.2 Sampling of rocks from faults

Fault rock samples (Fig. 4.4-3) were collected from a number of localities for thin section analysis. If pseudotachylite samples are fresh enough these will also be sent away for Ar-Ar dating.

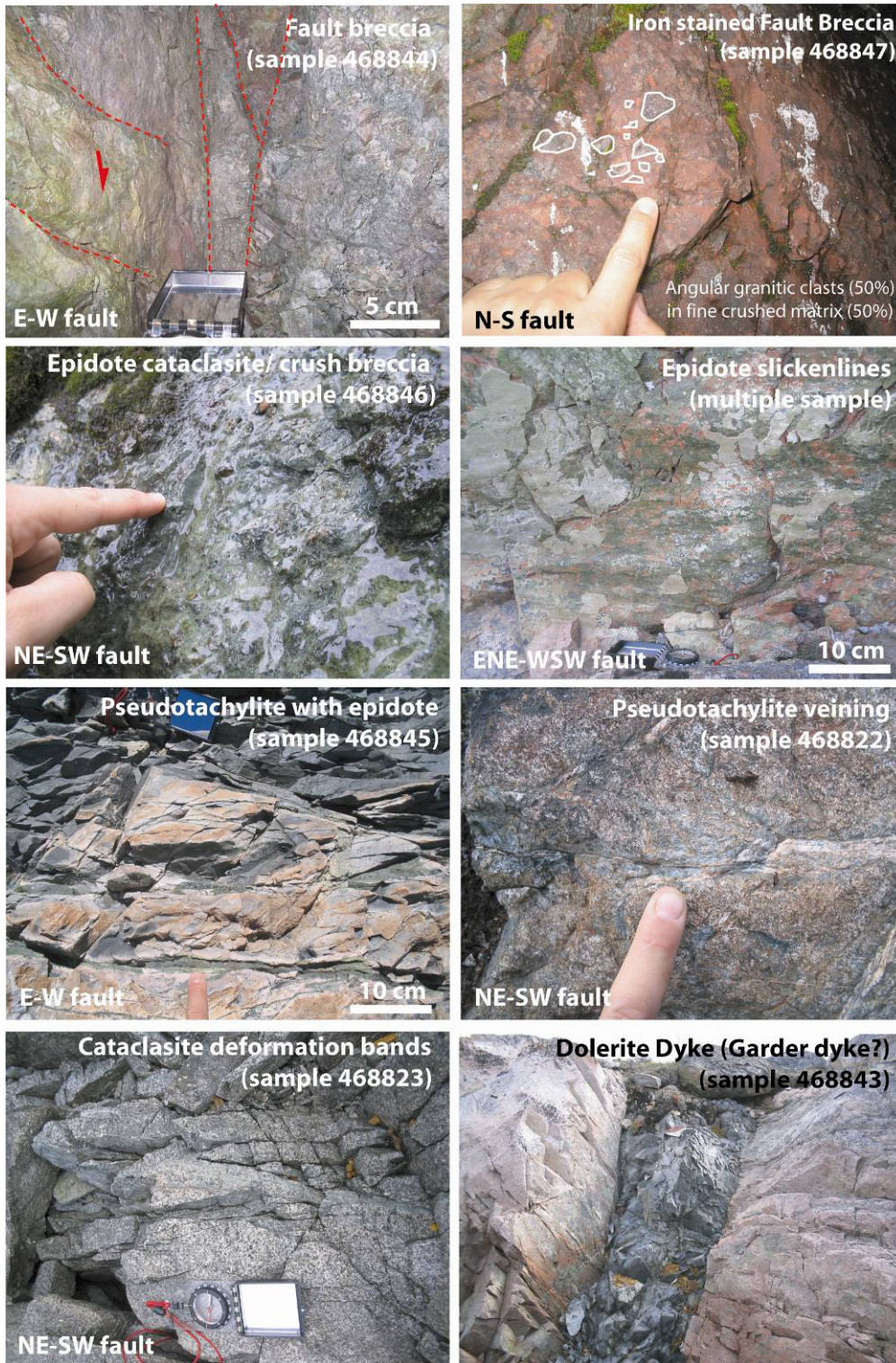


Figure 4.4-3. *Examples of fault rock samples collected*

4.5 Discussion

Fault patterns and movements all appear to be consistent with a regional NE–SW extension direction (Fig. 4.5-1a), and the orientation of strike-slip faults appears to fit with a system of Reidel shears associated with an E–W trending dextral wrench system (Fig. 4.5-1a). As the area studied lies in a left-lateral step on the rifted Labrador Sea margin, we suggest that this system may have developed as an oblique transfer zone during rifting (Fig. 4.5-1c).

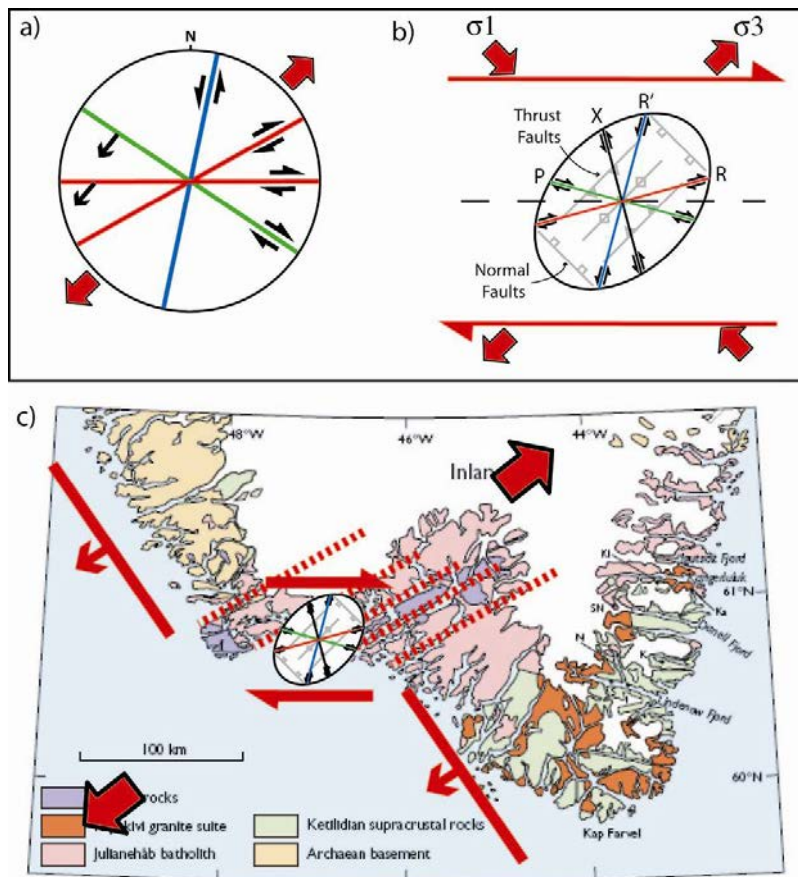


Figure 4.5-1. a) Summary of main fault trends and movements. b) E–W trending sinistral wrench system showing comparable movements to those shown in a). c) Regional structural model for fault patterns observed. Left stepping margin segment forms a dextral oblique transfer zone along the Labrador Sea margin.

If this left lateral step on the SW Greenland margin has developed through basement reactivation of Ketilidian structures during later rifting events, a key question is why has this not occurred on the eastern margin also? The answer to this may lie in the internal basement structure of the Ketilidian Orogenic Belt. Garde et al. (2002b) presented a model for mid crustal partitioning of deformation within the Ketilidian Orogen, where the upper crust underwent localised transpression along a number of discrete faults and shear zones, while the lower crust shows a more distributed zone of deformation (Fig. 4.5-2). Uplift and exhumation of Greenland's eastern margin has led to this lower crustal block being exposed along this margin, whereas it is the upper crustal block that is exposed in the west. This upper block is more likely to be prone to reactivation during rifting than the lower block as it con-

tains more discrete structures (also mineral phases in upper crustal shear zones are weaker). Therefore the western margin shows a stepped/ transfer zone geometry and the development of an oblique margin segment where as the east does not. This explains why the lithological contrast between the Archaean and Ketilidian terrane is not the controlling factor for the development of the topography.

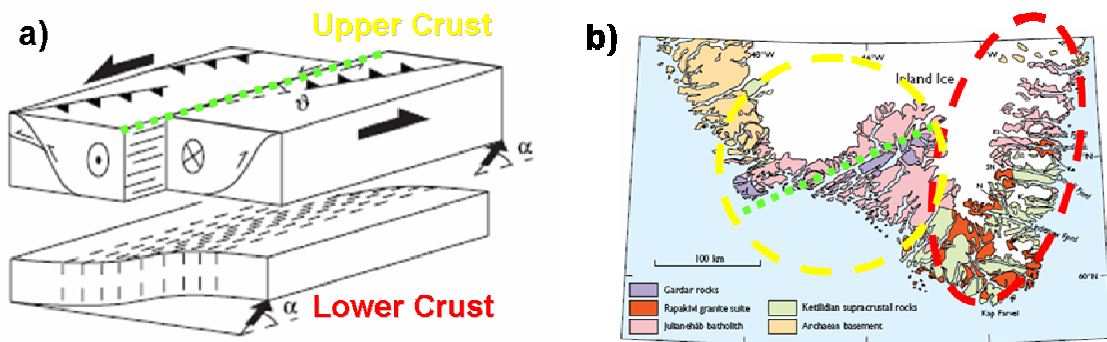


Figure 4.5-2. a) *Cartoon block model outlining crustal partitioning model for South Greenland (Garde et al. 2002b).* b) *Simplified geological map outlining upper (yellow) and lower (red) crustal blocks as suggested by Garde et al. (2002b).*

A key requirement of this model is that the present day basement exposures are similar to those at time of break-up and margin development (i.e. lower crustal block in east, upper in west). It is hoped that AFTA analysis of samples from across the region shall help to address this. However, the present day basement exposure may to a large extent be governed by pre-breakup tectonic movements at temperatures that were higher than 110°C and may thus not be recorded in the AFTA data.

Whereas the left stepping margin segment may be explained as a transfer zone related to the Mesozoic rifting, the present altitudes may be the result of the later development, as in West Greenland, where the present topography was due to late Neogene uplift of a mid-Cenozoic planation surface (e.g. Bonow et al. 2006a, Japsen et al. 2006). If this applies to southern Greenland, the present relief was formed subsequent to late Neogene tectonic movements. Furthermore, differential weathering controlled by lithological contrasts has contributed to the present contrasts in topography (e.g. between the Julianeåb granites and the Gardar intrusives). Such a hypothesis implies that the transfer zone along Kobberrminebugt may have been reactivated during the Neogene.

The preliminary analysis of the large-scale topography indicates a separate development of the eastern and western coasts of Greenland: the south-eastern coast is characterized by a elongated, anticlinal structure with elevations above 2 km almost to southern tip of Greenland at 60°N; the west coast is dominated by near-horizontal surfaces reaching 1 km southwards to the northern part of Kobberrminebugt at 61°N. How this configuration can be explained awaits the detailed follow-up on the fieldwork: A regional mapping of the landforms that may or may not verify a correlation with planation surfaces in central West Greenland and the analysis of the AFTA from the region, in particular from the elevated transect at Illerfissalik. The latter results may give insight into magnitude and timing of cooling events that have affected the region and reveal to what extent such events correlate with those established north of Sukkertoppen Iskappe.

5. Acknowledgements

The Fieldwork was made possible by funding from the Danish Natural Science Research Council (FNU) to the project 'Uplift, erosion and fault reactivation in Southwest Greenland', and further support from Nunaoil, GEUS and the University of Durham. The Carlsberg Foundation is thanked for generous support to the project 'Palæo-overflader og palæo-dale i Sydvestgrønland'. The plot of elevation of the bedrock (Fig. 2.5-1) is courtesy of Trine Dahl-Jensen, GEUS. Stefan Sølberg is thanked for producing the 3D diagrams in Figs 4.0-1 and 4.4-2.

6. References

- Allaart, J.H. 1976: Ketilidian mobile belt in South Greenland. In: Esher, A. & Watt, W.S. (eds): *Geology of Greenland*, 121–151. Copenhagen: Geological Survey of Greenland.
- Appel, P.W.U, Garde, A.A., Jørgensen, M.S., Moberg, E., Rasmussen, T.M., Schjøth, F., & Steinfeldt, A. 2003: Preliminary data of the economic potential of the greenstone belts in the Nuuk region. General geology and evaluation of compiled geophysical geochemical and ore geological data. Danmarks og Grønlands Geologiske Undersøgelse Rapport **2003/94**, 147 pp.
- Bonow, J.M. 2005: Re-exposed basement landforms in the Disko region, West Greenland - disregarded data for estimation of glacial erosion and uplift modelling. *Geomorphology* **72**, 106–127.
- Bonow, J.M., Lidmar-Bergström, K. & Japsen, P. 2006a: Palaeosurfaces in central West Greenland as reference for identification of tectonic movements and estimation of erosion. *Global and Planetary Change* **50** (3-4), 161–183.
- Bonow, J.M., Japsen, P. Lidmar-Bergström, K., Chalmers, J.A. & Pedersen, A.K. 2006b: Cenozoic uplift of Nuussuaq and Disko, West Greenland - elevated erosion surfaces as uplift markers of a passive margin. *Geomorphology* **80**, 325–337.
- Chadwick, B. & Garde, A.A. 1996: Palaeoproterozoic oblique plate convergence in South Greenland: a re-appraisal of the Ketilidian orogen. In: Brewer, T.S. (ed.): *Precambrian crustal evolution in the North Atlantic region*. Geological Society Special Publication (London) **112**, 179–196.
- Chalmers, J.A. 1997: The continental margin off southern Greenland: along-strike transition from an amagmatic to a volcanic margin. *Journal of the Geological Society (London)* **154**, 571–576.
- Chalmers, J.A. 2000: Offshore evidence for Neogene uplift in central West Greenland. *Global and Planetary Change* **24**, 311–318.
- Chalmers, J.A, in press: Labrador Sea, Davis Strait and Baffin Bay. *Phanerozoic Geology of the World*, Elsevier.
- Chalmers, J.A. & Laursen, K.H. 1995: Labrador Sea: the extent of continental and oceanic crust and the timing of the onset of seafloor spreading. *Marine and Petroleum Geology* **12**, 205–217.
- Chalmers, J.A. & Pulvertaft, T.C.R. 2001: Development of the continental margins of the Labrador Sea: a review. In Wilson, R. C. L., Whitmarsh, R. B., Taylor, B. & Froitzheim, N., *Non-volcanic Rifting of Continental Margins: A Comparison of Evidence from Land and Sea* Geological Society (London) Special Publication **187**, 79–107.
- Chalmers, J.A., Pulvertaft, T.C.R., Christiansen, F.G., Larsen, H.C., Laursen, K.H. & Ottesen, T.G. 1993: The southern West Greenland continental margin: rifting history, basin development, and petroleum potential. In Parker, J.R., (ed.) *Petroleum geology of Northwest Europe: proceedings of the 4th conference* (pp. 915–931). London: Geological Society.
- Chalmers, J.A., Pulvertaft, T.C.R., Marcussen, C. & Pedersen, A.K. 1999: New insight into structure of the Nuussuaq Basin, central West Greenland. *Marine and Petroleum Geology* **16**, 197–224.

- Chian, D. & Loudon, K.E. 1994: The continent-ocean crustal transition across the southwest Greenland margin. *Journal of Geophysical Research* **99**, 9117–9135.
- Escher, J.C. & Pulvertaft, T.C.R. 1995: Geological map of Greenland, 1:2 500 000. Copenhagen, Geological Survey of Denmark.
- Garde, A.A., Friend, C.R.L., Nutman, A.P. & Marker, M. 2000: Rapid maturation and stabilisation of middle Archaean continental crust: the Akia terrane, southern West Greenland. *Bulletin of the Geological Society of Denmark* **47**, 1–27.
- Garde, A.A., Hamilton, M.A., Chadwick, B., Grocott, J. & McCaffrey, K.J.W. 2002a: The Ketilidian orogen of South Greenland: Geochronology and tectonics, magmatism and forearc accretion during Palaeoproterozoic oblique convergence. *Canadian Journal of Earth Sciences* **39**, 765–793.
- Garde, A.A., Chadwick, B., Grocott, J., Hamilton, M.A., McCaffrey, K.J.W. & Swager, C.P. 2002b: Mid-crustal detachment during oblique convergence: implications of partitioned transpression in the magmatic arc and proximal forearc of the Palaeoproterozoic Ketilidian orogen, southern Greenland. *Journal of the Geological Society, London* **159**, 247–261.
- Green, P.F., Duddy, I.R., & Hegarty, K.E. 2002: Quantifying exhumation from apatite fission-track analysis and vitrinite reflectance data: precision, accuracy and latest results from the Atlantic margin of NW Europe, in: A.G. Doré, J.A. Cartwright, M.S. Stoker, J.P. Turner, N. White, (Eds.), *Exhumation of the North Atlantic Margin: Timing, Mechanisms and Implications for Petroleum Exploration*, Geol. Soc. London Spec. Publ. **196**, 331–354.
- Green, P.F. 2004: Thermal history of thirty three samples from outcrops and boreholes in West Greenland, based on AFTA. *Geotrack Report* **891**, 215 pp.
- Grocott, J., Garde, A.A., Chadwick, B., Cruden, A.R., & Swager, C. 1999: Emplacement of rapakivi granite and syenite by floor depression and roof uplift in the Palaeoproterozoic Ketilidian orogen, South Greenland. *Journal of the Geological Society, London* **156**, 15–24.
- Guilcher, A., Bodéré, J-C., Coudé, A., Hansom, J.D., Moign, A. & Peulvast, J-P., 1994: The strandflat problem in five high latitude countries. In: Evans. D.J.A. (Ed.), *Cold climate landforms*. John Wiley & Sons, Chichester, pp.351–393.
- Hancock, P.L. 1985: Brittle microtectonics: principles and practice. *Journal of Structural Geology* **7**, 437–457.
- Henriksen, N., Higgins, A.K., Kalsbeek, F. & Pulvertaft, T.C.R. 2000: Greenland from Archaean to Quaternary. Descriptive text to the Geological map of Greenland, 1:2 500 000. *Geology of Greenland Survey Bulletin* **185**, 93 pp. + map
- Holdsworth, R.E., Butler, C.A. & Roberts, A.M. 1997: The recognition of reactivation during continental deformation. *Journal of the Geological Society (London)* **154**, 73–78.
- Holtedahl, H. 1998: The Norwegian strandflat – a geomorphological puzzle. *Norsk Geologisk Tidsskrift* **78**, 46–66.
- Japsen, P., Bonow, J.M., Klint, K-E. & Jensen, F.K. 2002: Neogene uplift, erosion and re-sedimentation in West Greenland. Field report summer 2002. *Danmarks og Grønlands Geologiske Undersøgelse Rapport* **2002/71**, 118 pp.
- Japsen, P., Green, P.F. & Chalmers, J.A. 2005: Separation of Palaeogene and Neogene uplift on Nuussuaq, West Greenland, *Journal of the Geological Society, London* **162**, 299–314.

- Japsen, P., Bonow, J.M., Green, P.F., Chalmers, J.A. & Lidmar-Bergström, K. 2006: Elevated, passive continental margins: Long-term highs or Neogene uplifts. New evidence from West Greenland. *Earth Planet. Sc. Letters* **248**, 315–324.
- Larsen, L.M. 2006: Mesozoic to Palaeogene dyke swarms in West Greenland and their significance for the formation of the Labrador Sea and the Davis Strait. *Danmarks og Grønlands Geologiske Undersøgelse Rapport* **2006/34**, 84 pp.
- Layberry, R.L. & Bamber, J.L. 2001: A new ice thickness and bed data set for the Greenland ice sheet 2. Relationship between dynamics and basal topography. *Journal of Geophysical Research-Atmospheres* **106**, 33781–33788.
- McCaffrey, K., Chadwick, B., Garde, A.A., Hamilton, M., & Curtis, M. 1998: Preliminary results from the north-western border zone of the Ketilidian orogen, South Greenland. In: Wardle, R.J. & Hall, J. (compilers). *Lithoprobe eastern Canadian Shield onshore-offshore transect (ECSOOT): report of 1998 transect meeting*. Lithoprobe Report **68**, 103–114.
- McCaffrey, K., Grocott, J., Garde, A.A. & Hamilton, M.A. 2004: Attachment formation during partition of oblique convergence in the Ketilidian orogen, South Greenland. In: Grocott, J., McCaffrey, K.J.W., Taylor, G. & Tikoff, B. (eds): *Vertical coupling and decoupling in the lithosphere*. Geological Society Special Publication (London) **227**, 231–248.
- Peulvast, J.-P. 1985: Post-orogenic morphotectonic evolution of the Scandinavian Caledonides during the Mesozoic and Cenozoic. In: *The Caledonide Orogen - Scandinavia and related areas* (Ed. by D.G. Gee and B.A. Sturt), pp. 979–996. Wiley and Sons, Chichester.
- Peulvast, J.P. 1988: Pre-glacial landform evolution in two coastal high latitude mountains: Lofoten-Vesterålen (Norway) and Scoresby Sund area (Greenland). *Geografiska Annaler* **70A** (4), 351-360.
- Peulvast, J.P. & Claudino Sales, V. 2004: Stepped surfaces and palaeolandforms in the northern Brazilian «Nordeste»: constraints on models of morphotectonic evolution. *Geomorphology* **62**, 89–122.
- Peulvast, J.P. & Claudino Sales, V. 2005: Surfaces d'aplanissement et géodynamique. *Géomorphologie: relief, processus, environnement* **4**, 249–274.
- Reusch, H. 1894: Strandfladen, et nyt træk i Norges geografi. *Norges geologiske undersøkelse* **14**, 1–14.
- Schjøth, F., Garde, A.A., Jørgensen, M.S., Lind, M., Moberg, E., Nielsen, T.D.F., Rasmussen, T.M., Secher, K., Steinfeld, A., Stendal, H., Thorning, L. & Tukiainen, T. 2000: Mineral resource potential of South Greenland: the CD-ROM. *Danmarks og Grønlands Geologiske Undersøgelse Rapport* **2000/57**, 36 pp., 1 CD-ROM.
- Sørensen, A.B. 2006: Stratigraphy, structure and petroleum potential of the Lady Franklin and Maniitsoq Basins, offshore southern West Greenland. *Petroleum Geoscience* **12**, 221–234.
- Thomson, K., Green, P.F., Whitham, A.G., Price, S.P. & Underhill, J.R. 1999: New constraints on the thermal history of North-east Greenland from apatite fission track analysis. *Geological Society of America Bulletin* **111**, 1054–1068
- Wilson, R.W., Klint, K.E.S., van Gool, J.A.M., McCaffrey, K.J.W., Holdsworth, R.E. & Chalmers, J.A. in press: Faults and fractures in central West Greenland: onshore expression of continental break-up and sea-floor spreading in the Labrador-Baffin Bay Sea. *Geological survey of Denmark and Greenland Bulletin*.

Yardley, B.W.D. 1996: An Introduction to metamorphic petrology, Harlow, Longmans, 248 pp.

Maps

Saga map 1:250000, no. 2, Ivittuut, Narsarsuaq, Qaqortoq (undated). Based on topographic maps from Kort og Matrikelstyrelsen.

Saga map 1:250000, no. 6, Nuuk (undated). Based on topographic maps from Kort og Matrikelstyrelsen.

Saga map 1:500000, no. 1, Kalaallit Nunaata Kujataa (undated). Based on topographic maps from Kort og Matrikelstyrelsen.

60 V.1 Nord Nunarssuit. Geologisk kort over Grønland 1 : 100 000. Grønlands Geologiske Undersøgelse 1967. (Meddr. Grønland 175, no. 7 by T.C.R. Pulvertaft)

60 V.2 Nord Julianehåb. Geologisk kort over Grønland 1 : 100 000. Grønlands Geologiske Undersøgelse 1972. (Compilation by J.H. Allaart)

61 V.1 Syd Ivigtut. Geologisk kort over Grønland 1 : 100 000. Grønlands Geologiske Undersøgelse 1968. (Compilation by N. Henriksen)

61 V.3 Narssarsuaq. Geologisk kort over Grønland 1 : 100 000. Grønlands Geologiske Undersøgelse 1973. (Compilation by J.H. Allaart)

64 V.1 Nord Fiskefjord. Geologisk kort over Grønland 1 : 100 000. Grønlands Geologiske Undersøgelse 1988. (Compilation by A. Garde)

Appendix. Location maps and list of rocks sampled

Location maps for the study areas.

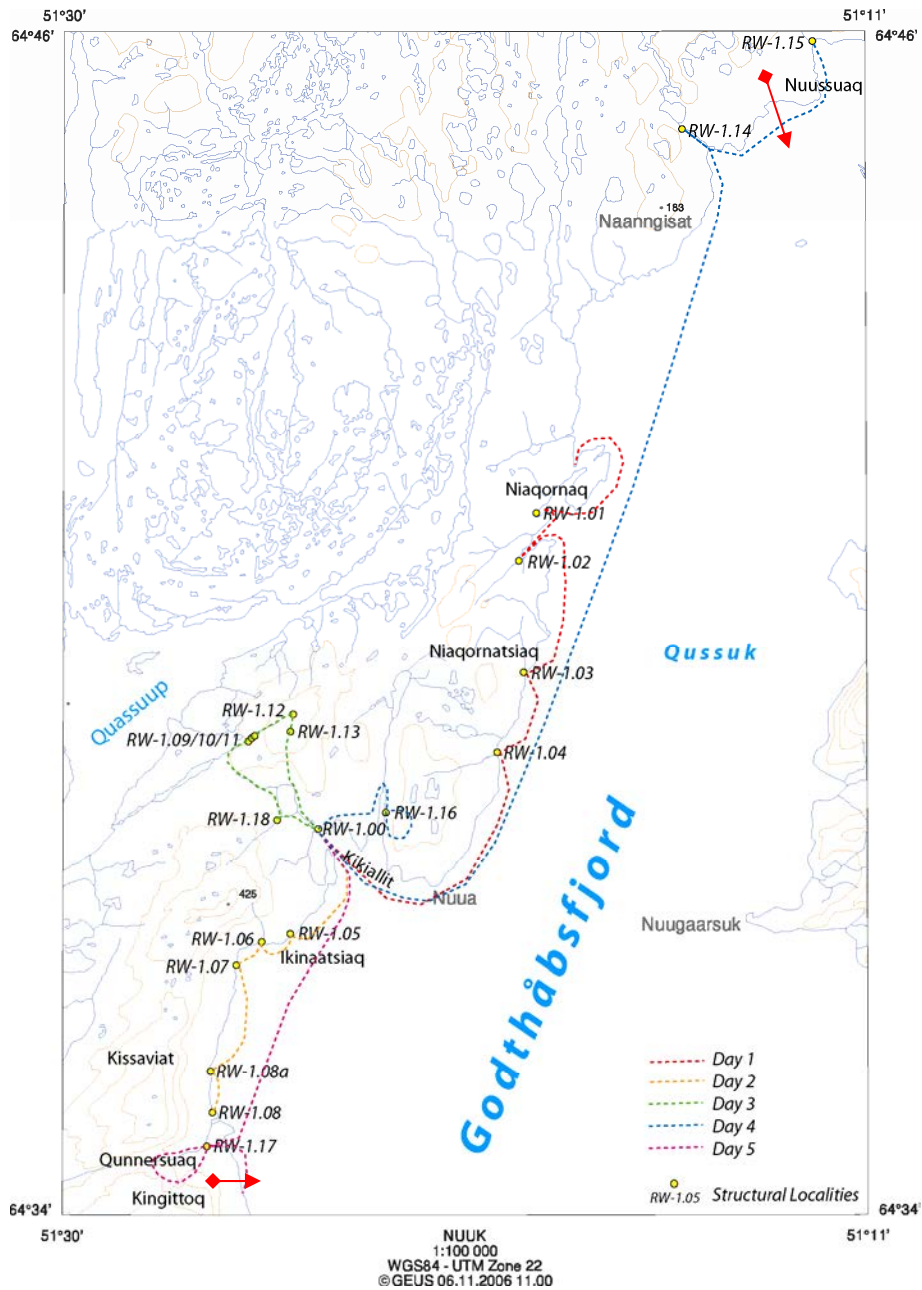
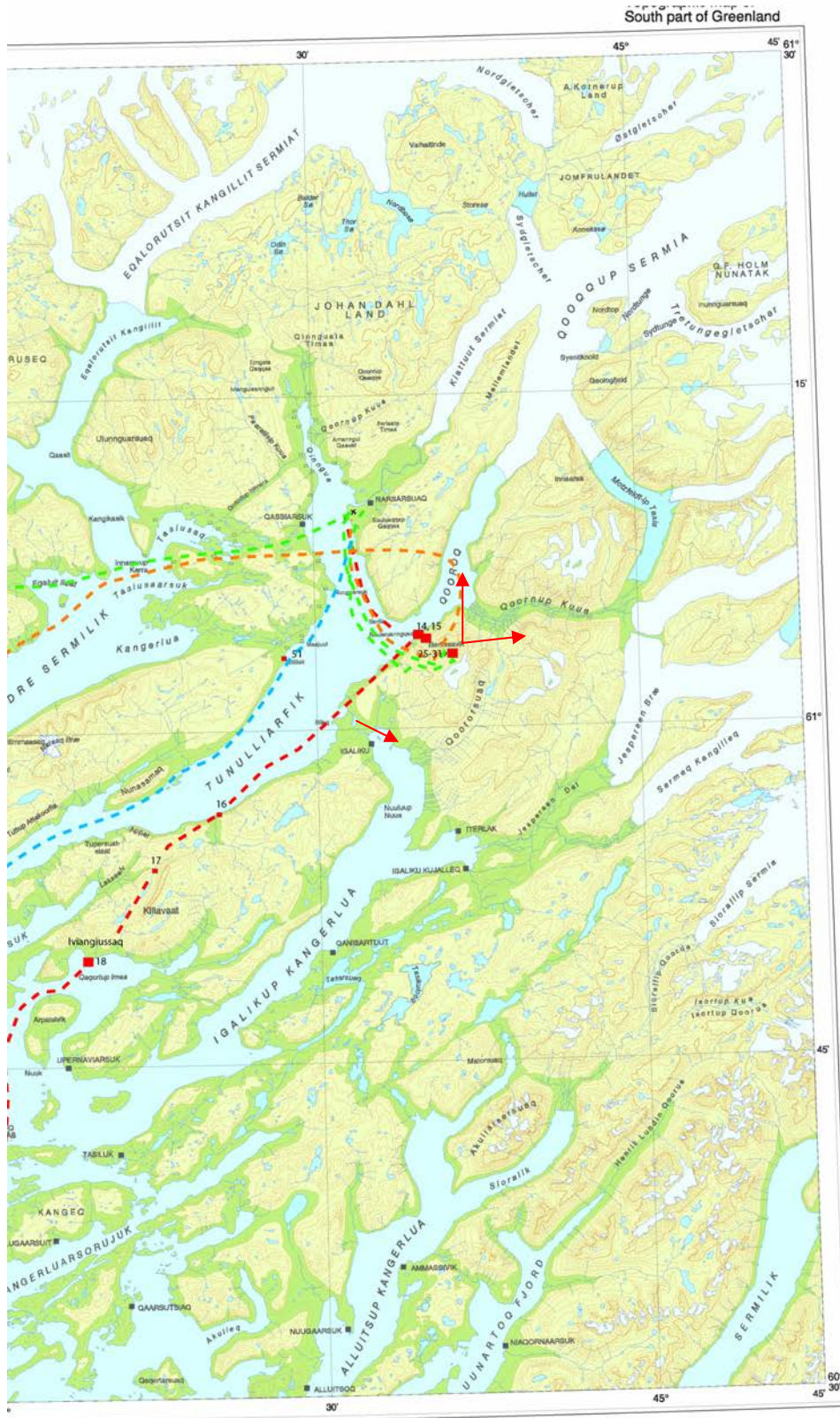


Figure A-1. Location map for Godthåbsfjord.



Figure A-3. Location map for SW Greenland (central part).



Geodetic reference: WGS84
 Projection: UTM 23
 South part of Greenland
 1:250 000

Figure A-4. Location map for SW Greenland (eastern part).

Table A. Rocks sampled.

Abbreviations, place names etc.

Place names for rock sampling localities are taken from the topographic maps.

ghf	Godthåbsfjord
kmb	Kobberminebugt
pst	pseudotachylyte

Altitudes in metres above sea level (a.s.l.) estimated by GPS.

Sample no.	UTM zone (W)	utm x (longitude)	utm y (latitude)	Altitude m a.s.l.	Locality	Region	Rock type	Rock age (Ma)	Date	Purpose	Initials	Comment
468801	22	484.834	7.170.446	5	Niaqornaq	ghf	weathered material	?	15-08-2006	clay minerals	jbon	fault zone
468802	22	484.834	7.170.446	5	Niaqornaq	ghf	weathered material	?	15-08-2006	clay minerals	pj	fault zone
468803	22	484.834	7.170.446	5	Niaqornaq	ghf	crushed rock	?	15-08-2006	clay minerals	pj	fault zone
468804	22	480.891	7.167.405	0	camp/ Kikiallit	ghf	gneiss	>1000	15-08-2006	AFTA	pj	
468805	22	479.875	7.165.360	2	Ikiaatsiaq	ghf	Cataclastite	?	16-08-2006	dating?	pj	fault zone
468806	22	478.912	7.162.124	6	Ikiaatsiaq	ghf	Cataclastite	?	16-08-2006	dating?	rww	fault zone
468807	22	480.382	7.169.442	217	Kikiallit	ghf	weathered rock	?	17-08-2006	clay minerals	jpp	between resistant rocks
468808	22	480.398	7.169.266	213	Kikiallit	ghf	gneiss	>1000	17-08-2006	AFTA	pj	
468809	22	478.866	7.162.851	0	Ikiaatsiaq	ghf	brittle deform.	?	16-08-2006	thin sect.	rww	fracture zone? Water fall
468810	22	490.320	7.182.266	0	Nuussuaq (Qussuk)	ghf	basement	>1000	18-06-2006	AFTA	pj	
468811	22	479.464	7.160.593	0	Qunnersuaq	ghf	basement	>1000	19-08-2006	AFTA	pj	
468812	22	478.227	7.161.320	90	Qunnersuaq	ghf	brittle deform.	?	19-08-2006	thin sect.	rww	
468813	22	479.953	7.167.488	86	Qunnersuaq	ghf	brittle/ductile deform.	?	19-08-2006	dating?	rww	
468814	23	479.527	6.768.732	4	Illerfissalik	Narsarsuaq	Nepheline syenite	>1000	21-08-2006	AFTA	pj	
468815	23	479.948	6.768.675	100	Illerfissalik	Narsarsuaq	Nepheline syenite	>1000	21-08-2006	AFTA	jbon	
468816	23	464.358	6.756.092	0	Qalilimmiut Qaqaa	Narsarsuaq	granite	>1000	21-08-2006	AFTA	pj	
468817	23	458.613	6.750.774	480	Redekammen, Killavaat	Narsarsuaq	Syenite	>1000	21-08-2006	AFTA	pj	
468818	23	453.094	6.744.136	0	Iviangiussaq	Qaqartog	granite	>1000	21-08-2006	AFTA	pj	

Sample no.	UTM zone (W)	utm x (longitude)	utm y (latitude)	Altitude m a.s.l.	Locality	Region	Rock type	Rock age (Ma)	Date	Purpose	Initials	Comment
468819	23	438.109	6.715.927	0	Uummannaq	Qaqartoq	granite	>1000	21-08-2006	AFTA	pj	
468820	23	443.609	6.731.910	11	Town	Qaqartoq	granite	>1000	22-08-2006	AFTA	pj	
468821	23	340.422	6.748.568	10	Amartajâq	kmb	granite	>1000	22-08-2006	AFTA	pj	
468822	23	341.147	6.748.253	9	Amartajâq	kmb	pst	?	22-08-2006	dating?	rww	
468823	23	341.950	6.747.735	0	Amartajâq	kmb	Cataclastite	?	22-08-2006	thin sect.	rww	
468824	22	661.528	6.756.100	0	Rinks Havn Qarmat Qaqaa	kmb	granite	>1000	23-08-2006	AFTA	pj	fault zone
468825	23	484.094	6.769.294	1757	Illerfissalik	Narsarsuaq	Nepheline syenite	>1000	23-08-2006	AFTA	pj	wp104
468826	23	484.051	6.766.799	1.366	Illerfissalik	Narsarsuaq	Nepheline syenite	>1000	23-08-2006	AFTA	pj	wp105
468827	23	483.200	6.767.085	1.124	Illerfissalik	Narsarsuaq	Nepheline syenite	>1000	23-08-2006	AFTA	pj	wp106
468828	23	482.012	6.768.307	915	Illerfissalik	Narsarsuaq	Nepheline syenite	>1000	23-08-2006	AFTA	pj	wp107
468829	23	481.449	6.767.475	698	Illerfissalik	Narsarsuaq	Nepheline syenite	>1000	23-08-2006	AFTA	pj	wp108
468830	23	481.029	6.769.131	450	Illerfissalik	Narsarsuaq	Nepheline syenite	>1000	23-08-2006	AFTA	pj	wp109
468831	23	479.240	6.767.985	211	Illerfissalik	Narsarsuaq	Nepheline syenite	>1000	23-08-2006	AFTA	pj	wp110
468832	23	353.876	6.766.229	46	Ikineq	kmb	mica schist	>1000	24-08-2006	AFTA	pj	apatite?
468833	22	663.099	6.745.248	154	Nunakuluut (Nunarsuit)	kmb	syenite	>1000	24-08-2006	AFTA	pj	
468834	22	656.627	6.747.786	80	Alannvorsuaq	kmb	granite	>1000	24-08-2006	AFTA	pj	
468835	22	642.894	6.748.784	41	Tulugartalik	kmb	syenite	>1000	24-08-2006	AFTA	pj	
368836	22	647.919	6.773.094	814	Tallorutit	kmb	gneiss	>1000	24-08-2006	AFTA	pj	
468837	22	650.421	6.772.983	453	Tallorutit	kmb	gneiss	>1000	24-08-2006	AFTA	pj	

Sample no.	UTM zone (W)	utm x (longitude)	utm y (latitude)	Altitude m a.s.l.	Locality	Region	Rock type	Rock age (Ma)	Date	Purpose	Initials	Comment
468838	22	652.008	6.772.927	251	Tallorutit	kmb	gneiss	>1000	24-08-2006	AFTA	pj	
468839	22	651.261	6.771.742	0	Tallorutit	kmb	gneiss	>1000	24-08-2006	AFTA	pj	
468840	23	346.257	6.762.355	0	Ikerasaaqqap Nunaa	kmb	dyke	?	25-08-2006	structure	rww	cut by fault
468841	23	348.513	6.761.144	0	Ilorleq, coast	kmb	metavolcanics?	>1000	25-08-2006	AFTA	jbon	anchor bay
468842	22	660.649	6.764.125	0	Sanerut (south)	kmb	gneiss	>1000	25-08-2006	AFTA	pj	
468843	22	656.466	6.747.855	106	week2-009	kmb	dolerite dyke	?	24-08-2006	dating?	rww	Garder age or younger?
468844	22	661.525	6.756.299	0	week2-004	kmb	unconsolidated fault breccia	?	23-08-2006	structure	rww	
468845	22	661.525	6.756.299	0	week2-004	kmb	pst?	?	23-08-2006	structure	rww	
468846	22	656.939	6.763.518	0	week2-016	kmb	fault breccia	?	26-08-2006	structure	rww	crushed Garder dyke
468847	22	657.317	6.752.457	30	Alannngorsuaq, Josvaminen	kmb	fault breccia	?	26-08-2006	structure	rww	
468848	22	654.290	6.738.161	0	Kap Desolation	kmb	granite	>1000	26-08-2006	AFTA	jbon	
468849	22	654.290	6.738.161	0	Kap Desolation	kmb	weathered rock	?	26-08-2006	clay minerals	jbon	
468850	23	398.534	6.736.424	0	Lille Tuttutooq, Niaqornaq	Bredefjord	granite	>1000	26-08-2006	AFTA	pj	
468851	23	470.960	6.769.140	5	Sillisit	Narsarsuaq	Sandstone, Eriksfjord Fm	>1000	26-08-2006	AFTA	pj	